

LIBRARY Michigan State University

This is to certify that the dissertation entitled

NEW COUPLED-CLUSTER METHODS FOR MOLECULAR POTENTIAL ENERGY SURFACES

presented by

Ian Sedrick O. Pimienta

has been accepted towards fulfillment of the requirements for the

Ph.D.	_ degree in	Chemistry		
		Doch		
Major Professor's Signature				
		/10/03		
		Date		

MSU is an Affirmative Action/Equal Opportunity Institution

PLACE IN RETURN BOX to remove this checkout from your record. TO AVOID FINES return on or before date due. MAY BE RECALLED with earlier due date if requested.

DATE DUE	DATE DUE	DATE DUE
AUG 2 2 2007		
AUG 2 9 2007		
	·	

6/01 c:/CIRC/DateDue.p65-p.15

NEW COUPLED-CLUSTER METHODS FOR MOLECULAR POTENTIAL ENERGY SURFACES

 $\mathbf{B}\mathbf{y}$

Ian Sedrick O. Pimienta

A DISSERTATION

Submitted to
Michigan State University
in partial fulfillment of the requirements
for the degree of

DOCTOR OF PHILOSOPHY

Department of Chemistry

2003

ABSTRACT

NEW COUPLED-CLUSTER METHODS FOR MOLECULAR POTENTIAL ENERGY SURFACES

By

Ian Sedrick O. Pimienta

The new single-reference approach to the many-electron correlation problem, termed the method of moments of coupled-cluster equations (MMCC), which can be used to extend the applicability of the standard CC methods to bond breaking, is further developed by considering the higher-than-quadruply excited moments of the CCSD (coupled-cluster singles and doubles) equations. The main idea behind the MMCC theory is that of the noniterative a posteriori energy corrections δ which, when added to the energies obtained in the standard CC calculations, recover the exact, full configuration interaction (CI), energies. In this study, the MMCC theory is extended by incorporating the generalized moments of the CCSD equations that correspond to projections of these equations on pentuply and hextuply excited configurations into the MMCC energy corrections. It is demonstrated that these higher-order moments can be very important in studies of the most difficult cases of multiple bond breaking. The trial wave functions that are used to calculate the MMCC energy corrections are provided by the relatively inexpensive CI methods and by the truncated forms of the exponential, CC-like, wave functions. The resulting CI-corrected MMCC methods and the quadratic MMCC (QMMCC) methods including higher-than-quadruply excited moments of the CCSD equations are tested in studies of different types of bond breaking, including the single bond breaking in the HF molecule, the simultaneous breaking of both O-H bonds in the water molecule, the complicated case of triple bond breaking in the nitrogen molecule, and the extremely difficult case of bond breaking in the C₂ molecule.

for Ria

ACKNOWLEDGMENTS

I would like to express my heartfelt thanks to the following people for their part in this work and in my graduate studies:

my advisor, Dr. Piotr Piecuch, for his endless support, guidance, and encouragement; Dr. Karol Kowalski, for his openness and willingness to help me in whatever capacity he could;

my advisorial committee, including Dr. James Harrison, the second reader, Dr. Katharine Hunt, Dr. James Jackson, and Dr. Simon Garrett, for their critical insights on various issues that facilitated my understanding of my research;

Mike, Peng-Dong, Maricris, Ruth, and DJ, for their friendship and companionship, for their willingness to help, and for listening to my practice seminars;

the MSU Filipino Club for all things "Pinoy";

Tita Luchie, Tita Estela, and Tito Amboy, for their unselfish love and support;

Ma and Dad, Lolo Flor, and my sister Ira, for their unconditional love and encouragement;

my wife Ria, for her love and friendship, and for everything she is; and finally, God Almighty, for without Him, there is nothing.

TABLE OF CONTENTS

List of Tables	vii
List of Figures	viii
1. Introduction	1
2. Project Objectives	15
3. The Method of Moments of Coupled-Cluster Equations: An Overview of the General Formalism	16
4. The Existing MMCC (m_A, m_B) Approximations 4.1. The CI-corrected MMCC $(2,3)$ and MMCC $(2,4)$ Methods	25 28
4.2. The Renormalized and Completely Renormalized CCSD[T], CCSD('and CCSD(TQ) Methods	1°), 37
5. The New MMCC (m_A, m_B) Approaches for Multiple Bond Breaking 5.1. The CI-corrected MMCC $(2,5)$ and MMCC $(2,6)$ Approximations 5.1.1. Theory	54 57 58
5.1.2. Examples of Applications 5.1.3. Conclusion	60 69
5.2. The Quasi-variational and Quadratic MMCC Approximations 5.2.1. Theory 5.2.2. Examples of Applications	71 72 86
5.2.3. Conclusion	98
6. Summary, Concluding Remarks, and Future Perspectives	100
Appendix A. An elementary derivation of Eq. (21)	106
Appendix B. The many-body diagrams for the generalized moments of the CCSD equations	110
Appendix C. Algebraic expressions for the $\mathcal{M}_{a_1 a_2 a_3}^{i_1 i_2 i_3}(2)$, $\mathcal{M}_{a_1 a_2 a_3 a_4}^{i_1 i_2 i_3 i_4}(2)$, $\mathcal{M}_{a_1 a_2 a_3 a_4 a_5}^{i_1 i_2 i_3 i_4 i_5 i_6}(2)$ moments of the CCSD equations	134
References	142

List of Tables

Table 1. A comparison of the standard CC, completely renormalized CCSD[T], CCSD(T), and CCSD(TQ), and CI-corrected MMCC(2,3) and MMCC(2,4) energies with the corresponding full CI, CISDt, and CISDtq results obtained for a few internuclear separations R of the HF molecule, as described by the DZ¹⁴¹ basis set.^a

154

Table 2. A comparison of the standard CC, completely renormalized CCSD[T], CCSD(T), and CCSD(TQ), and CI-corrected MMCC(2,3) and MMCC(2,4) energies with the corresponding full CI, CISDt, and CISDtq results obtained for the equilibrium and two displaced geometries of the H_2O molecule with the DZ¹⁴¹ basis set.^a

155

- Table 3. A comparison of the standard CC, completely renormalized CCSD[T], CCSD(T), and CCSD(TQ), and CI-corrected MMCC(2,3) and MMCC(2,4) energies with the corresponding full CI, CISDt, and CISDtq results for a few internuclear separations of the N_2 molecule, as described by the DZ¹⁴¹ basis set.^a 156
- Table 4. A comparison of the CI-corrected MMCC(2,5) and MMCC(2,6) energies and QMMCC(2,4), QMMCC(2,5), and QMMCC(2,6) energies with the results of the full CI, standard CC, and CISDtqp and CISDtqph calculations for the equilibrium and two displaced geometries of the H_2O molecule with the DZ^{141} basis set.^a 157
- Table 5. A comparison of the CI-corrected MMCC(2,5) and MMCC(2,6) energies and QMMCC(2,4), QMMCC(2,5), and QMMCC(2,6) energies with the results of the full CI, standard CC, and CISDtqp and CISDtqph calculations for a few internuclear separations of the N_2 molecule with the DZ^{141} basis set.^a 158
- Table 6. A comparison of the QMMCC(2,4), QMMCC(2,5), and QMMCC(2,6) energies with the results of the full CI and standard CC calculations for a few internuclear separations R of the HF molecule, as described by the DZ^{141} basis set.^a 159
- Table 7. A comparison of the QMMCC(2,4), QMMCC(2,5), and QMMCC(2,6) energies with the results of the full CI, standard CC, and completely renormalized CCSD(TQ) calculations for a few internuclear separations of the C₂ molecule with the DZ¹⁴¹ basis set.^a

List of Figures

- Fig. 1. The orbital classification used in the active-space CI and the CI-corrected MMCC(2,3), MMCC(2,4), MMCC(2,5), and MMCC(2,6) approaches. Core, active, and virtual orbitals are represented by solid, dashed, and dotted lines, respectively. Full and open circles represent core and active electrons of the reference configuration $|\Phi\rangle$.
- Fig. 2. Potential energy curves for the N_2 molecule, as described by the DZ basis set. A comparison of the results obtained with the CR-CC and CI-corrected MMCC(2,3) and MMCC(2,4) methods with the results of the standard CC and full CI calculations.

162

- Fig. 3. Potential energy curves for the N₂ molecule, as described by the DZ basis set. A comparison of the results obtained with the CI-corrected MMCC(2,5) and MMCC(2,6) methods with the results of the standard CC, CR-CCSD(TQ), and full CI calculations.
- Fig. 4. Potential energy curves for the N₂ molecule, as described by the DZ basis set. A comparison of the results obtained with the QMMCC methods with the results of the standard CC and full CI calculations.
- Fig. 5. Potential energy curves for the C₂ molecule, as described by the DZ basis set. A comparison of the results obtained with the QMMCC methods with the results of the standard CC, CR-CCSD(TQ), and full CI calculations.

1. Introduction

One of the most challenging problems that quantum chemists of today face is the accurate study of molecular potential energy surfaces (PESs) that involve breaking or making of chemical bonds. Bond breaking and bond making are difficult to describe with quantum mechanical methods, particularly when one is interested in high accuracies that are expected from modern computer simulation techniques. The early ab initio methods developed to obtain energies for atomic and molecular systems, such as the Hartree-Fock (HF) approach, 1,2 do not work when bond breaking or making is involved. The failure of the HF methods in describing bond breaking or making can be attributed to the lack of electron correlation in these methods. Because of the presence of the electron-electron repulsion terms in the molecular Hamiltonian, the motion of electrons in a molecule is highly correlated and difficult to describe. Although the bulk of the total electronic energy is obtained from the HF calculations (~99%), the remanent energy that the HF methods do not describe is involved in various chemical processes, including bond breaking and making. Other quantities of interest in chemistry (i.e. ionization potentials, electron affinities, electronic excitation energies, vibrational energies, etc.) are also sensitive in varying degrees to the many-electron correlation effects. The residual energy, known as the correlation energy obtained as the difference between the HF energy and the exact energy,3 is the single most important piece that quantum mechanical models must describe if we are to use them in accurate and predictive calculations for molecular systems.

There are a number of techniques that seek to improve the HF wave function. The

method of choice depends very much on the characteristics of the problem. Some of the desirable features of a method involving electron correlation are:⁴ (1) it should be well-defined, giving a continuous PES and a unique energy for any nuclear configuration, (2) it should be "size-consistent", i.e. the energy of a sum of non-interacting fragments should be exactly the sum of energies obtained in separate calculations on the fragments, (3) it should be exact when applied to a two-electron system, (4) it should be efficient, i.e. it should be applicable to larger basis sets, (5) it should be accurate enough to be an adequate approximation to the exact result, and (6) it should be variational, i.e. the energy should be an upper bound to the exact result. Unfortunately, no current method satisfies all of the above criteria!

Nowadays, there are three main ab initio approaches that describe the manyelectron correlation effects: (1) the configuration interaction (CI) method, 5-9 (2)
the many-body perturbation theory (MBPT), 10-14 and (3) the coupled-cluster (CC)
theory. 15-19 The conceptually simplest way of describing electron correlation is via the
CI method. CI uses a wave function which is a linear combination of the HF (or other
reference) determinant and Slater determinants obtained by promoting (exciting)
electrons from the occupied to unoccupied orbitals. The CI method is variational
and, if the expansion is complete (full CI), the exact correlation energy (and the
exact total energy) for a basis set used in the calculations is obtained. The number
of Slater determinants in full CI grows factorially with the system size, making the
method impractical for all but the smallest few-electron systems. For this reason
the CI expansion is usually truncated at some level of excitation. For example, in

determinants, in addition to the reference determinant, are considered while in the CISDT (CI with singles, doubles, and triples) approach, only the singly, doubly, and triply excited determinants are considered, and so on. The problem with all truncated CI methods is that the convergence of the CI results towards the full CI limit with the excitation level is often very slow. One has to use very long CI expansions to obtain high accuracies required in modern ab initio calculations. Another problem with the truncated CI approaches is that they are not size-extensive, i.e. the truncated CI methods incorrectly describe the dependence of electronic energies on the size of the system. For CISD, an approximate way to correct for the lack of size extensivity is by introducing the Davidson corrections.^{20,21}

Perhaps the easiest way to incorporate electron correlation into quantum chemical calculations is by using the MBPT. In this approach, the exact Hamiltonian is decomposed into the unperturbed part that corresponds to the HF (or some other single-determinantal) description and the perturbation that describes the many-electron correlation effects. The Rayleigh-Schrödinger perturbation theory is used to calculate the corrections to the HF (or other single-determinantal reference) wave function and energy. The MBPT energies are size-extensive, but not variational. Perturbation theory relies on the starting wave function being close to the exact wave function. When this is the case, i.e. when the electronic wave function is well represented by a single Slater determinant, the convergence of the MBPT series is usually rapid. However, when chemical bonds are stretched, the MBPT series becomes divergent. For molecules near their equilibrium geometries, the MBPT energies and properties are often more accurate than the corresponding limited (or truncated) CI results,

but unlike CI, the MBPT methods are usually useless when PESs involving bond breaking are examined.

The failing of MBPT is that it is basically an order-by-order perturbation approach. In many cases, it is necessary to go to higher orders of MBPT. A practical solution to this problem is provided by the CC theory. In the CC theory, an exponential form of the wave function in terms of the cluster operator T is employed. The advantage of all CC methods is that the higher-order excitations are partially included as products of the lower order excitations, making it possible to describe the high-order effects at a low level of approximation. The use of the infinite-order exponential ansatz guarantees the correct scaling of molecular properties with the number of electrons. Like MBPT, the CC results are not variational, and energies can go below their exact full CI counterparts, but this is never a problem when the closed-shell systems are considered, since in this case the CC methods are remarkably accurate. It is possible to combine some aspects of MBPT with CC theory to retain much of the infinite-order aspect of CC while saving significantly in the computational cost for higher cluster operators. This can be done iteratively or noniteratively (cf. the discussion below).

Over the past 30 years, the CC theory¹⁵⁻¹⁹ has become the most reliable computational method of electronic structure theory for the prediction of molecular energies and properties whenever high-accuracy results are desired. In 1966,¹⁵ and later in a review article published in 1969,¹⁶ Čížek laid down the foundations of the use of the CC method in electronic structure theory in formal terms. The sophisticated mathematical techniques that he used, such as diagrams and second-quantization, were,

unfortunately, beyond the experience of most quantum chemists at that time. In the 1970s, CC theory began to gain some interest in the quantum chemistry community. Čížek and Paldus¹⁷ derived expressions for coupled-cluster doubles (CCD) theory (at that time referred to as coupled-pair many-electron theory (CPMET)), using rather elementary mathematical techniques that could be easily understood by others. This was actually an algebraic re-derivation of the diagrammatic equations presented earlier by Čížek. 15 In 1972, 22 Paldus, Čížek, and Shavitt performed the first ab initio coupled cluster calculations using a variety of CC methods including singly, doubly, and even triply excited clusters, although computer programs that they developed were not of the general purpose type. At the end of 1970s, the first general purpose computer implementations of the CC theory began to appear. Pople et al.23 and Bartlett and Purvis²⁴ developed the first general purpose spin-orbital CCD codes. In the early 1980s, a particularly important achievement was that of Purvis and Bartlett, 25 who derived the vectorizable form of the CCSD (coupled-cluster with singles and doubles) equations and implemented them in a practical computer code that could be applied to a wide range of problems. At the end of the 1980s and throughout the 1990s, the popularity of CC methods grew at a rapid pace, as more effort was directed towards the construction of highly efficient CC codes, spin-adaptation of open-shell CC wave functions, calculations of properties other than energy, extensions of CC theory to excited states and multireference problems requiring a truly multideterminantal description, and inclusion of higher excitations in the CC wave function.²⁶⁻³⁰ Nowadays, accurate CC calculations for closed-shell and simple openshell molecular systems at their equilibrium geometries involving up to 20-30 light atoms or a few heavy atoms are routine.

The CC theory has grown to become one of the most popular methods in accurate electronic structure calculations, but severe problems have been discovered in applications of the CC methods to PESs involving bond breaking. From the time the CCSD²⁵⁻²⁹ method was implemented, numerous CC methods have been developed with the intention of improving the quality of PESs while maintaining the relatively low cost of the CC calculations. The CCSD method uses only the singly and doubly excited clusters in the CC expansion. It has been observed from many numerical calculations that the CCSD method fails to describe bond stretching or breaking, particularly when multiply bonded systems are considered (cf. the discussion below). The absence of the higher-than-doubly excited clusters in the expansion is one of the reasons why the CCSD method fails in the bond breaking region. As it turns out, the CCSD approach is often inadequate when high accuracy results for nuclear geometries near the equilibrium are sought. The inadequacy of the CCSD method prompted the quantum chemists to develop approximate methods that include higher-than-doubly excited clusters in the calculations. The most practical approximations that emerged from this effort include the noniterative $CCSD+T(CCSD) = CCSD[T]^{30-32}$ and the CCSD(T)³³ approaches, where the information about energy contributions due to triply excited clusters is obtained using MBPT. Later, similar methods were developed that account for the combined effect of triply and quadruply excited clusters. One such approach is the CCSD(TQ_f) method,³⁴ where one adds the relatively inexpensive corrections due to triply and quadruply excited clusters to the CCSD energies. Other inexpensive approaches, termed the approximate coupled-pair of approximate

CCSD methods accounting for triples, quadruples, and related higher-order clusters were developed by Piecuch et al.^{31,32} The addition of the triply and quadruply excited clusters, on which the CCSD[T], CCSD(T), and CCSD(TQ_f) approaches are based, to the CCSD energies has been proven time and time again in numerous molecular applications to produce methods that give the best compromise between high accuracy and relatively low computer cost in molecular applications.^{35–39}

Unfortunately, the CCSD[T], CCSD(T), and CCSD(TQ_f) methods fail in situations where bond breaking is involved, particularly when the spin-adapted restricted Hartree-Fock (RHF) configuration is used as a reference (cf., for example, Refs. 38, 40–53 and references therein). The failure of the CCSD[T], CCSD(T), and CCSD(TQ_f) approaches in describing breaking of chemical bonds is due to the following two factors: (i) the singly and doubly excited clusters, obtained in CCSD calculations, which are used to determine the energy corrections due to triples and quadruples in the CCSD[T], CCSD(T), and $CCSD(TQ_f)$ approaches, are significantly different from their exact values in the bond breaking region and (ii) the noniterative triples and quadruples corrections, defining the CCSD[T], CCSD(T), and CCSD(TQ_f) methods, which are based on the standard MBPT arguments, fail due to the divergent behavior of the MBPT series at larger internuclear separations. As a consequence, the PESs produced by the CCSD(T), CCSD(TQ_f), and other noniterative CC approaches are completely unphysical.^{38,40-53} As a matter of fact, even the iterative analogs of the CCSD[T], CCSD(T), and CCSD(TQ_f) methods, i.e. the CCSDT-n^{31,54-57} and CCSDTQ-1⁵⁸ approaches, and the higher-order noniterative CCSDT+Q(CCSDT) = $CCSDT[Q]^{58}$ and $CCSDT(Q_f)^{34}$ approximations that all use MBPT to evaluate higher-than-doubly excited clusters, fail in the bond breaking region, particularly when multiple bonds are broken.^{40,49} Thus, new CC methods that can be applied to molecular PESs involving single and multiple bond breaking must be developed.

One way to eliminate the failures of the perturbative, noniterative and iterative CC approximations in the bond breaking region is by the inclusion of the higherthan-doubly excited clusters, i.e. the triply, quadruply, and even the pentuply excited clusters, completely and in a fully iterative manner. Kállay and Surján developed a programming technique that allows one to write efficient computer codes for iterative CC methods of any rank.⁵⁹ The complete and iterative incorporation of the higherorder clusters in CC calculations helps to resolve the failures of the single-reference CC approaches, especially at larger internuclear separations. However, the resulting methods are much too expensive for routine applications. For example, the most expensive iterative steps of the full CCSDT approach (CC method with singly, doubly, and triply excited clusters)^{60,61} and its higher-level CCSDTQ (CC with singles, doubles, triples, and quadruples)⁶²⁻⁶⁵ and CCSDTQP (CC singles, doubles, triples, quadruples, and pentuples)⁶⁶ analogs scale as $n_o^3 n_u^5$, $n_o^4 n_u^6$, and $n_o^5 n_u^7$, respectively $(n_o$ (n_u) is the number of occupied (unoccupied) orbitals in the molecular orbital (MO) basis). This means that the computer time associated with the full CCSDT, CCS-DTQ, and CCSDTQP calculations grows as $\mathcal{N}^8,~\mathcal{N}^{10},$ and $\mathcal{N}^{12},$ respectively, with molecular size (\mathcal{N} is a general measure of the molecular size). On the other hand, the CCSD(T) calculation requires iterative steps that scale as $n_o^2 n_u^4$ (or \mathcal{N}^6) and noniterative steps that scale as $n_o^3 n_u^4$ (or \mathcal{N}^7). The expensive steps in the CCSDT, CCSDTQ, and CCSDTQP calculations restrict their applicability to very small systems, at best

consisting of 2–3 light atoms, using small basis sets. This should be contrasted with the fact that the CCSD(T) approach can be applied to systems with up to 30 light atoms or a few heavy atoms. In fact, Schütz and Werner performed CCSD(T) calculations for systems with $\sim \! 100$ atoms^{67–69} using the local correlation formalism of Pulay and Saebø.^{70–72}

One can eliminate the above problems with the single-reference CC methods by switching to the genuine multireference CC (MRCC) approaches of the state-universal^{35,38,73-88} or valence-universal^{35,38,89-92} type, which are specifically designed to handle general open-shell and quasi-degenerate states, including, at least in principle, all cases of bond breaking. However, the MRCC approaches are often plagued with intruder states and multiple, singular, or unphysical solutions (cf., e.g., Refs. 76, 81-85, 93-95). The standard single-reference CC methods do not suffer from such problems. Furthermore, the single-reference CC methods are much easier to use than their MRCC counterparts. The state-specific MRCC approaches (cf., e.g., Refs. 96-103), which are based on the genuine multireference formalism may change this situation, but none of the existing state-specific MRCC methods are simple or general enough to be as widely applicable as the standard CCSD, CCSD(T), and similar approaches.

The difficulties and problems associated with the use of the multireference approaches indicate that, in developing new methods for bond breaking, it may be more worthwhile to focus on methods that use only a single reference formalism. In recent years, a great deal of effort has been undertaken towards developing single-reference or single-reference-like approaches that would, potentially, eliminate the pervasive failing

of the standard CC approximations at larger internuclear separations, while avoiding the complexity of the genuine multireference theory and the astronomical costs of the CCSDTQ, CCSDTQP, and similar calculations. These include the reduced multireference CCSD (RMRCCSD) method, ^{38,104-110} the active-space CC approaches (which can also be classified as the state-selective MRCC methods), ^{41,43,44,48,65,111-125} the orbital-optimized CC methods, ^{126,127} the noniterative approaches based on the partitioning of the similarity-transformed Hamiltonian, ¹²⁸⁻¹³¹ and the renormalized (R) and completely renormalized (CR) CC methods. ^{45-51,53,134,136} The latter approaches are based on the more general formalism of the method of moments of CC equations (MMCC), ^{45-47,51,52,87,132-137} which can be applied to ground- and excited-state PESs. All of these methods have been developed with the intention of improving the description of bond breaking, while retaining the simplicity of the single-reference description based on the spin- and symmetry-adapted references of the RHF type.

The RMRCCSD method of Paldus and Li^{38,104-110} and the active-space CC approaches of Adamowicz, Piecuch and co-workers^{41,43,44,48,65,111-122} are interesting and worth further development. They have been proved to accurately describe quasi-degenerate ground states,^{43,65,104,107,118} bond breaking,^{41,43,44,48,105,106,108-110,115,116,119,122} ro-vibrational term values including highly excited states near dissociation,^{44,109,110} and property functions.¹²¹ In analogy to the genuine multireference approaches, the RMRCCSD and active-space CC approaches require choosing active orbitals, but this is done in such a way that the formal structure of the single-reference CC theory is largely preserved. The RMRCCSD and active-space CC methods definitely represent the step in the right direction, but the question remains if one could completely or

almost completely eliminate the elements of multireference calculations, such as active orbitals, and yet obtain a highly accurate description of PESs involving bond breaking.

The perturbative CC approaches developed by Head-Gordon et al., which are based on the partitioning of the similarity-transformed Hamiltonian, 128-131 and the renormalized (R) and completely-renormalized (CR) CC approaches developed by Piecuch et al., $^{45-51,53}$ which employ the MMCC formalism, $^{45-47,51,52,87,132-137}$ represent an attempt to entirely eliminate active orbitals and other elements of multireference theory from the calculations. These methods retain the simplicity and the "blackbox" character of the standard CC methods of the CCSD(T) type. The perturbative CC approaches developed by Head-Gordon et al. improve the description of bond breaking, but they are not as accurate as the MMCC methods and CR-CC approaches (cf., e.g., Ref. 48). Thus, pursuing the MMCC methodology is probably the best idea at this time, when it comes to relatively simple coupled-cluster methods that may improve the description of bond breaking with an effort similar to the singlereference calculations. In the MMCC formalism and the related R-CC and CR-CC approaches, noniterative energy corrections are computed which, when added to the energies obtained in the standard CC calculations, such as CCSD, recover the exact, i.e. full CI, energies. For example, in the renormalized and completely renormalized CCSD(T) and CCSD(TQ) approaches, one adds relatively inexpensive noniterative corrections due to triples or triples and quadruples to the CCSD energies. These methods preserve the conceptual and computational simplicity of the noniterative CC methods, such as CCSD(T) and CCSD(TQ_f), while improving the results in the

bond breaking region. At least part of the success of the MMCC approaches is due to the fact that in designing the MMCC approximations including the R-CC and CR-CC methods, we directly focus on the quantity of interest which is the difference between the full CI and CC energies.

Two types of the MMCC methods have been considered so far, namely, the CIschemes^{45,51,52,132-134} **MMCC** corrected and the R-CC and CR-CC methods. 45-51,53,134,136 In the CI-corrected MMCC approaches, one has to perform an a priori limited CI calculation to construct the noniterative corrections to the standard CC energies. $^{45,51,52,132-134}$ The R-CC and CR-CC methods $^{45-51,53,134,136}$ do not require any a priori non-CC calculations. Thus, they are as easy to use as the standard CC "black-boxes" of the CCSD(T) or CCSD(TQ_f) type. Furthermore, the R-CC and CR-CC methods can easily be incorporated in any electronic structure package that has the CCSD(T) and CCSD(TQ_f) options in it. In fact, the renormalized and completely renormalized CCSD[T] and CCSD(T) methods (the R-CCSD[T], R-CCSD(T), CR-CCSD[T], and CR-CCSD(T) methods, respectively) have recently been incorporated¹³⁸ in the popular GAMESS package.¹³⁹

It has been well-established by now that the CR-CCSD(T) and CR-CCSD(TQ) (completely renormalized CCSD(TQ)) methods provide an excellent description of entire PESs involving single and double bond dissociations, $^{45,46,48,50-52,134,136,138}$ highly-excited vibrational term values near dissociation, 50,51,134,138 and entire PESs for exchange chemical reactions of the general type: closed shell + closed shell \rightarrow doublet + doublet, 53,134,136 and for transition states having a diradical character. 140 The results obtained in the CR-CCSD(T) and CR-CCSD(TQ) calculations for triple bond break-

ing and for certain types of double bond dissociations, however, are somewhat less impressive. $^{47,51,134-136}$ In particular, for the double zeta (DZ) 141 model of N₂, the small \sim 1 millihartree errors, relative to full CI, near the equilibrium geometry R_e , obtained with variant "b" of the CR-CCSD(TQ) method increase to 10–25 millihartree at larger N-N separations (see Sect. 4.2 for the discussion on completely renormalized CC approaches; see Table 3 for the numerical results). These are still quite significant errors if one is aiming at high accuracy. Thus, for more complicated types of bond breaking, including cases where multiple bonds are stretched or broken, we need better methods than CR-CCSD(T) or CR-CCSD(TQ). The main challenge is in formulating methods that preserve the relative simplicity of the noniterative coupled-cluster approximations of the CCSD(T) or CCSD(TQ) type. We believe that such methods can be proposed if we use the higher-order MMCC approximations.

The main goal of this dissertation is the development, implementation, and testing of the new types of noniterative MMCC methods that lead to a highly accurate description of multiple bond breaking. We have formulated two classes of the MMCC methods that work especially well for double and triple bond breaking. The first class includes the CI-corrected MMCC(2,6) approach.¹³⁴ In this approach, a relatively inexpensive CI calculation is performed and the results are combined with the complete set of moments of the CCSD equations, including the previously ignored pentuply and hextuply excited moments (the CR-CCSD(T) and CR-CCSD(TQ) methods use only the triply and quadruply excited moments). The second class of approaches that we have developed, implemented, and tested includes the so-called quadratic MMCC (QMMCC) approach, ¹³⁴⁻¹³⁷ which is an approximate form of the more general quasi-

variational MMCC (QVMMCC) formalism. The QMMCC method can be viewed as a natural extension of the CR-CCSD(T) and CR-CCSD(TQ) methods mentioned earlier. In particular, the QMMCC approach preserves the "black-box" character of the CR-CCSD(T) and CR-CCSD(TQ) approximations. In the QMMCC method, as in the case of the CR-CCSD(T) and CR-CCSD(TQ) approaches, we add relatively straightforward noniterative corrections to the standard CCSD energies. Details of the CI-corrected MMCC(2,5) and MMCC(2,6) approaches and the QMMCC approximation are described in Sect. 5. Examples illustrating the performance of these new approaches in calculations of molecular PESs are described in Sect. 5, too.

2. Project Objectives

The main objectives of this work are:

- A. The development of the higher-order variants of the MMCC formalism, including higher-than-quadruply excited moments of the CCSD equations, that are capable of eliminating the failure or poorer performance of the existing standard and renormalized CC methods for cases involving multiple bond breaking. This will be accomplished by formulating and implementing the CI-corrected MMCC(2,6) method and the quadratic MMCC approximation mentioned in the previous section.
- B. Testing the proposed MMCC methods in benchmark calculations for various types of bond breaking, including single bond breaking in the HF molecule, simultaneous dissociation of two O-H bonds in the H₂O molecule, double bond breaking in the C₂ molecule, and triple bond breaking in N₂.

3. The Method of Moments of Coupled-Cluster Equations: An Overview of the General Formalism

In the single-reference CC theory, the ground-state wave function $|\Psi_0\rangle$ of an N-electron system, described by the Hamiltonian H, is written in the exponential form

$$|\Psi_0\rangle = e^T |\Phi\rangle \,, \tag{1}$$

where T is the cluster operator and $|\Phi\rangle$ is the independent-particle-model (IPM) reference configuration (e.g., the Hartree-Fock determinant) defining the Fermi vacuum. In the exact CC theory, T is a sum of all many-body cluster components that can be written for a given N-electron system. We have,

$$T = \sum_{n=1}^{N} T_n \,, \tag{2}$$

where the n-body cluster component T_n is defined as

$$T_{n} = \sum_{\substack{i_{1} < \dots < i_{n} \\ a_{1} < \dots < a_{n}}} t_{a_{1} \dots a_{n}}^{i_{1} \dots i_{n}} E_{i_{1} \dots i_{n}}^{a_{1} \dots a_{n}} = \left(\frac{1}{n!}\right)^{2} t_{a_{1} \dots a_{n}}^{i_{1} \dots i_{n}} E_{i_{1} \dots i_{n}}^{a_{1} \dots a_{n}}, \tag{3}$$

with

$$E_{i_1\dots i_n}^{a_1\dots a_n} = \prod_{\kappa=1}^n c^{a_\kappa} c_{i_\kappa} \tag{4}$$

and $t_{a_1...a_n}^{i_1...i_n}$ representing the corresponding excitation operators and cluster amplitudes, respectively. Whenever possible, the Einstein summation convention over repeated upper and lower indices is employed. In our notation, c^p (c_p) are the usual

creation (annihilation) operators ($c^p = c_p^{\dagger}$) associated with a given orthonormal spin-orbital basis set $\{p\}$. The letters i and a designate the occupied and unoccupied spin-orbitals, respectively, whereas p is a generic index that runs over all (occupied and unoccupied) spin-orbitals. The singly and doubly excited clusters, T_1 and T_2 , respectively, that are used in the CCSD calculations, are given by the following expressions:

$$T_1 = \sum_{\substack{i_1 \\ a_1}} t_{a_1}^{i_1} E_{i_1}^{a_1} \equiv t_{a_1}^{i_1} E_{i_1}^{a_1}, \qquad (5)$$

$$T_2 = \sum_{\substack{i_1 < i_2 \\ a_1 < a_2}} t_{a_1 a_2}^{i_1 i_2} E_{i_1 i_2}^{a_1 a_2} = \frac{1}{4} t_{a_1 a_2}^{i_1 i_2} E_{i_1 i_2}^{a_1 a_2}.$$
 (6)

The standard CC approximations are obtained by truncating the many-body expansion for T, Eq. (2), at a given excitation level $m_A < N$, so that

$$T \approx T^{(A)} = \sum_{n=1}^{m_A} T_n \,. \tag{7}$$

The standard CCSD method is obtained by setting $m_A = 2$ in Eq. (7). In the CCSDT method, m_A is set at 3; in the CCSDTQ approach, $m_A = 4$, etc. The cluster operator $T^{(A)}$, Eq. (7), defining the standard approximation A or the amplitudes $t_{a_1...a_n}^{i_1...i_n}$, $n = 1, ..., m_A$, which define it, is obtained by solving the system of nonlinear, energy-independent, algebraic equations,

$$Q_n \bar{H}^{(A)} |\Phi\rangle = 0, \quad n = 1, \dots, m_A, \qquad (8)$$

where

$$\bar{H}^{(A)} = e^{-T^{(A)}} H e^{T^{(A)}} = (H e^{T^{(A)}})_C \tag{9}$$

is the similarity-transformed Hamiltonian of the CC method A (subscript C designates the connected part of the corresponding operator expression (cf. Appendix B). Q_n is the projection operator onto the subspace spanned by all n-tuply excited configurations relative to reference $|\Phi\rangle$, i.e.,

$$Q_n = \sum_{\substack{i_1 < \dots < i_n \\ a_1 < \dots < a_n}} |\Phi_{i_1 \dots i_n}^{a_1 \dots a_n}\rangle \langle \Phi_{i_1 \dots i_n}^{a_1 \dots a_n}|, \qquad (10)$$

with

$$|\Phi_{i_1\dots i_n}^{a_1\dots a_n}\rangle = E_{i_1\dots i_n}^{a_1\dots a_n}|\Phi\rangle \tag{11}$$

representing the *n*-tuply excited configuration. For example, the standard CCSD equations for the singly and doubly excited cluster amplitudes $t_{a_1}^{i_1}$ and $t_{a_1a_2}^{i_1i_2}$ defining the operators T_1 and T_2 , respectively, look as follows:

$$Q_n \bar{H}^{\text{CCSD}} |\Phi\rangle = 0, \quad n = 1, 2,$$
 (12)

or, simply,

$$\langle \Phi_{i_1}^{a_1} | \bar{H}^{\text{CCSD}} | \Phi \rangle = 0, \qquad (13)$$

$$\langle \Phi_{i_1 i_2}^{a_1 a_2} | \bar{H}^{\text{CCSD}} | \Phi \rangle = 0, \quad i_1 < i_2, \ a_1 < a_2,$$
 (14)

where

$$\bar{H}^{\text{CCSD}} = e^{-(T_1 + T_2)} H e^{T_1 + T_2} = (H e^{T_1 + T_2})_C \tag{15}$$

is the similarity-transformed Hamiltonian of the CCSD approach. The system of CC equations, Eq. (8), is obtained by inserting the CC wave function $|\Psi_0\rangle$, Eq. (1), into the electronic Schrödinger equation $H|\Psi_0\rangle = E_0|\Psi_0\rangle$, premultiplying both sides of the Schrödinger equation on the left by e^{-T} and projecting the resulting connected cluster form of the Schrödinger equation, $\bar{H}|\Phi\rangle = E_0|\Phi\rangle$, with \bar{H} defined as $e^{-T}He^T$ (or $(He^T)_C$), in which $T = T^{(A)}$, onto the excited configurations $|\Phi^{a_1...a_n}_{i_1...i_n}\rangle$, $n = 1, ..., m_A$, included in $T^{(A)}$ (represented in Eq. (8) by the projection operators Q_n).

Once the system of equations, Eq. (8), is solved for $T^{(A)}$, we calculate the CC energy corresponding to the approximate CC method A by using the expression

$$E_0^{(A)} = \langle \Phi | \bar{H}^{(A)} | \Phi \rangle, \tag{16}$$

obtained by projecting the connected cluster form of the Schrödinger equation, $\bar{H}|\Phi\rangle = E_0|\Phi\rangle$, where $T=T^{(A)}$, onto $|\Phi\rangle$. For many-electron systems described by the Hamiltonians H containing up to two-body interactions, i.e., when

$$H = z_p^q c^p c_q + \frac{1}{4} v_{pq}^{rs} c^p c^q c_s c_r , \qquad (17)$$

the CC energy $E_0^{(A)}$ is calculated using only the T_1 and T_2 clusters, independent of the truncation scheme used to define $T^{(A)}$ (assuming that $m_A \geq 2$). We have

$$E_0^{(A)} = \langle \Phi | H | \Phi \rangle + \langle \Phi | [H_N(T_1 + T_2 + \frac{1}{2}T_1^2)]_C | \Phi \rangle, \qquad (18)$$

where $H_N = H - \langle \Phi | H | \Phi \rangle$ is the Hamiltonian in the normal-ordered form. The z_p^q and v_{pq}^{rs} coefficients defining Hamiltonian H, Eq. (17), are the usual one- and antisymmetrized two-electron molecular integrals, $\langle p|z|q\rangle$ and $\langle pq|v|rs\rangle_A = \langle pq|v|rs\rangle$ – $\langle pq|v|sr\rangle$, respectively.

In the ground-state MMCC formalism of Kowalski and Piecuch, $^{45-47}$ the energy $E_0^{(A)}$ obtained from the standard single-reference CC calculations with some approximate method A, Eq. (16), is improved upon by adding the suitably designed non-iterative correction $\delta_0^{(A)}$ to $E_0^{(A)}$, which in the exact limit recovers the exact full CI ground-state energy E_0 . The energy formula used by all MMCC methods can be written as

$$E_0^{\text{MMCC}} = E_0^{(A)} + \delta_0^{(A)}, \tag{19}$$

where $E_0^{(A)}$ is the standard CC (e.g., CCSD) energy and $\delta_0^{(A)}$ is the MMCC noniterative energy correction, which is described below. In the exact MMCC theory, E_0^{MMCC} becomes the exact full CI energy E_0 . The approximate MMCC methods are obtained by approximating the explicit many-body expression for $\delta_0^{(A)}$ described below.

The MMCC formula for the noniterative correction $\delta_0^{(A)}$ entering Eq. (19) is expressed in terms of the generalized moments of CC equations. We obtain these readily available quantities by projecting the CC equations for method A on the excited configurations that are not included in the calculations with method A. Thus, if $|\Phi_{i_1...i_k}^{a_1...a_k}\rangle$ designate the k-tuply excited configurations relative to $|\Phi\rangle$, the generalized moments $\mathcal{M}_{a_1...a_k}^{i_1...i_k}(m_A)$, corresponding to CC method A, are defined as

$$\mathcal{M}_{a_1\dots a_k}^{i_1\dots i_k}(m_A) = \langle \Phi_{i_1\dots i_k}^{a_1\dots a_k} | \bar{H}^{(A)} | \Phi \rangle. \tag{20}$$

Note that for $k \leq m_A$, the corresponding generalized moments $\mathcal{M}_{a_1...a_k}^{i_1...i_k}(m_A)$ vanish. This is a consequence of the fact that cluster operator $T^{(A)}$ satisfies Eq. (8). This implies that the exact correction $\delta_0^{(A)}$, defined as the difference between the full CI and CC energies, must be expressed in terms of the generalized moments $\mathcal{M}_{a_1...a_k}^{i_1...i_k}(m_A)$ with $k > m_A$. We obtain 45-47,134

$$\delta_0^{(A)} \equiv E_0 - E_0^{(A)} = \sum_{n=m_A+1}^N \sum_{k=m_A+1}^n \langle \Psi_0 | Q_n \, C_{n-k}(m_A) \, M_k(m_A) | \Phi \rangle / \langle \Psi_0 | e^{T^{(A)}} | \Phi \rangle , \quad (21)$$

where

$$C_{n-k}(m_A) = (e^{T^{(A)}})_{n-k} (22)$$

represents the (n-k)-body component of the CC wave operator $e^{T^{(A)}}$, defining the CC approximation A, $|\Psi_0\rangle$ is the exact ground-state wave function, and

$$M_{k}(m_{A})|\Phi\rangle \equiv Q_{k}\bar{H}^{(A)}|\Phi\rangle = \sum_{\substack{i_{1}<\dots< i_{k}\\a_{1}<\dots< a_{k}\\a_{1}<\dots< a_{k}}} \mathcal{M}_{a_{1}\dots a_{k}}^{i_{1}\dots i_{k}}(m_{A})|\Phi_{i_{1}\dots i_{k}}^{a_{1}\dots a_{k}}\rangle.$$
(23)

An elementary derivation of Eq. (21), based on applying the resolution of identity to an asymmetric energy expression, termed the MMCC functional, i.e.

$$\Lambda^{\rm CC}[\Psi] = \langle \Psi | (H - E_0^{(A)}) e^{T^{(A)}} | \Phi \rangle / \langle \Psi | e^{T^{(A)}} | \Phi \rangle , \qquad (24)$$

which gives the exact value of $\delta_0^{(A)}$ when $|\Psi\rangle$ is the full CI state $|\Psi_0\rangle$, is shown in Appendix A (the original proof is found in Appendix A of Ref. 46). An alternative derivation of Eq. (21), based on the analysis of the mathematical relationships between multiple solutions of nonlinear equations representing different CC approximations (CCSD, CCSDT, etc.), has been presented in Ref. 45.

Equation (21) is the basic equation of the MMCC formalism. According to this equation, we can obtain the exact full CI energy E_0 by determining the generalized moments $\mathcal{M}_{a_1...a_k}^{i_1...i_k}(m_A)$ with $k > m_A$ and by adding the resulting correction $\delta_0^{(A)}$, Eq. (21), to the CC energy $E_0^{(A)}$. In particular, we can use Eq. (21) to improve the results of the CCSD calculations (the $m_A = 2$ case). In this case, we must calculate moments $\mathcal{M}_{a_1...a_k}^{i_1...i_k}(2)$ with k = 3 - 6 (it can be shown that moments $\mathcal{M}_{a_1...a_k}^{i_1...i_k}(2)$ with k > 6 vanish) and use these moments to calculate the noniterative correction $\delta_0^{(\text{CCSD})}$ to the CCSD energy. According to Eq. (21), the explicit formula for the correction $\delta_0^{(\text{CCSD})}$ is

$$\delta_0^{(\text{CCSD})} \equiv E_0 - E_0^{(\text{CCSD})} = \sum_{n=3}^{N} \sum_{k=3}^{\min(n,6)} \langle \Psi_0 | Q_n \, C_{n-k}(2) \, M_k(2) | \Phi \rangle / \langle \Psi_0 | e^{T_1 + T_2} | \Phi \rangle \,, \quad (25)$$

where $E_0^{(CCSD)}$ is the CCSD energy, T_1 and T_2 are the singly and doubly excited cluster components obtained in the CCSD calculations,

$$C_{n-k}(2) = (e^{T_1 + T_2})_{n-k}, (26)$$

and

$$M_{k}(2)|\Phi\rangle = \sum_{\substack{i_{1}<\dots< i_{k}\\a_{1}<\dots< a_{k}}} \mathcal{M}_{a_{1}\dots a_{k}}^{i_{1}\dots i_{k}}(2)|\Phi_{i_{1}\dots i_{k}}^{a_{1}\dots a_{k}}\rangle, \quad k = 3-6,$$
(27)

with

$$\mathcal{M}_{a_{1}...a_{k}}^{i_{1}...i_{k}}(2) = \langle \Phi_{i_{1}...i_{k}}^{a_{1}...a_{k}} | (He^{T_{1}+T_{2}})_{C} | \Phi \rangle$$
 (28)

representing the generalized moments of the CCSD equations.

The exact MMCC corrections $\delta_0^{(A)}$, Eq. (21), or $\delta_0^{(\text{CCSD})}$, Eq. (25), have the form of the complete many-body expansions involving all n-tuply excited configurations with $n=m_A,\ldots,N$, where N is the number of electrons in a system (these n-tuply excited configurations are represented in Eqs. (21) and (25) by the projection operators Q_n). With an exception of very small few-electron systems, the complete many-body expansions of the type of Eq. (21) are not manageable. Thus, in order to come up with the practical MMCC schemes, based on Eqs. (21) or (25), we must truncate the many-body expansions for $\delta_0^{(A)}$ or $\delta_0^{(\text{CCSD})}$ at some reasonably low excitation level m_B . This leads to the so-called MMCC(m_A, m_B) schemes, in which we calculate the energy as follows: $^{45-47,51,52,87,132,133}$

$$E_0^{\text{MMCC}}(m_A, m_B) = E_0^{(A)} + \delta_0(m_A, m_B), \tag{29}$$

where the formula for $\delta_0(m_A, m_B)$ is

$$\delta_0(m_A, m_B) = \sum_{n=m_A+1}^{m_B} \sum_{k=m_A+1}^{n} \langle \Psi_0 | Q_n \, C_{n-k}(m_A) M_k(m_A) | \Phi \rangle / \langle \Psi_0 | e^{T^{(A)}} | \Phi \rangle. \tag{30}$$

Non-zero values of the correction $\delta_0(m_A,m_B)$ are obtained only when $m_B > m_A$.

When $m_B = N$ and when $|\Psi_0\rangle$ is exact, one obtains the exact MMCC theory described by Eq. (21). The renormalized and completely renormalized CCSD(T) and CCSD(TQ) methods mentioned in Sect. 1 are the MMCC(m_A , m_B) schemes with $m_A = 2$ and $m_B = 3$ (the CCSD(T) case) or $m_B = 4$ (the CCSD(TQ) case).

The only issue that has to be addressed before using Eqs. (29) and (30) in practice is the form of the wave function $|\Psi_0\rangle$ that enters the MMCC (m_A, m_B) energy expressions. The wave function $|\Psi_0\rangle$ that enters the formula for the exact correction $\delta_0^{(A)}$ or $\delta_0^{(CCSD)}$, Eqs. (21) and (25), respectively, is the full CI ground state, which we usually do not know. Thus, in order to propose computationally feasible approaches based on the MMCC theory, one must approximate $|\Psi_0\rangle$ with some inexpensive ab initio method. Several ways of approximating $|\Psi_0\rangle$ in the MMCC (m_A, m_B) energy expressions, Eqs. (29) and (30), are possible. The renormalized and completely renormalized CCSD(T) and CCSD(TQ) methods employ the low-order MBPT expressions to define $|\Psi_0\rangle$ in the MMCC(2,3) and MMCC(2,4) formulas.^{45-48,50,51,53,87,134,136} The CI-corrected MMCC approximations, 45,51,52,132-134 including the CI-corrected MMCC(2,6) approach developed in this work, use the wave functions $|\Psi_0\rangle$ originating from the limited CI calculations. Finally, the QMMCC methods, ¹³⁴⁻¹³⁷ also developed in this work, use the truncated forms of the exponential, CC-like, wave functions $|\Psi_0\rangle$. In general, it has been suggested that the wave functions $|\Psi_0\rangle$ used in the MMCC (m_A, m_B) formulas, Eqs. (29) and (30), do not contain higher-than- m_{B^-} tuply excited components relative to the reference $|\Phi\rangle$.

4. The Existing $\text{MMCC}(m_A, m_B)$ Approximations

We restrict our discussion to the MMCC(m_A , m_B) schemes with $m_A = 2$, which can be used to correct the results of the CCSD calculations. The MMCC($2,m_B$) energy expressions can be obtained by setting $m_A = 2$ in Eqs. (29) and (30) or by truncating the summation over n in the exact Eq. (25) at $n = m_B$. The simplest approximations belonging to the MMCC($2,m_B$) hierarchy are the MMCC($2,m_B$) and MMCC($2,m_B$) approaches. (45-53,132-134,136 They are obtained by setting $m_B = 3$ (the MMCC($2,m_B$) case) or $m_B = 4$ (the MMCC($2,m_B$) in Eqs. (29) and (30). In the MMCC($2,m_B$) approach, one computes the energy using the following expression:

$$E_0^{\text{MMCC}}(2,3) = E_0^{(\text{CCSD})} + \delta_0(2,3),$$
 (31)

where $E_0^{({
m CCSD})}$ is the CCSD energy and the correction $\delta_0(2,3)$ is defined as

$$\delta_0(2,3) = \langle \Psi_0 | Q_3 M_3(2) | \Phi \rangle / \langle \Psi_0 | e^{T_1 + T_2} | \Phi \rangle . \tag{32}$$

As in all MMCC(2, m_B) schemes, the T_1 and T_2 clusters entering Eq. (32) are obtained in the standard CCSD calculations. The $M_3(2)|\Phi\rangle$ quantities entering Eq. (32) are obtained using the formula,

$$M_3(2)|\Phi\rangle = \sum_{\substack{i_1 < i_2 < i_3 \\ a_1 < a_2 < a_3}} \mathcal{M}_{a_1 a_2 a_3}^{i_1 i_2 i_3}(2)|\Phi_{i_1 i_2 i_3}^{a_1 a_2 a_3}\rangle, \qquad (33)$$

where

$$\mathcal{M}_{a_1 a_2 a_3}^{i_1 i_2 i_3}(2) = \langle \Phi_{i_1 i_2 i_3}^{a_1 a_2 a_3} | (He^{T_1 + T_2})_C | \Phi \rangle, \tag{34}$$

represent the triply excited moments of the CCSD equations (the CCSD equations projected on the triply excited configurations $|\Phi_{i_1i_2i_3}^{a_1a_2a_3}\rangle$).

The MMCC(2,4) approach is an extension of the MMCC(2,3) scheme in which we use both the triply excited moments of the CCSD equations, $\mathcal{M}_{a_1 a_2 a_3}^{i_1 i_2 i_3}(2)$, Eq. (34), and the quadruply excited moments,

$$\mathcal{M}_{a_1 a_2 a_3 a_4}^{i_1 i_2 i_3 i_4}(2) = \langle \Phi_{i_1 i_2 i_3 i_4}^{a_1 a_2 a_3 a_4} | (He^{T_1 + T_2})_C | \Phi \rangle, \tag{35}$$

where $|\Phi_{i_1i_2i_3i_4}^{a_1a_2a_3a_4}\rangle$ are the quadruply excited configurations relative to $|\Phi\rangle$. The MMCC(2,4) energy is computed as follows:

$$E_0^{\text{MMCC}}(2,4) = E_0^{(\text{CCSD})} + \delta_0(2,4) \tag{36}$$

where

$$\delta_0(2,4) = \langle \Psi_0 | \{ Q_3 M_3(2) + Q_4 [M_4(2) + T_1 M_3(2)] \} | \Phi \rangle / \langle \Psi_0 | e^{T_1 + T_2} | \Phi \rangle. \tag{37}$$

The triexcited moments $\mathcal{M}_{a_1 a_2 a_3}^{i_1 i_2 i_3}(2)$ enter Eq. (37) through quantities $M_3(2)|\Phi\rangle$, defined by Eq. (33). The quadruply excited moments $\mathcal{M}_{a_1 a_2 a_3 a_4}^{i_1 i_2 i_3 i_4}(2)$ enter Eq. (37) through quantities $M_4(2)|\Phi\rangle$, which are defined as

$$M_4(2)|\Phi\rangle = \sum_{\substack{i_1 < i_2 < i_3 < i_4 \\ a_1 < a_2 < a_3 < a_4}} \mathcal{M}_{a_1 a_2 a_3 a_4}^{i_1 i_2 i_3 i_4}(2)|\Phi_{i_1 i_2 i_3 i_4}^{a_1 a_2 a_3 a_4}\rangle. \tag{38}$$

The explicit expressions for the triply and quadruply excited moments of the CCSD equations, $\mathcal{M}_{a_1a_2a_3}^{i_1i_2i_3}(2)$ and $\mathcal{M}_{a_1a_2a_3a_4}^{i_1i_2i_3i_4}(2)$, respectively, along with their higher-level pentuply and hextuply excited $\mathcal{M}_{a_1a_2a_3a_4a_5}^{i_1i_2i_3i_4i_5}(2)$ and $\mathcal{M}_{a_1a_2a_3a_4a_5a_6}^{i_1i_2i_3i_4i_5i_6}(2)$ counterparts, which will be needed to formulate the CI-corrected and quadratic MMCC(2,5) and MMCC(2,6) schemes (cf. Sect. 5), in terms of molecular integrals defining the Hamiltonian and cluster amplitudes defining T_1 and T_2 , are shown in Appendix C. These expressions are obtained by drawing all relevant Hugenholtz diagrams for the CCSD equations projected onto triply, quadruply, pentuply, and hextuply excited configurations, as shown in Appendix B.

Different types of the MMCC(2,3) and MMCC(2,4) approximations can be proposed by using different choices of $|\Psi_0\rangle$ in Eqs. (31)–(38). So far, only the CI-corrected MMCC(2,3) and MMCC(2,4) methods, in which the wave fuction $|\Psi_0\rangle$ is provided by the multireference, CI-like, CISDt and CISDtq calculations, respectively, and the renormalized and completely renormalized CCSD[T], CCSD(T), and CCSD(TQ) methods, in which the wave function $|\Psi_0\rangle$ is obtained from the second-order MBPT expressions, have been developed. The CI-corrected MMCC(2,3) and MMCC(2,4) methods are discussed in Sect. 4.1. The renormalized and completely renormalized CCSD[T], CCSD(T), and CCSD(TQ) methods are discussed in Sect. 4.2. In both cases, the mathematical and computational concepts are illustrated by examples of applications to molecular systems.

4.1. The CI-corrected MMCC(2,3) and MMCC(2,4) Methods

The CI-corrected MMCC(2,3) and MMCC(2,4) methods use simple forms of the wave functions $|\Psi_0\rangle$ in which higher-than-doubly excited components are defined through active orbitals. Thus, one uses the wave functions $|\Psi_0\rangle$ obtained in the active-space CISDt^{45,51,52} and CISDtq⁵² calculations, which provide the qualitatively correct description of bond breaking, to construct the $\delta_0(2,3)$ and $\delta_0(2,4)$ corrections to the CCSD energy. In order to define the CISDt and CISDtq wave functions $|\Psi_0\rangle$ for the MMCC(2,3) and MMCC(2,4) calculations, one divides the available spin-orbitals into core spin-orbitals (i₁, i₂, ...), active spin-orbitals occupied in the reference determinant $|\Phi\rangle$ (I₁, I₂, ...), active spin-orbitals unoccupied in $|\Phi\rangle$ (A₁, A₂, ...), and virtual spin-orbitals (a₁, a₂, ...) (see Fig. 1). Once the active orbitals are selected (typically, active orbitals correspond to the valence orbitals of a molecule), we define the CISDt and CISDtq wave functions $|\Psi_0\rangle$ as follows:^{45,51,52}

$$|\Psi_0^{\text{CISDt}}\rangle = (C_0 + C_1 + C_2 + c_3)|\Phi\rangle,$$
 (39)

$$|\Psi_0^{\text{CISDtq}}\rangle = (C_0 + C_1 + C_2 + c_3 + c_4)|\Phi\rangle,$$
 (40)

where $C_0|\Phi\rangle$, $C_1|\Phi\rangle$, and $C_2|\Phi\rangle$ are the reference, singly excited, and doubly excited components of $|\Psi_0^{\text{CISDt}}\rangle$ and $|\Psi_0^{\text{CISDtq}}\rangle$ and

$$c_3|\Phi\rangle = \sum_{\substack{\mathbf{I_1}>i_2>i_3\\a_1>a_2>\mathbf{A_3}}} c_{\mathbf{I_1}i_2i_3}^{a_1a_2\mathbf{A_3}} |\Phi_{\mathbf{I_1}i_2i_3}^{a_1a_2\mathbf{A_3}}\rangle, \qquad (41)$$

$$c_{4}|\Phi\rangle = \sum_{\substack{\mathbf{I}_{1} > \mathbf{I}_{2} > i_{3} > i_{4} \\ a_{1} > a_{2} > \mathbf{A}_{8} > \mathbf{A}_{4}}} c_{\mathbf{I}_{1} \mathbf{I}_{2} i_{3} i_{4}}^{a_{1} a_{2} \mathbf{A}_{8} \mathbf{A}_{4}} |\Phi_{\mathbf{I}_{1} \mathbf{I}_{2} i_{3} i_{4}}^{a_{1} a_{2} \mathbf{A}_{8} \mathbf{A}_{4}} \rangle.$$
(42)

As one can see, the CISDt wave function $|\Psi_0^{\text{CISDt}}\rangle$, Eq. (39), which is used to calculate the $\delta_0(2,3)$ correction of the CI-corrected MMCC(2,3) method is a limited CI wave function including all singles and doubles from $|\Phi\rangle$ and a relatively small set of internal and semi-internal triples containing at least one active occupied and one active unoccupied spin-orbital index (cf. Eq. (41)). The CISDtq wave function $|\Psi_0^{\text{CISDtq}}\rangle$, Eq. (40), which is used to construct the correction $\delta_0(2,4)$ of the CI-corrected MMCC(2,4) approach, is obtained by including all singles and doubles from $|\Phi\rangle$, a relatively small set of internal and semi-internal triples containing at least one active occupied and one active unoccupied spin-orbital index, and a relatively small set of quadruples containing at least two active occupied and at least two active unoccupied spin-orbital indices (cf. Eqs. (41) and (42)). The CI coefficients that define the CISDt and CISDtq wave functions are determined variationally.

There are two main factors contributing to the relatively low computer costs of the CI-corrected MMCC(2,3) and MMCC(2,4) calculations: (1) the use of active orbitals in the process of constructing the CISDt and CISDtq wave functions $|\Psi_0\rangle$ and (2) the noniterative character of the $\delta_0(2,3)$ and $\delta_0(2,4)$ corrections. The most expensive steps in the CISDt and CISDtq methods scale as $N_o N_u n_o^2 n_u^4$ and $N_o^2 N_u^2 n_o^2 n_u^4$, respectively $(N_o \ (N_u)$ is the number of active orbitals occupied (unoccupied) in $|\Phi\rangle$). Since N_o and N_u are typically much smaller than n_o and n_u , respectively, the costs of the CISDt and CISDtq calculations represent a small fraction of the parent CISDT (CI

singles, doubles, and triples) and CISDTQ (CI singles, doubles, triples, and quadruples) calculations. In fact, the CISDt and CISDtq calculations are often only a few times more expensive than the CCSD or CISD calculations. Thus, the use of a small set of triples and quadruples in the CISDt and CISDtq calculations greatly reduces the cost of the CI-corrected MMCC(2,3) and MMCC(2,4) calculations. The storage requirements for the CISDt and CISDtq calculations are also greatly reduced because only small fractions of the total numbers of triples and quadruples are being used when the number of active orbitals is small. The numbers of triples and quadruples considered in the CISDt and CISDtq calculations are $N_o N_u n_o^2 n_u^2$ and $N_o^2 N_u^2 n_o^2 n_u^2$, respectively, which is much less than the total number of triples and quadruples $(n_o^3 n_u^3)$ and $(n_o^4 n_u^4)$, respectively).

Once the wave functions $|\Psi_0^{\text{CISDt}}\rangle$ and $|\Psi_0^{\text{CISDtq}}\rangle$ are obtained by performing the variational CISDt and CISDtq calculations, one has to construct the corrections $\delta_0(2,3)$ and $\delta_0(2,4)$ using Eqs. (32) and (37). The costs of constructing the $\delta_0(2,3)$ and $\delta_0(2,4)$ corrections, which normally are $n_o^3 n_u^4$ and $n_o^2 n_u^5$, respectively, are reduced further when one uses the CISDt (the MMCC(2,3) case) and CISDtq (the MMCC(2,4) case) wave functions $|\Psi_0\rangle$ since only the generalized moments of the CCSD equations corresponding to projections of these equations on the internal and semi-internal triples and quadruples present in the CISDt and CISDtq wave functions have to be considered.

The CI-corrected MMCC(2,3) and MMCC(2,4) approaches were tested by us by calculating the PESs for the single bond breaking in the HF molecule and the simultaneous dissociation of the two O-H bonds in the H₂O molecule.⁵² We used the

RHF reference and a DZ¹⁴¹ basis set (see Tables 1 and 2). The active spaces used to define the CISDt and CISDtq wave functions employed in these tests were the 3σ , 1π , 2π , and 4σ orbitals for the HF molecule and the $1b_1$, $3a_1$, $1b_2$, $4a_1$, $2b_1$, and 2b₂ orbitals for the H₂O molecule. In other words, we used small numbers of active orbitals resulting from the valence shells of the relevant H, F, and O atoms. In the case of the HF molecule (see Table 1), the 1.634 millihartree error in the CCSD result relative to full CI at the equilibrium geometry, $R=R_{\rm e}=1.7328$ bohr (R is the H-F internuclear separation), which increases to 12.291 millihartree in the dissociation region $(R = 5R_e)$, is reduced to 1.195 millihartree at $R = R_e$ and to 3.255 millihartree at $R = 5R_e$, when the CI-corrected MMCC(2,3) approach is employed, and to 1.207 and 3.066 millihartree at $R = R_e$ and $R = 5R_e$, respectively, when the CI-corrected MMCC(2,4) calculation is performed. In the $R=R_{\rm e}-2R_{\rm e}$ region, the CCSD[T], CCSD(T), and CCSD(TQ_f) methods, which represent standard ways of correcting the CCSD energies for the effects of triples and quadruples, perform quite well. However, once the H-F bond is significantly stretched $(R \geq 3R_e)$, the errors resulting from the CCSD[T], CCSD(T), and CCSD(TQ_f) calculations dramatically increase. For example, the CCSD(T) and CCSD(TQ_f) methods produce large negative errors of -53.183 and -35.078 millihartree, respectively, at $R = 5R_e$. The CI-corrected MMCC(2,3) and MMCC(2,4) approaches are capable of reducing these large errors to a few millihartree.

Interestingly enough, the CISDt method itself is not capable of providing a quantitative description of the bond breaking in HF. The 16–34 millihartree errors in the CISDt calculations in the $R>2R_e$ region are substantial. In spite of the poor perfor-

mance of the CISDt method, the CISDt-corrected MMCC(2,3) results are excellent when the H-F bond is broken. This indicates the robust nature of the MMCC energy corrections. We can use a relatively poor source of the wave function $|\Psi_0\rangle$ in constructing the MMCC corrections δ and yet obtain excellent results for bond breaking when the MMCC corrections δ are added to the (also poor) CCSD energies.

One of the reasons for the very good performance of the MMCC approximations in the bond breaking region is the presence of the $\langle \Psi_0|e^{T_1+T_2}|\Phi\rangle$ denominator in the MMCC(2,3) and MMCC(2,4) energy expressions. These denominators increase with R, damping the unphysically large negative triples corrections of the CCSD(T) and similar approximations. For example, the CISDt $\langle \Psi_0|e^{T_1+T_2}|\Phi\rangle$ denominator ranges from \sim 1.0 at $R=R_e$ to 2.3–2.4 at $R=5R_e$ in the case of HF.

The HF molecule represents a case where T_4 clusters play a very small role so that the CISDt-corrected MMCC(2,3) approach, which describes the effects due to singles, doubles, and triples only, suffices. The CISDtq-corrected MMCC(2,4) results are not much more accurate than the CISDt-corrected MMCC(2,3) results in the HF case. Let us, therefore, examine the performance of the CI-corrected MMCC(2,3) and MMCC(2,4) methods in the case of the double dissociation of H_2O , where both the T_3 and T_4 clusters play a significant role (cf. the CCSDT – CCSD and CCSDTQ – CCSDT differences in Table 2, which are -11.544 and 2.319 millihartree, respectively at $R = 2R_e$; R is the O-H bond length).

The standard noniterative CC approximations such as the CCSD[T], CCSD(T), and CCSD(TQ_f) are incapable of dealing with the large T_3 and T_4 effects characterizing the situation where both O-H bonds in H₂O are stretched by a factor of 2 (the

 $R=2R_e$ case in Table 2). Indeed, the unsigned errors in the CCSD[T], CCSD(T), and CCSD(TQ_f) results, relative to full CI, are 11.220, 7.699, and 5.914 millihartree, respectively, at $R=2R_e$. Only the complete inclusion of the T_3 and T_4 clusters via the expensive CCSDTQ method reduces the error at $R=2R_e$ to 0.108 millihartree. The full CCSDT approach produces a negative, -2.211 millihartree, error at this geometry, which is an indication of the breakdown of the CCSDT method in the $R>2R_e$ region, due to the lack of important T_4 clusters. The CCSD[T], CCSD(T), and CCSD(TQ_f), work well in the $R \leq 1.5R_e$ region, but they give large negative errors at $R=2R_e$, which is an indication of the complete breakdown of these methods when both O-H bonds in H₂O are broken.

The CI-corrected MMCC(2,3) and MMCC(2,4) approximations provide excellent results at stretched geometries of H_2O , when compared to the standard CC approaches, such as CCSD[T], CCSD(T), and CCSD(TQ_f). In fact, the simplest CISDt-corrected MMCC(2,3) method, which requires a very small computer effort in the process of constructing the triples energy correction $\delta_0(2,3)$, outperforms the expensive full CCSDT approach at $R=2R_e$. With the choice of the active orbitals mentioned earlier (the three highest-energy occupied orbitals, $1b_1$, $3a_1$, and $1b_2$, and the three lowest-energy unoccupied orbitals, $4a_1$, $2b_1$, and $2b_2$), the description of the entire $R=R_e-2R_e$ region by the CISDt-corrected MMCC(2,3) approximation is excellent, in spite of the poor performance of the underlying CISDt approach. The MMCC(2,3) method reduces the large \sim 19 millihartree error in the CISDt result at $R=1.5R_e$ and the huge \sim 50 millihartree error in the CISDt energy at $R=2R_e$, to the very small 2.407 and 1.631 millihartree errors, respectively.

The CI-corrected MMCC(2,4) approach offers a more balanced description of the simultaneous breaking of both O-H bonds in H₂O, when compared to the CI-corrected MMCC(2,3) method. Indeed, the errors in the CI-corrected MMCC(2,3) results initially increase, from \sim 0.8 millihartree at $R=R_{\rm e}$ to \sim 2.5 millihartree at $R=1.5R_{\rm e}$, and then decrease to \sim 1.6 millihartree at $R=2R_{\rm e}$. This might be the first sign of the breakdown of the CI-corrected MMCC(2,3) approximation at very large distances R due to the lack of T_4 corrections in the MMCC(2,3) energy expressions. This behavior should be contrasted with the slow and monotonic increase of errors in the CI-corrected MMCC(2,4) results with increasing R (from 0-5 millihartree at $R=R_{\rm e}$ to 2.416 millihartree at $R=2R_{\rm e}$).

The excellent performance of the CISDtq-based MMCC(2,4) approach in the calculations for double bond breaking in H_2O is due to several factors. One of the factors is the fact that the CISDtq method, which is used to construct the wave function $|\Psi_0\rangle$ entering the MMCC(2,4) energy expressions, provides a much better description of the simultaneous breaking of both O-H bonds in H_2O than the CISDt method used in the MMCC(2,3) calculations (see Table 2). The incorporation of the quadruply excited moments of the CCSD equations in the MMCC(2,4) calculations provides improvements, too, particularly in the $R > 1.5R_e$ region. As already mentioned, one of the strengths of the MMCC(2,3), MMCC(2,4), and similar methods is the ability of these approaches to produce excellent results even when the wave functions $|\Psi_0\rangle$ that are used to construct the relevant energy corrections are themselves rather poor. In the case of double dissociation of H_2O , this is particularly true for the CISDt-corrected MMCC(2,3) method. Another factor that helps to improve the

MMCC(2,3) and MMCC(2,4) results at stretched nuclear geometries is the presence of the $\langle \Psi_0 | \mathrm{e}^{T_1 + T_2} | \Phi \rangle$ denominators in the MMCC(2,3) and MMCC(2,4) energy expressions. In the case of double bond breaking in H₂O, these denominators increase their values from ~1.0 at $R = R_{\mathrm{e}}$ to 1.5–1.7 at $R = 2R_{\mathrm{e}}$. Without these denominators, the MMCC(2,3) and MMCC(2,4) results would be almost as bad as the CCSD(T) and CCSD(TQ_f) results.

We also tested the CI-corrected MMCC(2,3) and MMCC(2,4) methods in the calculations for N_2 , which is the most difficult case involving triple bond breaking (see Table 3 and Fig. 2). The active orbitals used by us in the CI-corrected MMCC calculations included the $3\sigma_g$, $1\pi_u$, $2\pi_u$, $1\pi_g$, $2\pi_g$, and $3\sigma_u$ orbitals correlating with the 2p shells of the N atoms. As in the case of HF and H_2O , we used the DZ basis set, for which the exact full CI energies are available.⁴⁷

The N₂ molecule is an example of the catastrophic failure of all standard single-reference CC methods. The standard CCSD(T), CCSD(TQ_f), CCSDT, and CCSDT(Q_f) methods work well in the equilibrium, $R = R_e$, region, providing errors as low as 0.323 and 0.010 millihartree at $R = R_e$ when the CCSD(TQ_f) and CCSDT(Q_f) methods are employed, but at $R = 2R_e$ or $R > 2R_e$ the results of the standard CC calculations are disastrous. The CCSD(T) method provides a curve that goes hundreds of millihartree below the full CI curve (similarly for the CCSD curve). The CCSD(TQ_f) and CCSDT(Q_f) approaches, which include triples and quadruples, produce curves that go hundreds of millihartree above the full CI curve in the $R > 1.75R_e$ region. The CISDt-corrected MMCC(2,3) approximation reduces these large errors somewhat, but the MMCC(2,3) curve at larger R values is com-

pletely unphysical. Clearly, one needs higher-than-triply excited clusters to obtain a better description of the N_2 curve. The corrections due to T_4 clusters are present in the CISDtq-corrected MMCC(2,4) method, but they are insufficient to provide a high quality curve for N_2 . The CISDtq-corrected MMCC(2,4) curve is clearly much better than all other curves provided by the standard CC methods, but the (-16) – (-31) millihartree negative errors in the results of the CISDtq-corrected MMCC(2,4) calculations in the $R \geq 2R_e$ region indicate the need for the inclusion of the effects due to higher-than-quadruply excited determinants in the CI-corrected MMCC calculations, if we are to achieve a highly accurate description of triple bond breaking by the MMCC theory. New classes of the MMCC methods that can handle triple bond stretching or breaking will be discussed in Sect. 5.

In summary, the CI-corrected MMCC(2,3) and MMCC(2,4) methods work very well for single and double bond breaking, but they are not sufficiently accurate to provide a good description of triple bond breaking. For cases involving single or double bond dissociations, they are capable of eliminating the failures of the CCSD(T), CCSD(TQ_f), and CCSDT(Q_f) methods by reducing large errors in the standard single-reference CC calculations to a few millihartree, but they are not capable of handling more complicated cases of multiple bond breaking. The CI-corrected MMCC(2,3) and MMCC(2,4) methods are capable of providing excellent results in spite of the use of the rather inaccurate CI approximations to construct the relevant corrections $\delta_0(2,3)$ and $\delta_0(2,4)$. This stresses the robust nature of the MMCC theory. Although the CI-corrected MMCC(2,3) and MMCC(2,4) approximations are capable of providing high quality results, they require performing the a priori CI calculations

and choosing active orbitals. The MMCC(2,3) and MMCC(2,4) methods that provide results of similar quality for single and double bond breaking, but which do not require performing any additional calculations or choosing active orbitals, are discussed next.

4.2. The Renormalized and Completely Renormalized CCSD[T], CCSD(T), and CCSD(TQ) Methods

In the renormalized and completely renormalized CC methods, the low-order MBPT expressions are used to define the wave function $|\Psi_0\rangle$ in the MMCC (m_A, m_B) energy formulas. $^{45-51,53,134-138}$ Thus, in the renormalized and completely renormalized CCSD[T], CCSD(T), and CCSD(TQ) methods, MBPT(2)-like (second-order MBPT-like) wave functions $|\Psi_0\rangle$ are combined with the MMCC(2,3) and MMCC(2,4) approximations introduced earlier (cf. Eqs. (31) and (36)). Just as their standard CCSD[T], CCSD(T), and CCSD(TQ_f) counterparts, the renormalized and completely renormalized CCSD[T], CCSD(T), and CCSD(TQ) approaches can be used to correct the results of the CCSD calculations through simple noniterative corrections. The difference between the standard and renormalized or completely renormalized CC methods is that only the latter methods can be used to study bond breaking.

The completely renormalized CCSD(T) method (the CR-CCSD(T) approach), which is the basic renormalized CC approximation, is an example of the MMCC(2,3) scheme, in which the wave function $|\Psi_0\rangle$ is replaced by the very simple, MBPT(2)[SDT]-

like, expression,

$$|\Psi^{\text{CCSD(T)}}\rangle = (1 + T_1 + T_2 + T_3^{[2]} + Z_3)|\Phi\rangle,$$
 (43)

where T_1 and T_2 are the singly and doubly excited clusters obtained by solving the CCSD equations, the $T_3^{[2]}$ term,

$$T_3^{[2]}|\Phi\rangle = R_0^{(3)}(V_N T_2)_C |\Phi\rangle,\tag{44}$$

in Eq. (43) is a CCSD analog of the connected triples contribution to the MBPT(2) wave function, and

$$Z_3|\Phi\rangle = R_0^{(3)} V_N T_1 |\Phi\rangle \tag{45}$$

is the disconnected triples correction that is needed to distinguish between the (T) triples corrections and the [T] corrections due to triples discussed below. In the above expressions, $R_0^{(3)}$ designates the three-body component of the MBPT reduced resolvent and V_N represents the two-body part of the Hamiltonian in the normal-ordered form. The energy formula defining the CR-CCSD(T) method is (cf. Eq. (32))^{45-48,50,51,53,134,136,138}

$$E_0^{\text{CR-CCSD(T)}} = E_0^{(\text{CCSD})} + \langle \Psi^{\text{CCSD(T)}} | Q_3 M_3(2) | \Phi \rangle / \langle \Psi^{\text{CCSD(T)}} | e^{T_1 + T_2} | \Phi \rangle, \tag{46}$$

where $E_0^{(\text{CCSD})}$ is the CCSD energy, $|\Psi^{\text{CCSD}(T)}\rangle$ is defined by Eq. (43), and $M_3(2)|\Phi\rangle$ is the quantity defined in terms of triexcited moments $\mathcal{M}_{a_1 a_2 a_3}^{i_1 i_2 i_3}(2)$, as shown in Eq. (33). One can also consider the completely renormalized CCSD[T] method (the CR-

CCSD[T] approach), in which $|\Psi_0\rangle$ in the MMCC(2,3) energy expression is replaced by another MBPT(2)[SDT]-like wave function,

$$|\Psi^{\text{CCSD[T]}}\rangle = (1 + T_1 + T_2 + T_3^{[2]})|\Phi\rangle,$$
 (47)

where $T_3^{[2]}$ is defined by Eq. (44). The only difference between the wave functions $|\Psi^{\text{CCSD[T]}}\rangle$ and $|\Psi^{\text{CCSD(T)}}\rangle$ is in the $Z_3|\Phi\rangle$ term, Eq. (45), which appears in the CR-CCSD(T) theory, but is not included in the CR-CCSD[T] approach. The CR-CCSD[T] energy expression is (cf. Eq. (32))^{45-48,50,51,53,134,136,138}

$$E_0^{\text{CR-CCSD[T]}} = E_0^{(\text{CCSD})} + \langle \Psi^{\text{CCSD[T]}} | Q_3 M_3(2) | \Phi \rangle / \langle \Psi^{\text{CCSD[T]}} | e^{T_1 + T_2} | \Phi \rangle. \tag{48}$$

Typically, the CR-CCSD(T) method provides somewhat better and more balanced results than the CR-CCSD[T] approach (cf. Tables 1 and 2). It is important, however, to discuss the CR-CCSD[T] theory to understand the connection between the CR-CC methods and their higher-order QMMCC counterparts.

In addition to the CR-CCSD[T] and CR-CCSD(T) methods, it is worth considering the renormalized CCSD[T] and CCSD(T) approaches (the R-CCSD[T] and R-CCSD(T) approaches). The R-CCSD[T] and R-CCSD(T) methods are obtained by replacing the $\mathcal{M}_{a_1a_2a_3}^{i_1i_2i_3}(2)$ moments in the CR-CCSD[T] and CR-CCSD(T) formulas, Eqs. (48) and (46), respectively, by their lowest-order estimates, i.e. $\langle \Phi_{i_1i_2i_3}^{a_1a_2a_3}|(V_NT_2)_C|\Phi\rangle$. The R-CCSD[T] and R-CCSD(T) energies are defined as follows: $^{45-48,50,51,53,134}$

$$E_0^{\text{R-CCSD[T]}} = E_0^{\text{(CCSD)}} + \langle \Psi^{\text{CCSD[T]}} | Q_3 (V_N T_2)_C | \Phi \rangle / \langle \Psi^{\text{CCSD[T]}} | e^{T_1 + T_2} | \Phi \rangle, \qquad (49)$$

$$E_0^{\text{R-CCSD(T)}} = E_0^{\text{(CCSD)}} + \langle \Psi^{\text{CCSD(T)}} | Q_3 (V_N T_2)_C | \Phi \rangle / \langle \Psi^{\text{CCSD(T)}} | e^{T_1 + T_2} | \Phi \rangle. \tag{50}$$

In practice, the calculations of PESs involving bond breaking require using the CR-CCSD[T] and CR-CCSD(T) methods rather than their simplified R-CCSD[T] and R-CCSD(T) versions. 45,46,48,50,51,53,134 However, the R-CCSD[T] and R-CCSD(T) approaches allow us to understand the relationship between the standard and completely renormalized CC approaches.

The relationship between the CCSD(T) (or CCSD[T]) and CR-CCSD(T) (or CR-CCSD[T]) approaches can be best understood by rewriting the CR-CCSD[T], CR-CCSD(T), R-CCSD[T], and R-CCSD(T) energies, Eqs. (48), (46), (49), and (50), respectively, in the following form: ^{134,138}

$$E_0^{\text{CR-CCSD[T]}} = E_0^{(\text{CCSD})} + N^{\text{CR[T]}}/D^{[\text{T}]},$$
 (51)

$$E_0^{\text{CR-CCSD(T)}} = E_0^{(\text{CCSD})} + N^{\text{CR(T)}}/D^{(\text{T})},$$
 (52)

$$E_0^{\text{R-CCSD[T]}} = E_0^{\text{(CCSD)}} + N^{\text{[T]}}/D^{\text{[T]}},$$
 (53)

$$E_0^{\text{R-CCSD(T)}} = E_0^{(\text{CCSD})} + N^{(\text{T})}/D^{(\text{T})},$$
 (54)

where the $N^{CR[T]}$, $N^{CR(T)}$, $N^{[T]}$, and $N^{(T)}$ numerators, entering the above expressions,

are defined as

$$N^{\text{CR[T]}} = \langle \Phi | (T_3^{[2]})^{\dagger} M_3(2) | \Phi \rangle,$$
 (55)

$$N^{\text{CR(T)}} = N^{\text{CR[T]}} + \langle \Phi | (Z_3)^{\dagger} M_3(2) | \Phi \rangle, \tag{56}$$

$$N^{[T]} = \langle \Phi | (T_3^{[2]})^{\dagger} (V_N T_2)_C | \Phi \rangle, \tag{57}$$

$$N^{(T)} = N^{[T]} + \langle \Phi | (Z_3)^{\dagger} (V_N T_2)_C | \Phi \rangle, \tag{58}$$

and the $D^{[T]}$ and $D^{(T)}$ denominators, representing the overlaps between $|\Psi^{\text{CCSD}[T]}\rangle$ and $|\Psi^{\text{CCSD}(T)}\rangle$ and the CCSD ground state, are calculated as

$$D^{[T]} \equiv \langle \Psi^{\text{CCSD[T]}} | e^{T_1 + T_2} | \Phi \rangle = 1 + \langle \Phi | T_1^{\dagger} T_1 | \Phi \rangle + \langle \Phi | T_2^{\dagger} \left(T_2 + \frac{1}{2} T_1^2 \right) | \Phi \rangle$$
$$+ \langle \Phi | \left(T_3^{[2]} \right)^{\dagger} \left(T_1 T_2 + \frac{1}{6} T_1^3 \right) | \Phi \rangle, \tag{59}$$

$$D^{(T)} \equiv \langle \Psi^{CCSD(T)} | e^{T_1 + T_2} | \Phi \rangle = D^{[T]} + \langle \Phi | Z_3^{\dagger} (T_1 T_2 + \frac{1}{6} T_1^3) | \Phi \rangle.$$
 (60)

The $N^{[T]}$ and $N^{(T)}$ numerators defining the R-CCSD[T] and R-CCSD(T) energies, Eqs. (53) and (54), respectively, are related to the noniterative triples corrections

$$E_{\rm T}^{[4]} = \langle \Phi | (T_3^{[2]})^{\dagger} (V_N T_2)_C | \Phi \rangle, \tag{61}$$

and

$$E_{\rm ST}^{[5]} = \langle \Phi | (Z_3)^{\dagger} (V_N T_2)_C | \Phi \rangle, \tag{62}$$

defining the standard CCSD[T] and CCSD(T) energies, 30,33,31

$$E_0^{\text{CCSD[T]}} = E_0^{\text{(CCSD)}} + E_T^{[4]}, \tag{63}$$

and

$$E_0^{\text{CCSD(T)}} = E_0^{\text{CCSD[T]}} + E_{\text{ST}}^{[5]} = E_0^{\text{(CCSD)}} + E_{\text{T}}^{[4]} + E_{\text{ST}}^{[5]}, \tag{64}$$

respectively. We can write

$$N^{[T]} = E_T^{[4]}, (65)$$

$$N^{(T)} = E_T^{[4]} + E_{ST}^{[5]}. (66)$$

One can clearly see from the above equations that the R-CCSD[T] and R-CCSD(T) approximations, which are obtained by simplifying the CR-CCSD[T] and CR-CCSD(T) methods, reduce to the standard CCSD[T] and CCSD(T) approaches, when the $D^{[T]}$ and $D^{(T)}$ denominators in Eqs. (49) and (50) or (53) and (54) are replaced by 1. The approximation of the $D^{[T]}$ and $D^{(T)}$ denominators by 1 is a justified step from the point of view of MBPT, since both denominators equal 1 plus terms which are at least of the second order in perturbation V_N (see Eqs. (59) and (60); the lowest-order $T_2^{\dagger}T_2$ term (excluding 1) in Eqs. (59) and (60) is at least of the second order in V_N). The presence of the $D^{[T]}$ and $D^{(T)}$ denominators in Eqs. (51)-(54) is not important at equilibrium geometries, where these denominators are usually very close to 1. However, these denominators are essential for improving the results of the standard CC calculations in the bond breaking region. In the bond breaking region, the values of $D^{[T]}$ and $D^{(T)}$ are significantly greater than 1, damping the excessively large negative triples corrections to the CCSD energies, which cause the failures of the standard CCSD[T] and CCSD(T) approximations at larger internuclear separations. 46,47

From the above analysis, it follows that the R-CCSD[T], R-CCSD(T), CR-CCSD[T], and CR-CCSD(T) methods can be viewed as the MMCC-based extensions of the standard CCSD[T] and CCSD(T) approaches. Very similar extensions can be formulated for other noniterative CC approaches. For example, one can use the MMCC formalism to renormalize the CCSD(TQ_f) method of Ref. 34, in which the correction due to the combined effect of triples and quadruples is added to the CCSD energy. The resulting completely renormalized CCSD(TQ) (CR-CCSD(TQ)) approaches are examples of the MMCC(2,4) approximation, defined by Eq. (36). As in the case of the CR-CCSD[T] and CR-CCSD(T) methods, one uses MBPT(2)-like expressions to define the wave function $|\Psi_0\rangle$ in the CR-CCSD(TQ) energy formulas (this time, however, we include the leading terms due to triples as well as quadruples in $|\Psi_0\rangle$). Two variants of the CR-CCSD(TQ) method, labeled by extra letters "a" and "b", are particularly useful. The CR-CCSD(TQ),a and CR-CCSD(TQ),b energies are defined as follows: 45-48,50,51,134,136

$$E_0^{\text{CR-CCSD(TQ)},x} = E_0^{(\text{CCSD})} + \langle \Psi^{\text{CCSD(TQ)},x} | \{ Q_3 M_3(2) + Q_4 [T_1 M_3(2) + M_4(2)] \} | \Phi \rangle /$$

$$\langle \Psi^{\text{CCSD(TQ)},x} | e^{T_1 + T_2} | \Phi \rangle \quad (x = a, b), \tag{67}$$

where $M_3(2)|\Phi\rangle$ and $M_4(2)|\Phi\rangle$ are the quantities expressed in terms of the triply and quadruply excited moments $\mathcal{M}_{a_1a_2a_3}^{i_1i_2i_3}(2)$ and $\mathcal{M}_{a_1a_2a_3a_4}^{i_1i_2i_3i_4}(2)$, respectively, according to

Eqs. (33) and (38).

$$|\Psi^{\text{CCSD(TQ)},a}\rangle = |\Psi^{\text{CCSD(T)}}\rangle + \frac{1}{2}T_2T_2^{(1)}|\Phi\rangle, \tag{68}$$

and

$$|\Psi^{\text{CCSD(TQ)},b}\rangle = |\Psi^{\text{CCSD(T)}}\rangle + \frac{1}{2}T_2^2|\Phi\rangle,$$
 (69)

are the relevant MBPT(2)[SDTQ]-like wave functions that enter the CR-CCSD(TQ), a and CR-CCSD(TQ), b corrections to CCSD energy. The $|\Psi^{\text{CCSD}(T)}\rangle$ wave function entering Eqs. (68) and (69) is given by Eq. (43), and the $T_2^{(1)}$ operator entering Eq. (68) is the first-order MBPT estimate of the cluster operator T_2 . In analogy to the CR-CCSD[T] and CR-CCSD(T) methods, one can rewrite the formulas for the CR-CCSD(TQ), a and CR-CCSD(TQ), b energies, Eq. (67), in a more compact form:

$$E_0^{\text{CR-CCSD(TQ)},x} = E_0^{(\text{CCSD})} + N^{\text{CR(TQ)},x} / D^{(\text{TQ)},x} \quad (x = a, b),$$
 (70)

where

$$N^{\text{CR(TQ)},a} = N^{\text{CR(T)}} + \frac{1}{2} \langle \Phi | T_2^{\dagger} (T_2^{(1)})^{\dagger} [T_1 M_3(2) + M_4(2)] | \Phi \rangle, \tag{71}$$

$$N^{\text{CR(TQ),b}} = N^{\text{CR(T)}} + \frac{1}{2} \langle \Phi | (T_2^{\dagger})^2 [T_1 M_3(2) + M_4(2)] | \Phi \rangle, \tag{72}$$

$$D^{(TQ),a} = \langle \Psi^{CCSD(TQ),a} | e^{T_1 + T_2} | \Phi \rangle$$

$$= D^{(T)} + \frac{1}{2} \langle \Phi | T_2^{\dagger} (T_2^{(1)})^{\dagger} (\frac{1}{2} T_2^2 + \frac{1}{2} T_1^2 T_2 + \frac{1}{24} T_1^4) | \Phi \rangle, \tag{73}$$

and

$$D^{(TQ),b} = \langle \Psi^{CCSD(TQ),b} | e^{T_1 + T_2} | \Phi \rangle$$

$$= D^{(T)} + \frac{1}{2} \langle \Phi | (T_2^{\dagger})^2 (\frac{1}{2} T_2^2 + \frac{1}{2} T_1^2 T_2 + \frac{1}{24} T_1^4) | \Phi \rangle, \tag{74}$$

with $N^{\text{CR}(\text{T})}$ and $D^{(\text{T})}$ defined by Eqs. (56) and (60), respectively. One can also introduce the renormalized CCSD(TQ) (R-CCSD(TQ)) methods by considering the lowest-order estimates of the $\mathcal{M}_{a_1 a_2 a_3}^{i_1 i_2 i_3}(2)$ and $\mathcal{M}_{a_1 a_2 a_3 a_4}^{i_1 i_2 i_3 i_4}(2)$ moments, which enter Eq. (67) via quantities $M_3(2)|\Phi\rangle$ and $M_4(2)|\Phi\rangle$, and by dropping the higher-order $T_1 M_3(2)$ term in Eq. (67). Several types of the R-CCSD(TQ) methods can be considered. (67). Several types of the R-CCSD(TQ) methods, one replaces $\mathcal{M}_{a_1 a_2 a_3}^{i_1 i_2 i_3}(2)$ by $\langle \Phi_{i_1 i_2 i_3}^{a_1 a_2 a_3}|(V_N T_2)_C|\Phi\rangle$ and $\mathcal{M}_{a_1 a_2 a_3 a_4}^{i_1 i_2 i_3 i_4}(2)$ by $\langle \Phi_{i_1 i_2 i_3 i_4}^{a_1 a_2 a_3 a_4}|[V_N(\frac{1}{2}T_2^2 + T_3^{[2]})]_C|\Phi\rangle$, where $T_3^{[2]}$ is defined by Eq. (44). In the R-CCSD(TQ)-2,x methods, one replaces $\mathcal{M}_{a_1 a_2 a_3}^{i_1 i_2 i_3}(2)$ by $\langle \Phi_{i_1 i_2 i_3}^{a_1 a_2 a_3}|[V_N(T_2 + \frac{1}{2}T_2^2)]_C|\Phi\rangle$ and $\mathcal{M}_{a_1 a_2 a_3 a_4}^{i_1 i_2 i_3 i_4}(2)$ by $\langle \Phi_{i_1 i_2 i_3 i_4}^{a_1 a_2 a_3 a_4}|(\frac{1}{2}V_N T_2^2)_C|\Phi\rangle$. For example, the R-CCSD(TQ)-1,x energies, x = a, b, are calculated as follows:

$$E_0^{\text{R-CCSD(TQ)-1,x}} = E_0^{\text{(CCSD)}} + N^{\text{(TQ)-1,x}} / D^{\text{(TQ),x}} \quad (x = a, b),$$
 (75)

where

$$N^{(\text{TQ})-1,a} = N^{(\text{T})} + \frac{1}{2} \langle \Phi | T_2^{\dagger} (T_2^{(1)})^{\dagger} [V_N(\frac{1}{2}T_2^2 + T_3^{[2]})]_C | \Phi \rangle, \tag{76}$$

and

$$N^{(\text{TQ})-1,b} = N^{(\text{T})} + \frac{1}{2} \langle \Phi | (T_2^{\dagger})^2 [V_N(\frac{1}{2}T_2^2 + T_3^{[2]})]_C | \Phi \rangle, \tag{77}$$

with $N^{(T)}$ and $T_3^{[2]}$ defined by Eqs. (58) and (44), respectively.

In analogy to the R-CCSD[T] and R-CCSD(T) approaches and their standard CCSD[T] and CCSD(T)counterparts, be shown that the it can R-CCSD(TQ)-1,a scheme, obtained by simplifying the CR-CCSD(TQ),x (x=a,b) equations according to Eqs. (75) and (76), reduces to the factorized CCSD(TQ_f) approach of Kucharski and Bartlett,³⁴ when the D^{(TQ),a} denominator in the R-CCSD(TQ)-1, a energy expression, Eq. (75), is replaced by 1. Indeed, the $CCSD(TQ_f)$ energy can be given the following form:

$$E_0^{\text{CCSD(TQ_f)}} = E_0^{\text{(CCSD)}} + N^{\text{(TQ)-1,a}},$$
 (78)

where $N^{(\text{TQ})-1,a}$ is defined by Eq. (76).³⁴ Clearly, one can immediately obtain Eq. (78) from the R-CCSD(TQ)-1,a energy formula, Eq. (75), by replacing $D^{(\text{TQ}),a}$ in the latter equation by 1. This very simple relationship between the R-CCSD(TQ)-1,a and CCSD(TQ_f) methods, combined with the fact that all R-CCSD(TQ) methods are obtained by simplifying the CR-CCSD(TQ) energy expressions, implies that the R-CCSD(TQ) and CR-CCSD(TQ) approaches represent MMCC extensions of the standard CCSD(TQ_f) method of Ref. 34. As in the case of the (C)R-CCSD[T] and (C)R-CCSD(T) approaches, the presence of the $D^{(\text{TQ}),x}$ denominators, Eqs. (73) and (74), in the (C)R-CCSD(TQ),x (x = a, b) energy expressions is essential for improving the results of the standard CCSD(TQ_f) calculations at larger internuclear separations. The overlaps of the $|\Psi^{\text{CCSD}(\text{TQ}),x}\rangle$ (x = a, b) and CCSD wave functions, defining the $D^{(\text{TQ}),x}$ denominators, increase with the internuclear distance, damping the exces-

sively large and, thus, completely unphysical values of the noniterative triples and quadruples corrections resulting from the standard CCSD(TQ_f) calculations, which cause the failure of the CCSD(TQ_f) approach in the bond breaking region.^{46,47}

The simple relationships between the renormalized and completely renormalized CCSD[T], CCSD(T), and CCSD(TQ) methods and their standard counterparts, discussed above, imply that the computer costs of the R-CCSD[T], R-CCSD(T), CR-CCSD[T], CR-CCSD(T), R-CCSD(TQ)-n, and CR-CCSD(TQ), (n = 1, 2, x = a, b) calculations are essentially identical to the costs of the standard CCSD[T], CCSD(T), and CCSD(TQ_f) calculations. In analogy to the standard CCSD[T] and CCSD(T) methods, the R-CCSD[T], R-CCSD(T), CR-CCSD[T], and CR-CCSD(T) approaches are $n_o^3 n_u^4$ procedures in the noniterative steps involving triples and $n_o^2 n_u^4$ procedures in the iterative CCSD steps. More specifically, the CR-CCSD[T] and CR-CCSD(T) approaches are twice as expensive as the standard CCSD[T] and CCSD(T) approaches in the steps involving noniterative triples corrections, whereas the costs of the R-CCSD[T] and R-CCSD(T) calculations are the same as the costs of the CCSD[T] and CCSD(T) calculations. ¹³⁸ The memory and disk storage requirements characterizing the R-CCSD[T], R-CCSD(T), CR-CCSD[T], and CR-CCSD(T) methods are essentially identical to those characterizing the standard CCSD[T] and CCSD(T) approaches (see Ref. 138 for further details). In complete analogy to the noniterative triples corrections, the costs of the R-CCSD(TQ)-n,x calculations are identical to the costs of the $CCSD(TQ_f)$ calculations (the $CCSD(TQ_f)$ method is an $n_o^3 n_u^4$ procedure in the triples part and an $n_o^2 n_u^5$ procedure in the noniterative steps involving quadruples). Again, the CR-CCSD(TQ),x approaches are only

twice as expensive as the $CCSD(TQ_f)$ method in the steps involving the noniterative energy corrections due to triples and quadruples.

These relatively low computer costs, combined with the ease-of-use of the completely renormalized CCSD[T], CCSD(T), and CCSD(TQ) methods that can only be matched by the standard CCSD[T], CCSD(T), and CCSD(TQ_f) approaches and with the fact that the CR-CCSD[T], CR-CCSD(T), and CR-CCSD(TQ),x approaches remove the failing of the CCSD[T], CCSD(T), and CCSD(TQ_f) methods at larger internuclear separations, make the CR-CCSD[T], CR-CCSD(T), and CR-CCSD(TQ),x approaches attractive alternatives to the existing multireference methods, such as multireference CI (MRCI). The MRCI methods describe bond breaking in a correct manner, but the effort involved is significantly larger and one has to define many additional elements, such as reference configurations, active orbitals, etc. to set up multireference calculations. None of these elements has to be considered in the CR-CCSD[T], CR-CCSD(T), and CR-CCSD(TQ),x calculations. As shown in earlier works, 45-48,50,51,53,134,138 the CR-CCSD[T], CR-CCSD(T), and CR-CCSD(TQ),x methods provide a highly accurate description of molecular PESs that can compete with the results of multireference calculations. The R-CCSD[T], R-CCSD(T), and R-CCSD(TQ)-n,x approaches are capable of improving the results of the standard CCSD[T], CCSD(T), and $CCSD(TQ_f)$ calculations for the intermediate stretches of chemical bonds, but the overall behavior of the R-CC methods at larger distances is not as good as the behavior of the CR-CC methods, so that the use of the R-CC approaches for studies of entire molecular PESs is not recommended. The CR-CC methods are more trustworthy in this regard.

To illustrate the performance of the completely renormalized CCSD[T], CCSD(T), and CCSD(TQ) methods, we review the results of the CR-CCSD[T], CR-CCSD(T), and CR-CCSD(TQ) calculations for the HF, H2O, and N2 molecules. As shown in Table 1, already the simple CR-CCSD[T] and CR-CCSD(T) methods provide considerable improvements over the poor description of the potential energy curve for the HF molecule by the standard CCSD, CCSD[T], and CCSD(T) approaches. The CR-CCSD[T], CR-CCSD(T), and CR-CCSD(TQ) methods are particularly effective at larger internuclear separations. For example, the 11.596 millihartree error in the CCSD result and the large -38.302, -24.480, and -18.351 millihartree errors in the CCSD[T], CCSD(T), and CCSD(TQ_f) results, respectively, at $R = 3R_e$ reduce to 2.508, 2.100, 0.425, and 0.316 millihartree when the CR-CCSD[T], CR-CCSD(T), CR-CCSD(TQ), a, and CR-CCSD(TQ), b methods are employed (cf. Table 1). The reduction of errors in the CCSD[T], CCSD(T), and CCSD(TQ_f) results at $R = 5R_e$, offered by the CR-CCSD[T], CR-CCSD(T), and CR-CCSD(TQ) methods, is even more impressive. The huge -75.101, -53.183, and -35.078 millihartree errors, relative to full CI, obtained with the CCSD[T], CCSD(T), and CCSD(TQ_f) calculations, respectively, are reduced to 3.820, 1.650, 0.454, and 0.689 millihartree when one switches to the CR-CCSD[T], CR-CCSD(T), CR-CCSD(TQ), a, and CR-CCSD(TQ), b methods. The CR-CCSD[T], CR-CCSD(T), CR-CCSD(TQ), a, and CR-CCSD(TQ), b results for geometries near the equilibrium $(R \approx R_e)$ are as good as the CCSD[T], CCSD(T), and $CCSD(TQ_f)$ results, producing very small errors not exceeding 0.5 millihartree. The excellent results obtained with the CR-CCSD[T] and CR-CCSD(T) methods for the HF molecule imply that already the simplest CR-CC approximations

are sufficient to obtain accurate PESs for single bond breaking. The CR-CCSD(TQ) approaches provide further improvements in this case, but their use is not essential to obtain high quality results.

The CR-CCSD[T] and CR-CCSD(T) methods are also sufficiently accurate for cases involving a simultaneous dissociation of two single bonds. This is illustrated in Table 2, where we consider a simultaneous breaking of both O-H bonds of the H₂O molecule. As shown in Table 2, the CR-CCSD[T], CR-CCSD(T), and CR-CCSD(TQ), x = a,b methods reduce the large -11.220, -7.699, and -5.914 millihartree, errors in the CCSD[T], CCSD(T), and CCSD(TQ_f) results at $R = 2R_e$ to the small 1.163, 1.830, 1.461, and 2.853 millihartree errors, respectively. The < 2.5 millihartree errors, relative to full CI, obtained with the CR-CCSD[T] and CR-CCSD(T) methods in the entire $R=R_e-2R_e$ region for the doubly dissociating water molecule indicate that there is no apparent need to use the higher-level CR-CCSD(TQ), x (x=a,b) methods in cases involving a simultaneous stretching of two single bonds. However, the CR-CCSD(TQ),x (x=a,b) approaches provide a more stable description of the double dissociation of H₂O, when compared with the CR-CCSD[T] and CR-CCSD(T) methods. Indeed, the initially small, 0.560 millihartree, error in the CR-CCSD[T] result at $R = R_e$ increases to 2.053 millihartree at $R = 1.5R_e$, to decrease again to 1.163 millihartree at $R = 2R_e$ (see Table 2). A similar behavior is observed for the CR-CCSD(T) approach. The non-monotonic error changes in the CR-CCSD[T] and CR-CCSD(T) results are the first signs of the possible eventual breakdown of these methods in the $R > 2R_e$ region. The CR-CCSD(TQ),x (x=a,b) methods behave much better in this regard, since the small errors in the CR-CCSD(TQ),x energies, relative to full CI, increase monotonically with the O-H separation.

Although the CR-CCSD[T] and CR-CCSD(T) approaches seem to be accurate enough to describe the simultaneous stretching of two single bonds, the stretching or breaking of multiple bonds requires using the higher-order CR-CC theories, such as CR-CCSD(TQ),b. For example, when one applies the CR-CCSD(T) method to triple bond breaking in the N_2 molecule, the resulting potential energy curve has a hump at the N-N separation $R \approx 1.75R_e$ and the CR-CCSD(T) curve is located below the full CI curve at larger N-N separations (see Table 3 and Fig. 2). The N_2 molecule is characterized by large T_3 as well as T_4 effects, even at the equilibrium geometry $R = R_e$. It is quite possible that higher-than-quadruply excited clusters play an important role when the N-N internuclear separation becomes large. The apparent importance of the higher-order clusters in the N_2 case, which cannot be easily approximated using the conventional MBPT or CC arguments, explains why the CR-CCSD(T) approach fails in this case.

The results of the CR-CCSD(TQ), a and CR-CCSD(TQ), b calculations for the DZ model of N_2 are shown in Table 3 and Fig. 2. We can immediately see that these methods, particularly variant "b" of the CR-CCSD(TQ) approach, provide significant improvements in the standard CC and CR-CCSD(T) results. The CR-CCSD(TQ), b method, which is a relatively simple modification of the conventional CCSD(TQ_f) approach and which uses elements of MBPT to estimate the effects due to T_3 and T_4 , provides a potential energy curve which is quite close to the exact full CI curve. For example, at $R = 2.25R_e$, the huge 334.985 millihartree error in

the CCSD(TQ_f) result and the 133.313 millihartree error in the CR-CCSD(T) result reduce to 14.796 millihartree, when the CR-CCSD(TQ), b method is employed (see Table 3). The CR-CCSD(TQ),b curve is located above the full CI curve in the entire $R = 0.75R_e - 2.25R_e$ region and almost all pathologies observed in the standard single-reference CC and CR-CCSD(T) calculations are eliminated when the CR-CCSD(TQ), b method is employed. The huge humps on the CCSD, CCSD(T), CR-CCSD(T), and CCSDT curves and a nearly singular behavior of the CCSD(T), $CCSD(TQ_f)$, and $CCSDT(Q_f)$ approaches at large R values are almost entirely eliminated by the CR-CCSD(TQ), b approach (cf. Table 3 and Fig. 2). Although there is a hump on the CR-CCSD(TQ), b curve, the size of this hump, as measured by the difference between the CR-CCSD(TQ), be energies at the maximum corresponding to the hump and at $R = 2.25R_e$, is small (~4.9 millihartree). There are 10-25 millihartree differences between the CR-CCSD(TQ),b and full CI energies at the intermediate values of R, but the fact that one can obtain a reasonably accurate potential energy curve for the triply bonded N₂ molecule, which is also located above the full CI curve in the entire $R = 0.75R_e - 2.25R_e$ region, with the ease of use characterizing the standard noniterative CC "black-boxes" of the CCSD(TQ_f) type, is an encouraging finding. However, in spite of the remarkable improvements offered by the CR-CCSD(TQ),b method in the N₂ case, the 10-25 millihartree errors in the region of the intermediate N-N separations are not sufficiently small for high accuracy calculations. It would also be great to be able to eliminate or, at least, further reduce the ~4.9 millihartree hump in the CR-CCSD(TQ), b curve. As shown in Sect. 5.1, the hump on the CR-CCSD(TQ), b curve can be completely eliminated by the new CISDtqph-corrected

MMCC(2,6) approach, which is an extension of the CISDtq-corrected MMCC(2,4) method described in Sect. 4.1 that incorporates the corrections due to pentuply and hextuply excited moments of the CCSD equations in addition to triply and quadruply excited moments present in the MMCC(2,4) approaches. The CISDtqph-corrected MMCC(2,6) method provides a virtually exact description of the N_2 potential energy curve. Similar improvements in the CR-CCSD(TQ),b description of the triple bond breaking in N_2 are obtained when we use the quadratic MMCC approach, developed in this thesis work and discussed in Sect. 5.2.

5. The New MMCC (m_A, m_B) Approaches for Multiple Bond Breaking

The MMCC(2,3) approximation, on which the CISDt-corrected MMCC(2,3) method and the (C)R-CCSD[T] and (C)R-CCSD(T) approaches are based, uses only the triply excited CCSD moments, $\mathcal{M}_{a_1a_2a_3}^{i_1i_2i_3}(2)$, corresponding to projections of the CCSD equations on triply excited configurations $|\Phi_{i_1i_2i_3}^{a_1a_2a_3}\rangle$, whereas the MMCC(2,4) scheme, on which the CISDtq-corrected MMCC(2,4) approach and the R-CCSD(TQ)n,x and CR-CCSD(TQ), x (n=1,2, x=a,b) methods are based, uses the triply and quadruply excited moments, $\mathcal{M}_{a_1a_2a_3}^{i_1i_2i_3}(2)$ and $\mathcal{M}_{a_1a_2a_3a_4}^{i_1i_2i_3i_4}(2)$, respectively, corresponding to projections of the CCSD equations on triply and quadruply excited configurations. The presence of the triply and quadruply excited moments in the MMCC(2,3) and MMCC(2,4) energy expressions (cf. Eqs. (31) and (36) with $\delta_0(2,3)$ and $\delta_0(2,4)$ defined by Eqs. (32) and (37), respectively) is usually sufficient to obtain a highly accurate description of single and double bond dissociation, but triple bond dissociation and other complicated types of multiple bond breaking may require a more accurate treatment. From the numerical experiments with the MMCC-based renormalized and completely renormalized CCSD[T], CCSD(T), and CCSD(TQ) methods and their CI-corrected counterparts, it follows that it may be necessary to incorporate the pentuply and hextuply excited moments of the CCSD equations, $\mathcal{M}_{a_1...a_k}^{i_1...i_k}(2)$, k = 5 and 6, respectively, if we are to formulate accurate MMCC approximations for multiple (e.g. triple) bond breaking. The inclusion of the $\mathcal{M}_{a_1a_2a_3a_4a_5}^{i_1i_2i_3i_4i_5}(2)$ and $\mathcal{M}_{a_1 a_2 a_3 a_4 a_5 a_6}^{i_1 i_2 i_3 i_4 i_5 i_6}(2)$ moments, in addition to the $\mathcal{M}_{a_1 a_2 a_3}^{i_1 i_2 i_3 i_4}(2)$ and $\mathcal{M}_{a_1 a_2 a_3 a_4}^{i_1 i_2 i_3 i_4}(2)$ moments that are already present in the MMCC(2,3) and MMCC(2,4) approaches, leads to the MMCC(2,5) and MMCC(2,6) approximations.

The MMCC(2,5) and MMCC(2,6) approximations are obtained by fixing the value of m_A in Eqs. (29) and (30) at 2 and by setting $m_B = 5$ (the MMCC(2,5) case) and $m_B = 6$ (the MMCC(2,6) case) in the resulting expressions. The formulas defining the MMCC(2,5) and MMCC(2,6) approaches are as follows:¹³⁴⁻¹³⁷

$$E_0^{\text{MMCC}}(2,5) = E_0^{\text{(CCSD)}} + \delta_0(2,5),$$
 (79)

$$E_0^{\text{MMCC}}(2,6) = E_0^{\text{(CCSD)}} + \delta_0(2,6),$$
 (80)

where

$$\delta_0(2,5) = \langle \Psi_0 | \{ Q_3 M_3(2) + Q_4 [M_4(2) + T_1 M_3(2)]$$

$$+ Q_5 [M_5(2) + T_1 M_4(2) + (T_2 + \frac{1}{2} T_1^2) M_3(2)] \} | \Phi \rangle$$

$$/ \langle \Psi_0 | e^{T_1 + T_2} | \Phi \rangle,$$
(81)

$$\delta_{0}(2,6) = \langle \Psi_{0} | \{ Q_{3} M_{3}(2) + Q_{4} [M_{4}(2) + T_{1} M_{3}(2)]$$

$$+ Q_{5} [M_{5}(2) + T_{1} M_{4}(2) + (T_{2} + \frac{1}{2} T_{1}^{2}) M_{3}(2)]$$

$$+ Q_{6} [M_{6}(2) + T_{1} M_{5}(2) + (T_{2} + \frac{1}{2} T_{1}^{2}) M_{4}(2)$$

$$+ (T_{1} T_{2} + \frac{1}{6} T_{1}^{3}) M_{3}(2)] \} |\Phi\rangle / \langle \Psi_{0} | e^{T_{1} + T_{2}} |\Phi\rangle .$$

$$(82)$$

The quantities $M_3(2)|\Phi\rangle$ and $M_4(2)|\Phi\rangle$ in Eqs. (81) and (82) are defined by Eqs. (33)

and (38), respectively. The $M_3(2)|\Phi\rangle$ and $M_4(2)|\Phi\rangle$ quantities are expressed in terms of triply and quadruply excited moments, $\mathcal{M}_{a_1a_2a_3}^{i_1i_2i_3}(2)$ and $\mathcal{M}_{a_1a_2a_3a_4}^{i_1i_2i_3i_4}(2)$, respectively. The new quantities $M_5(2)|\Phi\rangle$ and $M_6(2)|\Phi\rangle$ are defined as

$$M_{5}(2)|\Phi\rangle = \sum_{\substack{i_{1} < i_{2} < i_{3} < i_{4} < i_{5} \\ a_{1} < a_{2} < a_{3} < a_{4} < a_{5}}} \mathcal{M}_{a_{1}a_{2}a_{3}a_{4}a_{5}}^{i_{1}i_{2}i_{3}i_{4}i_{5}}(2)|\Phi_{i_{1}i_{2}i_{3}i_{4}i_{5}}^{a_{1}a_{2}a_{3}a_{4}a_{5}}\rangle, \tag{83}$$

and

$$M_{6}(2)|\Phi\rangle = \sum_{\substack{i_{1} < i_{2} < i_{3} < i_{4} < i_{5} < i_{6} \\ a_{1} < a_{2} < a_{3} < a_{4} < a_{5} < a_{6}}} \mathcal{M}_{a_{1}a_{2}a_{3}a_{4}a_{5}a_{6}}^{i_{1}i_{2}i_{3}i_{4}i_{5}i_{6}}(2)|\Phi_{i_{1}i_{2}i_{3}i_{4}i_{5}i_{6}}^{a_{1}a_{2}a_{3}a_{4}a_{5}a_{6}}\rangle, \tag{84}$$

where

$$\mathcal{M}_{a_{1}a_{2}a_{3}a_{4}a_{5}}^{i_{1}i_{2}i_{3}i_{4}i_{5}}(2) = \langle \Phi_{i_{1}i_{2}i_{3}i_{4}i_{5}}^{a_{1}a_{2}a_{3}a_{4}a_{5}} | (He^{T_{1}+T_{2}})_{C} | \Phi \rangle, \tag{85}$$

and

$$\mathcal{M}_{a_1 a_2 a_3 a_4 a_5 a_6}^{i_1 i_2 i_3 i_4 i_5 i_6}(2) = \langle \Phi_{i_1 i_2 i_3 i_4 i_5 i_6}^{a_1 a_2 a_3 a_4 a_5 a_6} | (He^{T_1 + T_2})_C | \Phi \rangle, \tag{86}$$

are the pentuply and hextuply excited moments of the CCSD equations, obtained by projecting these equations on the pentuply and hextuply excited configurations, $|\Phi_{i_1i_2i_3i_4i_5}^{a_1a_2a_3a_4a_5}\rangle$ and $|\Phi_{i_1i_2i_3i_4i_5}^{a_1a_2a_3a_4a_5a_6}\rangle$, respectively.

As in all MMCC(2, m_B) energy formulas, the MMCC(2,5) and MMCC(2,6) energies are expressed in terms of the generalized moments of the CCSD equations and the ground-state wave function $|\Psi_0\rangle$. The generalized moments of the CCSD equations can be easily determined using the converged CCSD cluster amplitudes, $t_{a_1}^{i_1}$ and $t_{a_1a_2}^{i_1i_2}$, respectively (see Appendix B), whereas $|\Psi_0\rangle$ must be replaced by some approximate form of the ground-state wave function. If we want to use the MMCC(2,5)

and MMCC(2,6) approximations in practice, we must use a simple form of $|\Psi_0\rangle$ that facilitates the calculations. In order to satisfy this "simplicity" requirement, we have formulated two classes of the MMCC(2,5) and MMCC(2,6) methods: (i) the CI-corrected MMCC(2,5) and MMCC(2,6) approaches, which can be viewed as extensions of the CI-corrected MMCC(2,3) and MMCC(2,4) methods where a priori limited CI calculations are performed to obtain $|\Psi_0\rangle$, and (ii) the quasi-variational and quadratic MMCC approaches, which are extensions of the CR-CCSD(T) and CR-CCSD(TQ) methods where the exponential, CC-like, form of the wave function $|\Psi_0\rangle$ is used to construct the $\delta_0(2,5)$ and $\delta_0(2,6)$ corrections. These two new classes of the MMCC approximations are discussed in Sects. 5.1 and 5.2, respectively.

5.1. The CI-corrected MMCC(2,5) and MMCC(2,6) Approximations

The CI-corrected MMCC(2,3) and MMCC(2,4) approaches, described in Sect. 4.1, provide very good results for single and double bond breaking. However, when triple bonds (e.g. in N₂) are broken, the results of the CI-corrected MMCC(2,3) and MMCC(2,4) calculations are less impressive. As shown in Table 3 and Fig. 2, the relatively small (a few millihartree) errors in the CISDtq-corrected MMCC(2,4) results for the N-N separations $R < 1.5R_e$ ($R = R_e$ is the equilibrium N-N bond length) become relatively large (> 10 millihartree) for $R \ge 1.5R_e$. At large internuclear separations, such as $R = 2R_e$, the CISDt-corrected MMCC(2,3) approach and the CISDtq-corrected MMCC(2,4) method suffer from non-variational collapse, similar to

that plaguing the standard CCSD(T) approximation, although the $\lesssim 30$ millihartree absolute errors in the CISDtq-corrected MMCC(2,4) results for $R \leq 2.25R_e$ are an order of magnitude smaller than the analogous errors characterizing the CCSD(T) and CCSD(TQ_f) results (cf. Table 3). In cases like this, we have to switch to the CI-corrected MMCC(2,6) method in which, in addition to moments $\mathcal{M}_{a_1a_2a_3}^{i_1i_2i_3i_4}$ (2) and $\mathcal{M}_{a_1a_2a_3a_4}^{i_1i_2i_3i_4i_5}$ (2) Eqs. (34) and (35), respectively, we consider moments $\mathcal{M}_{a_1a_2a_3a_4a_5}^{i_1i_2i_3i_4i_5}$ (2) and $\mathcal{M}_{a_1a_2a_3a_4a_5a_6}^{i_1i_2i_3i_4i_5i_6}$ (2), Eqs. (85) and (86), respectively, corresponding to projections of the CCSD equations on pentuply and hextuply excited configurations. As we will see, the CI-corrected MMCC(2,5) approximation is not sufficiently accurate for triple bond breaking in the region of larger internuclear separations, although the situation dramatically changes when we consider the quadratic version of the quasi-variational MMCC(2,5) theory described in Sect. 5.2.

5.1.1. Theory

In analogy to the CI-corrected MMCC(2,3) and MMCC(2,4) methods, the wave functions $|\Psi_0\rangle$ entering the MMCC(2,5) and MMCC(2,6) energy corrections, Eqs. (81) and (82), respectively, are obtained by solving the limited CI equations. Thus, in the CI-corrected MMCC(2,5) approach, the wave function $|\Psi_0\rangle$ in Eq. (81) is replaced by the wave function obtained in the CISDtqp calculation. The CISDtqp wave function is calculated by solving the CI eigenvalue problem with all singles and doubles, internal and semi-internal triples and quadruples defined by Eqs. (41) and

(42), and internal and semi-internal pentuply excited configurations defined by the excitation operator

$$c_{5}|\Phi\rangle = \sum_{\substack{\mathbf{I}_{1}>\mathbf{I}_{2}>\mathbf{I}_{8}>i_{4}>i_{5}\\a_{1}>a_{2}>\mathbf{A}_{8}>\mathbf{A}_{4}>\mathbf{A}_{5}\\a_{1}>a_{2}>\mathbf{A}_{8}>\mathbf{A}_{4}>\mathbf{A}_{5}}} c_{\mathbf{I}_{1}\mathbf{I}_{2}\mathbf{I}_{8}i_{4}i_{5}}^{a_{1}a_{2}\mathbf{A}_{8}\mathbf{A}_{4}\mathbf{A}_{5}} |\Phi_{\mathbf{I}_{1}\mathbf{I}_{2}\mathbf{I}_{8}i_{4}i_{5}}^{a_{1}a_{2}\mathbf{A}_{8}\mathbf{A}_{4}\mathbf{A}_{5}} \rangle,$$
(87)

where I_1 , I_2 , and I_3 indices represent active occupied spin-orbitals and A_3 , A_4 , and A_5 indices represent active unoccupied spin-orbitals (cf. Fig. 1). In a similar manner, the CI-corrected MMCC(2,6) method requires that we first perform the CISDtqph calculation by solving the CI eigenvalue problem with all singles and doubles, internal and semi-internal triples and quadruples defined by Eqs. (41) and (42), internal and semi-internal pentuples defined by Eq. (87), and internal and semi-internal hextuply excited configurations defined by the excitation operator

$$c_{6}|\Phi\rangle = \sum_{\substack{\mathbf{I}_{1}>\mathbf{I}_{2}>\mathbf{I}_{8}>\mathbf{I}_{4}>i_{5}>i_{6}\\a_{1}>a_{2}>\mathbf{A}_{8}>\mathbf{A}_{4}>\mathbf{A}_{5}>\mathbf{A}_{6}}} c_{\mathbf{I}_{1}\mathbf{I}_{2}\mathbf{I}_{8}\mathbf{I}_{4}i_{5}i_{6}}^{a_{1}a_{2}\mathbf{A}_{8}\mathbf{A}_{4}\mathbf{A}_{5}\mathbf{A}_{6}} |\Phi_{\mathbf{I}_{1}\mathbf{I}_{2}\mathbf{I}_{8}\mathbf{I}_{4}i_{5}i_{6}}^{a_{1}a_{2}\mathbf{A}_{8}\mathbf{A}_{4}\mathbf{A}_{5}\mathbf{A}_{6}}\rangle,$$
(88)

where I_1 , I_2 , I_3 , and I_4 are active occupied spin-orbitals and A_3 , A_4 , A_5 , and A_6 are active unoccupied spin-orbitals. The CISDtqph-corrected MMCC(2,6) energy expression is obtained by replacing the wave function $|\Psi_0\rangle$ in Eq. (82) by the wave function obtained in the CISDtqph calculation, as described above.

As in the case of the CI-corrected MMCC(2,3) and MMCC(2,4) approaches, the use of the active orbitals in defining the selected pentuples and hextuples entering Eqs. (87) and (88) significantly reduces the computer costs of the CI-corrected MMCC(2,5) and MMCC(2,6) calculations, since we do not have to determine all pentuply and hextuply excited moments of the CCSD equations. It is sufficient to calculate moments

 $\mathcal{M}_{a_1a_2\mathbf{A_8A_4A_5}}^{\mathbf{I_1\mathbf{I_2\mathbf{I_3}\mathbf{I_4}i_5}i_6}}(2)$ and $\mathcal{M}_{a_1a_2\mathbf{A_8A_4A_5}a_6}^{\mathbf{I_1\mathbf{I_2\mathbf{I_3}\mathbf{I_4}i_5}i_6}}(2)$, corresponding to projections of the CCSD equations on a relatively small set of internal and semi-internal pentuply and hextuply excited configurations of the $|\Phi_{\mathbf{I_1\mathbf{I_2}\mathbf{I_3}i_4i_5}}^{a_1a_2\mathbf{A_3A_4A_5}}\rangle$ and $|\Phi_{\mathbf{I_1\mathbf{I_2}\mathbf{I_3}\mathbf{I_4}i_5i_6}}^{a_1a_2\mathbf{A_3A_4A_5}}\rangle$ types. Our experience with the CI-corrected MMCC(2,5) and MMCC(2,6) methods indicates that these are the only types of projections of the CCSD equations on the pentuply and hextuply excited configurations that matter in calculations of triple bond breaking. This will be seen by analyzing the results of the CI-corrected MMCC(2,5) and MMCC(2,6) calculations for the triple bond breaking in the N₂ molecule.

5.1.2. Examples of Applications

The CI-corrected MMCC(2,5) and MMCC(2,6) methods developed in this thesis project were implemented using the explicit expressions for the generalized moments of the CCSD equations given in Appendix B. As in the case of the MMCC(2,3) and MMCC(2,4) calculations, the T_1 and T_2 cluster amplitudes were obtained with the orthogonally spin-adapted CCSD method of Ref. 29 using computer programs developed by Piecuch and Paldus. The required RHF calculations and the transformation from the atomic to molecular basis set were performed with the GAMESS codes. 139

We begin our discussion of the CI-corrected MMCC(2,5) and MMCC(2,6) results with the DZ model of H₂O. In this case, the simultaneous dissociation of both O-H bonds is reasonably well described by the CI-corrected MMCC(2,3) and MMCC(2,4) approaches (see Table 2), but it is interesting to examine if one can further reduce the

1-2 millihartree errors resulting from the CI-corrected MMCC(2,3) and MMCC(2,4) calculations at stretched nuclear geometries of H₂O by performing the higher-level MMCC(2,5) and MMCC(2,6) calculations.

The results of the CI-corrected MMCC(2,5) and MMCC(2,6) calculations for the double dissociation of H_2O are shown in Table 4. As in the case of the CI-corrected MMCC(2,3) and MMCC(2,4) calculations discussed in Sect. 4.1, the active space used in the CI-corrected MMCC(2,5) and MMCC(2,6) calculations consisted of the $1b_1$, $3a_1$, $1b_2$, $4a_1$, $2b_1$, and $2b_2$ valence orbitals. As one can see, the 0.811-2.407 millihartree errors in the CISDt-corrected MMCC(2,3) results and the 0.501-2.416 millihartree errors in the CISDtq-corrected MMCC(2,4) results in the $R = R_e - 2R_e$ region reduce to 0.421-0.730 millihartree when we switch to the CISDtqp-corrected MMCC(2,5) approach (see Table 4). The CISDtqph-corrected MMCC(2,6) method reduces the very small errors resulting from the CISDtqp-corrected MMCC(2,5) calculations even further, to 0.417 millihartree at $R = R_e$, 0.477 millihartree at $R = 1.5R_e$, and 0.538 millihartree at $R = 2R_e$.

These excellent results obtained with the CI-corrected MMCC(2,5) and MMCC(2,6) approaches are, at least in part, a consequence of the relatively good description of the double dissociation of H_2O by the CISDtqp and CISDtqph methods that are used to generate wave functions $|\Psi_0\rangle$ for constructing the MMCC(2,5) and MMCC(2,6) corrections, $\delta_0(2,5)$ and $\delta_0(2,6)$, respectively. The CISDtqph method is particularly good in this case, producing the relatively small 1.922–2.600 millihartree errors in the entire $R = R_e - 2R_e$ region. It is interesting to observe, though, that the MMCC theory is capable of reducing the small 2.628–3.732 millihartree errors in the CISDtqp

results and even smaller 1.922–2.600 millihartree errors in the CISDtqph results by a relatively large factor of 4–6, once the CISDtqp and CISDtqph wave functions $|\Psi_0\rangle$ are inserted into the MMCC(2,5) and MMCC(2,6) energy expressions, Eqs. (79) and (80), respectively. One might expect that the use of these high-quality wave functions $|\Psi_0\rangle$ in the MMCC calculations would only lead to small improvements in the results for H_2O . This is not the case. The reduction of errors in the CISDtqp and CISDtqph results for the double dissociation of H_2O by a factor of 4–6 is not as impressive as the reduction of large errors in the CISDt results, when the rather poor CISDt wave function $|\Psi_0\rangle$ is inserted into the MMCC(2,3) energy formula (cf. Tables 2 and 5), but the reduction of the ~ 2 –4 millihartree errors in the CISDtqp and CISDtqph results to as little as 0.4–0.7 millihartree is very encouraging.

We have already seen that neither the CI-corrected MMCC(2,3) theory nor its CI-corrected MMCC(2,4) extension is accurate enough to study the most challenging types of multiple bond breaking, including the triple bond breaking in N_2 (see Table 3 and Fig. 2). The N_2 molecule is characterized by large T_3 and T_4 effects and, for stretched nuclear geometries, by sizable contributions due to higher-than-quadruply excited clusters, in addition to the huge T_3 and T_4 effects. The effect of T_3 clusters at the equilibrium geometry ($R = R_e$) and for the DZ basis set in N_2 , obtained as the difference of the CCSDT and CCSD energies, is -6.182 millihartree (see Tables 3 and 5). The difference of the CCSDTQ and CCSDT energies, which measures the effect of T_4 clusters, is -1.912 millihartree.⁴⁷ The full CCSDTQ method is virtually exact in this case. For geometries near the equilibrium, the T_3 and T_4 effects are accurately described by the perturbative CCSD(T) and CCSD(TQ_f) approaches. For example,

the difference between the CCSD(T) and CCSD energies of -6.133 millihartree at $R = R_e$ is virtually identical to the -6.182 millihartree difference between the CCSDT and CCSD energies. However, the situation becomes much more complicated when the N-N bond is stretched. The 8.289 millihartree difference between the full CI and CCSD energies at $R = R_e$, which measures the combined effect of all higher-thandoubly excited clusters, rapidly increases to 33.545 millihartree at $R=1.5R_e$ (see Tables 3 and 5). At $R \approx 1.75 R_e$, the CCSD potential energy curve has an unphysical hump, and for the N-N distances greater than 3.74 bohr, the CCSD potential energy curve goes significantly below the exact full CI curve (see Tables 3 and 5 and Figs. 2 and 3). Similar remarks apply to the CCSDT curve, which has a well-pronounced hump at larger N-N separations. All of these imply that we need to incorporate T_4 clusters to obtain a correct description of the N_2 curve. It is quite likely that higher-than-quadruply excited clusters play an important role too when R becomes large, since triple bond breaking in N₂ requires at least some hextuple excitations in a CI sense. This can be seen by comparing the CISDtqph and CISDtqp energies. The CISDtop approach, which neglects the hextuple excitations altogether, provides a significantly worse description of bond breaking in N₂ than the CISDtqph method (see Table 5). It can also be shown that the difference between the CISDTQ (CI singles, doubles, triples, and quadruples) and full CI energies at $R=2R_e$ is almost 40 millihartree, 106 indicating the possible need for higher-than-quadruply excited clusters at larger N-N separations.

As mentioned in Sect. 4, the CCSD(T) and CCSD(TQ_f) approximations, which describe the effects due to triply and quadruply excited clusters perturbatively, lead

to completely erroneous results at larger N-N distances (cf. Tables 3 and 5 and Figs. 2 and 3). The relatively small 2.156 millihartree difference between the CCSD(T) and full CI energies at $R=R_e$ increases (in absolute value) to 51.869 millihartree at R= $1.75R_e$, 246.405 millihartree at $R=2R_e$, and 387.448 millihartree at $R=2.25R_e$. The $CCSD(TQ_f)$ approach fails, too, giving 92.981 and 334.985 millihartree errors at R = $2R_e$ and $2.25R_e$, respectively. As shown in Figs. 2 and 3, the potential energy curves obtained in the CCSD(T) and $CCSD(TQ_f)$ calculations are completely pathological. At larger internuclear separations, the CCSD(T) curve is located significantly below the full CI curve, and there is a well-pronounced hump on the CCSD(T) curve for the intermediate values of R. The $CCSD(TQ_f)$ potential energy curve is located significantly above the full CI curve. None of the standard single-reference methods of improving the poor CCSD results at larger N-N separations, based on adding the noniterative corrections due to triples and quadruples to the RHF-based CCSD energies, leads to a satisfactory description of bond breaking in N₂. In fact, even the CCSDT(Q_f) method, in which the effects due to T₄ clusters are added to the CCSDT energies, fails (see Table 3). The failure of the CCSD(T), CCSD(TQ_f), and $CCSDT(Q_f)$ approaches at larger N-N distances is a consequence of the divergent nature of the MBPT series and the failure of the CCSD and CCSDT methods to provide reasonable information about the T_1 , T_2 and (in the case of CCSDT) T_3 cluster amplitudes, which are used to construct the relevant (T) and (Q_f) corrections.

The MMCC formalism provides us with two different ways of removing the failures of the standard single-reference CC approximations at larger N-N separations in N₂. The excellent results for the triple bond breaking in N₂ can be obtained either by using

the CISDtqph-corrected MMCC(2,6) method or by employing the quadratic MMCC approximation. In this section, we focus on the CISDtqph-corrected MMCC(2,6) results. The quadratic MMCC calculations are discussed in Sect. 5.2.

The results of the CISDtqph-corrected MMCC(2,6) calculations and their CISDtqp-corrected MMCC(2,5) analogs can be found in Table 5 and Fig. 3. As in the CI-corrected MMCC(2,3) and MMCC(2,4) calculations, the active space used in the CI-corrected MMCC(2,5) and MMCC(2,6) calculations consisted of the $3\sigma_g$, $1\pi_u$, $2\pi_u$, $1\pi_g$, $2\pi_g$, and $3\sigma_u$ valence orbitals.

As one can see, the CISDtqph-corrected MMCC(2,6) approach reduces the huge errors in the results of the CCSD, CCSD(T), and other standard CC calculations at large N-N distances R to as little as 4.443 millihartree at $R=2R_e$ and 4.552 millihartree at $R=2.25R_e$. The errors in the MMCC(2,6) calculations for N₂ range between 1.217 and 4.552 millihartree in the entire $R = 0.75R_e - 2.25R_e$ region. This is an excellent (and intriguing) result considering the fact that the MMCC(2,6) calculations utilize the generalized moments of the failing CCSD approach. This result clearly demonstrates that the MMCC formalism can handle all kinds of problems, including the most difficult problem of triple bond breaking. In spite of the unphysical shape of the CCSD PES at the intermediate and larger N-N distances, the MMCC(2,6) corrections to the CCSD energies lead to an excellent potential energy curve, which is located only slightly above the exact full CI curve (see Fig. 3). The dissociation energy D_e , defined here as the difference of energies at $R=2.25R_e$ and $R = R_e$, resulting from the MMCC(2,6) calculations, is 6.68 eV, in excellent agreement with the exact full CI value of 6.61 eV. This should be contrasted with

the fact that it is impossible to calculate D_e for the standard RHF-based singlereference CC methods due to unphysical shapes of the potential energy curves resulting from the single-reference CC calculations. It is, therefore, very encouraging that the MMCC(2,6) method employing the RHF reference is capable of providing an accurate representation of the PES of N₂, even at larger N-N separations, where all standard CC approximations fail. The 2.022 millihartree error in the MMCC(2,6) result at $R=R_e$ is not as small as the 0.323 or ~ 1 millihartree errors in the standard and completely renormalized CCSD(TQ) results (cf. Table 3), but the overall performance of the CISDtqph-corrected MMCC(2,6) approximation is much better than the performance of the standard and renormalized CCSD(T) and CCSD(TQ) methods. The only other noniterative CC method, employing the cluster amplitudes obtained in the CCSD calculations, that can provide results that are comparable with the results of the CI-corrected MMCC(2,6) calculations, is the aforementioned quadratic MMCC approach discussed in Sect. 5.2.

The results of the CI-corrected MMCC(2,3), MMCC(2,4), and MMCC(2,5) calculations are not as good as the CI-corrected MMCC(2,6) results. This clearly indicates that the MMCC(2,3), MMCC(2,4), and MMCC(2,5) levels of the MMCC theory are not sufficient to obtain an accurate description of the triple bond breaking in N₂, when the limited CI wave functions are used as the wave functions $|\Psi_0\rangle$ in constructing the relevant energy corrections. As mentioned in Sect. 4.1, the CI-corrected MMCC(2,3) approach completely fails for N₂ (cf. Table 3 and Fig. 2). The CI-corrected MMCC(2,4) and MMCC(2,5) results are good for $R \leq 1.75R_e$, with errors not exceeding a few millihartree (see Tables 3 and 5). However, for $R \geq 2R_e$, the

energies obtained in the CI-corrected MMCC(2,4) and MMCC(2,5) calculations are significantly below the corresponding full CI energies. At larger N-N separations, the CI-corrected MMCC(2,4) and MMCC(2,5) approaches suffer from a non-variational collapse similar to that characterizing the CCSD and CCSD(T) approximations. On the other hand, the CI-corrected MMCC(2,4) and MMCC(2,5) approaches performed much better than the CCSD, CCSD(T), and other standard noniterative CC methods. The negative errors relative to full CI in the results of the CI-corrected MMCC(2,4) and MMCC(2,5) calculations for larger values of R, which for $R = 2R_e$ are approximately -20 millihartree, are much smaller (in absolute value) than the errors in the CCSD, CCSD(T), CCSD(TQ_f), and CCSDT(Q_f) results. We can, therefore, conclude that the CI-corrected MMCC(2,4) and MMCC(2,5) methods provide significant improvements in the results of the standard single-reference calculations for triple bond breaking in N_2 . The only problem is that the improvements offered by the CI-corrected MMCC(2,4) and MMCC(2,5) approximations at larger N-N separations are not as great as we would like them to be. This behavior of the CI-corrected MMCC methods is in sharp contrast to the behavior of the quadratic MMCC approximations which will be discussed in Sect. 5.2. As we will see in the next section, already the quadratic MMCC approaches of the MMCC(2,5) type are capable of providing very small, at most a few millihartree, errors in the entire $R = 0.75R_e - 2.25R_e$ region of the ground-state PES of N₂. As a matter of fact, the most expensive moments of the CCSD theory, i.e. $\mathcal{M}_{a_1 a_2 a_3 a_4 a_5}^{i_1 i_2 i_3 i_4 i_5}(2)$ and $\mathcal{M}_{a_1 a_2 a_3 a_4 a_5 a_6}^{i_1 i_2 i_3 i_4 i_5 i_6}(2)$, can be ignored in the quadratic MMCC calculations for N₂ without significant loss of accuracy at larger N-N separations. This is in great contrast with the CI-corrected MMCC methods

discussed in this section, since the only level of the CI-corrected MMCC theory that guarantees very good results for the triple bond breaking in N_2 is the MMCC(2,6) level, which includes the entire set of the generalized moments of the CCSD equations.

From the results in Tables 3 and 5 and Figs. 2 and 3, it immediately follows that the CI-corrected MMCC methods provide the correct shape of the potential energy curve and small errors relative to full CI only when the limited CI wave functions $|\Psi_0\rangle$ used to construct the MMCC energy corrections provide a qualitatively correct description of bond breaking. Clearly, the CISDtqph method, on which the CI-corrected MMCC(2,6) approach is based, provides a qualitatively correct representation of the potential energy curve of N₂ (see Table 5). In consequence, the CISDtqph-corrected MMCC(2,6) method provides excellent results for all N-N separations. It is interesting to note that the CISDtqph-corrected MMCC(2,6) approximation reduces the 5.390-8.372 millihartree errors in the CISDtqph results for N_2 by a factor of 2-4. As expected, the use of the CISDt, CISDtq, and CISDtqp wave functions, which lack the important contributions from the hextuply excited configurations, results in a poor performance of the CISDt, CISDtq, and CISDtqp methods and their CI-corrected MMCC(2,3), MMCC(2,4), and MMCC(2,5) analogs at larger N-N separations.

The CISDtqph-corrected MMCC(2,6) method is essentially the only approach among all CI-corrected MMCC approximations that provides excellent and well-balanced results for smaller and larger N-N distances. For simpler types of bond breaking, including various examples of single and double bond breaking, very good results can already be obtained with the MMCC(2,3) and MMCC(2,4) approximations (cf. Sect. 4.1). The results in Tables 4 and 5 and the earlier results in Tables

1-3 show that the MMCC formalism always offers considerable improvements in the results of the limited CI calculations that are used to provide wave functions $|\Psi_0\rangle$ for constructing the MMCC energy corrections, but one has to use the right form of the CI wave function $|\Psi_0\rangle$ for a given type of bond breaking to obtain highly accurate CI-corrected MMCC results (CISDt for single bond breaking, CISDtq for double bond breaking, and CISDtqph for triple bond breaking).

5.1.3. Conclusion

The results for various types of bond breaking reported in Tables 1–5 and Figs. 2 and 3 show the systematic behavior of the CI-corrected MMCC approximations. The CI-corrected MMCC results systematically improve when we go from the basic MMCC(2,3) approach to the intermediate MMCC(2,4) and MMCC(2,5) levels and to the highest-level MMCC(2,6) approximation. The systematic improvements in the results of the CI-corrected MMCC calculations in a sequence of the MMCC(2,3) \rightarrow MMCC(2,4) \rightarrow MMCC(2,5) \rightarrow MMCC(2,6) approximations are a consequence of the fact that along with incorporating higher and higher moments of the CCSD equations, we are also systematically improving the quality of the CI wave functions that enter the MMCC(2, m_B), $m_B = 2 - 6$, energy expressions (from CISDt in the MMCC(2,3) case to CISDtqph in the MMCC(2,6) case).

With a judicious choice of the CI wave function $|\Psi_0\rangle$, the CI-corrected MMCC methods are capable of providing very good results for all kinds of bond breaking. The

choice of active orbitals in the CI-corrected MMCC calculations is usually straightforward since we often know which valence orbitals are involved in the bond breaking process under consideration, but clearly it would be very useful to be able to describe PESs involving bond breaking without having to select active orbitals. Undoubtedly, it would be desirable to have robust approaches, which combine the simplicity of the "black-box" noniterative CC methods, such as CCSD(T), with the efficiency with which active-space or MRCC and MRCI approaches describe quasi-degenerate electronic states and bond breaking. Noniterative single-reference CC approaches which are flexible and powerful enough that they can handle bond breaking in spite of using elements of MBPT, would be particularly desirable in situations where it is not easy to define the appropriate active space. The completely renormalized CCSD(T) and CCSD(TQ) methods that were described in Sect. 4.2 and the new quasi-variational and quadratic MMCC approaches developed in this thesis work and described in Sect. 5.2 are good candidates for such "black-box"-type methods. The quasi-variational and quadratic MMCC approaches can be viewed as extensions of the completely renormalized CCSD(T) and CCSD(TQ) methods which work for single as well as multiple bond breaking, including triple bond breaking in N₂.

5.2. The Quasi-variational and Quadratic MMCC Approximations

The excellent results obtained with the CISDtqph-corrected MMCC(2,6) approach for the triple bond breaking in N₂ indicate that in searching for the "black-box" extensions of the completely renormalized CCSD(T) and CCSD(TQ) methods that might provide an excellent description of triple bond breaking, one should consider approximations involving the pentuply and hextuply excited moments of the CCSD equations, $\mathcal{M}_{a_1a_2a_3a_4a_5}^{i_1i_2i_3i_4i_5}(2)$ and $\mathcal{M}_{a_1a_2a_3a_4a_5a_6}^{i_1i_2i_3i_4i_5i_6}(2)$, respectively. This implies that, in designing the extensions of CR-CCSD(T) and CR-CCSD(TQ) methods for multiple bond breaking, we can no longer use the MBPT(2)-like wave functions, defined by Eqs. (68) or (69), as the wave functions $|\Psi_0\rangle$ in the relevant MMCC expressions, since they do not contain higher-than-quadruply excited components that must be present in the formula for $|\Psi_0\rangle$, if we are to benefit from the presence of the $\mathcal{M}_{a_1a_2a_3a_4a_5}^{i_1i_2i_3i_4i_5}(2)$ and $\mathcal{M}_{a_1a_2a_3a_4a_5a_6}^{i_1i_2i_3i_4i_5i_6}(2)$ contributions to the higher-order MMCC(2,5) and MMCC(2,6) energy expressions. The MBPT(3) wave function is the lowest-order wave function that has the pentuply and hextuply excited contributions, which can engage the pentuply and hextuply excited moments of the CCSD equations in Eq. (25) to give a nonzero MMCC(2,6) correction $\delta_0(2,6)$ (cf., also, Eq. (82)). Unfortunately, in spite of several attempts, we have not succeeded in improving the CR-CCSD(TQ) results for triple bond breaking, reported in Ref. 47 and discussed in Sect. 4.2, by using the MBPT(3)-like expressions for $|\Psi_0\rangle$. Clearly, a different way of designing the MMCC corrections is required if we are to improve the CR-CCSD(TQ) results for multiple bond breaking by adding noniterative corrections to CCSD energies that are solely

based on the CCSD values of T_1 and T_2 . This new way of designing "black-box" MMCC methods for multiple bond breaking is discussed in this section.

As part of this thesis research, we have suggested a new idea of exploiting the exponential, CC-like, forms of $|\Psi_0\rangle$ in Eq. (25) for the MMCC-based $\delta_0^{(CCSD)}$ correction to the CCSD energy, instead of the more usual MBPT-like forms used in the CR-CCSD(T) and CR-CCSD(TQ) approaches. As shown in this section, the CC-like functions $|\Psi_0\rangle$ or their truncated variants are much more effective in introducing the higher-order terms into Eq. (25) than the finite-order MBPT expressions exploited in the existing CR-CCSD(T) and CR-CCSD(TQ) approaches. The resulting quasivariational and quadratic MMCC methods provide excellent results for multiple bond breaking, while preserving the ease of use of the standard and completely renormalized CCSD(T) and CCSD(TQ) approaches.

5.2.1. Theory

Since the MBPT(3)-like wave functions $|\Psi_0\rangle$ proved to be inefficient in constructing the highly accurate corrections $\delta_0^{(CCSD)}$ for multiple bond breaking, we decided to consider an alternative approach, in which we replace $|\Psi_0\rangle$ in Eqs. (21) or (25) by a CC-like exponential wave function^{134–137}

$$|\Psi_0^{\text{QVMMCC}}\rangle = e^{\Sigma}|\Phi\rangle,$$
 (89)

where, in practice, the excitation operator Σ is an approximation to the exact cluster operator T. By inserting Eq. (89) into Eqs. (21) and (25) and by choosing different forms of Σ in Eq. (89), a hierarchy of the so-called quasi-variational MMCC (QVMMCC) approximations can be proposed. In general, the QVMMCC noniterative energy correction to the standard CC energy $E_0^{(A)}$ is defined as follows (cf. Eq. (21)):¹³⁴⁻¹³⁷

$$\delta_0^{(A)}(\text{QVMMCC}) \equiv E_0^{\text{QVMMCC}} - E_0^{(A)}$$

$$= \sum_{n=m_A+1}^{N} \sum_{k=m_A+1}^{n} \langle \Phi | e^{\Sigma^{\dagger}} Q_n C_{n-k}(m_A) M_k(m_A) | \Phi \rangle /$$

$$\langle \Phi | e^{\Sigma^{\dagger}} e^{T^{(A)}} | \Phi \rangle. \tag{90}$$

If the CC method A represents the CCSD theory, the corresponding QVMMCC energy, E_0^{QVMMCC} , is calculated by adding the correction

$$\delta_0^{(\text{CCSD})}(\text{QVMMCC}) = \sum_{n=3}^{N} \sum_{k=3}^{\min(n,6)} \langle \Phi | e^{\Sigma^{\dagger}} Q_n C_{n-k}(2) M_k(2) | \Phi \rangle /$$

$$\langle \Phi | e^{\Sigma^{\dagger}} e^{T_1 + T_2} | \Phi \rangle$$
(91)

to the CCSD energy. The name "quasi-variational" in reference to the MMCC approximations based on Eqs. (90) or (91) is related to the fact that the QVMMCC energy

$$E_0^{\text{QVMMCC}} = E_0^{(A)} + \delta_0^{(A)}(\text{QVMMCC})$$
(92)

represents an upper bound to the exact energy E_0 , if Σ in Eq. (90) equals $T^{(A)}$ (or

 Σ in Eq. (91) equals $T_1 + T_2$). Indeed, by replacing $|\Psi_0\rangle$ in Eqs. (21) and (24) by $|\Psi_0^{\text{QVMMCC}}\rangle$, Eq. (89), we immediately obtain

$$\delta_0^{(A)}(\text{QVMMCC}) = \langle \Phi | e^{\Sigma^{\dagger}} H e^{T^{(A)}} | \Phi \rangle / \langle \Phi | e^{\Sigma^{\dagger}} e^{T^{(A)}} | \Phi \rangle - E_0^{(A)}, \tag{93}$$

so that

$$E_0^{\text{QVMMCC}} = \langle \Phi | e^{\Sigma^{\dagger}} H e^{T^{(A)}} | \Phi \rangle / \langle \Phi | e^{\Sigma^{\dagger}} e^{T^{(A)}} | \Phi \rangle. \tag{94}$$

When $\Sigma = T^{(A)}$, the QVMMCC energy E_0^{QVMMCC} , Eq. (94), reduces to the expectation value of the Hamiltonian with the CC wave function $e^{T^{(A)}}|\Phi\rangle$, which provides an upper bound to the exact ground-state energy E_0 .

Clearly, the QVMMCC theory becomes exact if Σ in Eqs. (90) or (91) is the exact cluster operator T. Also, the exponential form of $|\Psi_0\rangle$, Eq. (89), used to define the QVMMCC corrections $\delta_0^{(A)}(\text{QVMMCC})$, Eq. (90), or $\delta_0^{(\text{CCSD})}(\text{QVMMCC})$, Eq. (91), guarantees that the resulting energies E_0^{QVMMCC} , Eq. (92), are rigorously size-extensive. The question is if we can propose efficient computational schemes, based on Eqs. (90) or (91), that would allow us to obtain a highly accurate description of multiple bond breaking. In developing these practical schemes, the form of the operator Σ entering Eqs. (90) and (91) plays an important role.

The simplest choice of Σ in Eq. (91) might be $\Sigma = T_1 + T_2$, with T_1 and T_2 obtained in the standard CCSD calculations. As shown above, the resulting corrections $\delta_0^{(\text{CCSD})}(\text{QVMMCC})$, when added to the CCSD energies, would provide upper bounds to the exact energies. Thus, the choice of $\Sigma = T_1 + T_2$ in Eq. (91), in analogy to

the variational CCD theory, ^{142,143} would lead to a qualitatively correct description of triple bond breaking in N₂. In particular, the non-variational collapse of the standard CCSD approach at larger N-N separations discussed in the earlier sections would be entirely eliminated. However, we do not obtain the desired improvements in the quantitative description of multiple bond breaking when the wave function $|\Psi_0^{\text{QVMMCC}}\rangle$, Eq. (89), with $\Sigma = T_1 + T_2$, is used to calculate the correction $\delta_0^{\text{(CCSD)}}(\text{QVMMCC})$, Eq. (91), to the CCSD energy. This is a consequence of the fact that the choice of $\Sigma = T_1 + T_2$ in Eq. (91) is not bringing any meaningful information about the connected triply excited clusters T_3 , which are very important in all quantitative calculations (particularly when chemical bonds are stretched or broken).

The T_3 clusters can be approximated by considering the MBPT(2)-like expression, Eq. (44), used in the CCSD[T], CCSD(T), (C)R-CCSD[T], and (C)R-CCSD(T) methods. Thus, based on the fact that the T_3 cluster components are essential in studies of bond breaking, we can suggest the following form of the cluster operator Σ for the energy calculations based on Eq. (91):

$$\Sigma = T_1 + T_2 + T_3^{[2]}. \tag{95}$$

The cluster operator Σ , Eq. (95), represents an approximation to the exact cluster operator T, which is correct through the second order of the MBPT wave function (T_1 and T_3 contribute, for the first time, in the second order and T_2 contributes, for the first time, in the first order; T_4 , T_5 , etc. do not contribute in the first two orders of MBPT). We can, of course, think of some other, more elaborate, forms of Σ in Eq.

(95), but all of our benchmark calculations to date indicate that a simple definition of Σ given by Eq. (95) is sufficient to provide very good results for multiple bond breaking.

The use of the exponential wave function $|\Psi_0^{\text{QVMMCC}}\rangle$, Eq. (89), in calculating the noniterative corrections $\delta_0^{(\text{CCSD})}$, has only one practical drawback, namely, all many-body terms resulting from the presence of $e^{\Sigma^{\dagger}}$ in Eq. (91), including the *N*-body ones, where *N* is the number of electrons, contribute to the correction $\delta_0^{(\text{CCSD})}$ (QVMMCC). Although this does not change the fact that the generalized moments of the CCSD equations, corresponding to projections of those equations on higher-than-hextuply excited configurations, vanish (so that the summation over k in Eq. (91) is still limited to the k=3-6 terms), the full use of the exponential wave function $|\Psi_0^{\text{QVMMCC}}\rangle$ requires that we deal with the full CI expansion of $|\Psi_0^{\text{QVMMCC}}\rangle$ in calculating $\delta_0^{\text{(CCSD)}}$. In order to alleviate this situation, we have decided to consider approximate forms of Eq. (91), in which the power series expansion for $e^{\Sigma^{\dagger}}$, i.e.,

$$e^{\Sigma^{\dagger}} = \sum_{\ell=0}^{N} \frac{(\Sigma^{\dagger})^{\ell}}{\ell!},\tag{96}$$

with Σ defined by Eq. (95), is truncated in Eq. (91) at some low power of Σ^{\dagger} . Two approximations are particularly important here, namely, the linearized QVMMCC (LMMCC) model, in which $e^{\Sigma^{\dagger}}$ in Eq. (91) is truncated at the linear terms in Σ^{\dagger} , so that the wave function $|\Psi_0^{\text{QVMMCC}}\rangle$, Eq. (89), is approximated by

$$|\Psi_0^{\text{LMMCC}}\rangle = (1+\Sigma)|\Phi\rangle,$$
 (97)

and the quadratic QVMMCC (QMMCC) model, in which $e^{\Sigma^{\dagger}}$ in Eq. (91) is truncated at the $(\Sigma^{\dagger})^2$ terms, so that the wave function $|\Psi_0^{\text{QVMMCC}}\rangle$ is approximated by

$$|\Psi_0^{\text{QMMCC}}\rangle = (1 + \Sigma + \frac{1}{2}\Sigma^2)|\Phi\rangle. \tag{98}$$

Cubic, quartic, and other QVMMCC models based on truncating the power series expansion for $|\Psi_0^{\rm QVMMCC}\rangle$ at higher powers of Σ can be proposed, too, although it seems to us that the LMMCC and QMMCC approximations are usually sufficiently accurate.

It can be easily shown that the LMMCC model with Σ defined by Eq. (95) is equivalent to the CR-CCSD[T] method, introduced in Refs. 45 and 46 and overviewed in Sect. 4.2. As such, the LMMCC method cannot describe multiple bond breaking due to the absence of the quadratic $\frac{1}{2}T_2^2$ terms and other nonlinear terms in the wave function $|\Psi_0\rangle$ defining the relevant energy correction $\delta_0^{(CCSD)}$ (cf., e.g., Ref. 47). The $LMMCC \equiv CR-CCSD[T]$ method and its CR-CCSD(T) analog work well for the PESs involving single bond breaking. The QMMCC model can be thought of as the extension of the CR-CCSD[T] and CR-CCSD(T) methods that includes terms that are quadratic in Σ^{\dagger} . In particular, the QMMCC method contains the quadratic $\frac{1}{2}T_2^2$ terms in the wave function $|\Psi_0\rangle$ that can also be found in variant "b" of the CR-CCSD(TQ) theory, introduced in Ref. 47 and discussed in Sect. 4.2. In addition to the $\frac{1}{2}T_2^2$ terms in $|\Psi_0\rangle$ (the $\frac{1}{2}(T_2^{\dagger})^2$ terms in Eq. (91)), the QMMCC energy expression contains other terms that are bilinear in cluster amplitudes, such as $T_2^{\dagger}(T_3^{[2]})^{\dagger}$, which are not present in the CR-CCSD(TQ) method. These additional bilinear terms are essential for obtaining a highly accurate description of multiple bond breaking.

We begin our description of the QMMCC energy expressions by considering the complete QMMCC theory within the $T^{(A)} = T_1 + T_2$ and $\Sigma = T_1 + T_2 + T_3^{[2]}$ approximations, referred to as the QMMCC(2,6) method. By replacing Σ in Eq. (91) by Eq. (95) and by truncating the power series expansion for $e^{\Sigma^{\dagger}}$ in Eq. (91) at the $(\Sigma^{\dagger})^2$ term, we obtain the following expression for the QMMCC(2,6) energy:

$$E_0^{\text{QMMCC}(2,6)} = E_0^{(\text{CCSD})} + \delta_0^{(\text{CCSD})}(\text{QMMCC}(2,6)),$$
 (99)

where

$$\delta_0^{(CCSD)}(QMMCC(2,6)) = N^{QMMCC(2,6)}/D^{QMMCC(2,6)},$$
 (100)

with the numerator

$$N^{\text{QMMCC}(2,6)} = \sum_{n=3}^{6} \sum_{k=3}^{n} \langle \Psi_{0}^{\text{QMMCC}} | Q_{n} C_{n-k}(2) M_{k}(2) | \Phi \rangle$$

$$= \langle \Phi | [T_{1}^{\dagger} T_{2}^{\dagger} + (T_{3}^{[2]})^{\dagger}] M_{3}(2)$$

$$+ [\frac{1}{2} (T_{2}^{\dagger})^{2} + T_{1}^{\dagger} (T_{3}^{[2]})^{\dagger}] [M_{4}(2) + T_{1} M_{3}(2)]$$

$$+ T_{2}^{\dagger} (T_{3}^{[2]})^{\dagger} [M_{5}(2) + T_{1} M_{4}(2) + (T_{2} + \frac{1}{2} T_{1}^{2}) M_{3}(2)]$$

$$+ \frac{1}{2} [(T_{3}^{[2]})^{\dagger}]^{2} [M_{6}(2) + T_{1} M_{5}(2) + (T_{2} + \frac{1}{2} T_{1}^{2}) M_{4}(2)$$

$$+ (T_{1} T_{2} + \frac{1}{6} T_{1}^{3}) M_{3}(2)] | \Phi \rangle, \qquad (101)$$

and the denominator

$$\begin{split} D^{\mathrm{QMMCC}(2,6)} &= \langle \Psi_0^{\mathrm{QMMCC}} | e^{T_1 + T_2} | \Phi \rangle \\ &= 1 + \langle \Phi | T_1^{\dagger} T_1 | \Phi \rangle + \langle \Phi | [T_2^{\dagger} + \frac{1}{2} (T_1^{\dagger})^2] (T_2 + \frac{1}{2} T_1^2) | \Phi \rangle \\ &+ \langle \Phi | [T_1^{\dagger} T_2^{\dagger} + (T_3^{[2]})^{\dagger}] (T_1 T_2 + \frac{1}{6} T_1^3) | \Phi \rangle \\ &+ \langle \Phi | [\frac{1}{2} (T_2^{\dagger})^2 + T_1^{\dagger} (T_3^{[2]})^{\dagger}] (\frac{1}{2} T_2^2 + \frac{1}{2} T_1^2 T_2 + \frac{1}{24} T_1^4) | \Phi \rangle \\ &+ \langle \Phi | T_2^{\dagger} (T_3^{[2]})^{\dagger} (\frac{1}{2} T_1 T_2^2 + \frac{1}{6} T_1^3 T_2 + \frac{1}{120} T_1^5) | \Phi \rangle \\ &+ \langle \Phi | \frac{1}{2} [(T_3^{[2]})^{\dagger}]^2 (\frac{1}{6} T_2^3 + \frac{1}{4} T_1^2 T_2^2 + \frac{1}{24} T_1^4 T_2 + \frac{1}{720} T_1^6) | \Phi \rangle. \end{split}$$
(102)

As we can see, the QMMCC(2,6) method introduces the $T_2^{\dagger}(T_3^{[2]})^{\dagger}$ and $\frac{1}{2}[(T_3^{[2]})^{\dagger}]^2$ components into the energy expression. These components originate from the $(\Sigma^{\dagger})^2$ terms in Eq. (91). Their presence in Eq. (101) leads to the appearance of the $M_5(2)|\Phi\rangle$ and $M_6(2)|\Phi\rangle$ quantities and, in consequence, the pentuply and hextuply excited moments, $\mathcal{M}_{a_1 a_2 a_3 a_4 a_5}^{i_1 i_2 i_3 i_4 i_5}(2)$ and $\mathcal{M}_{a_1 a_2 a_3 a_4 a_5 a_6}^{i_1 i_2 i_3 i_4 i_5 i_6}(2)$, respectively, in Eq. (99). The linear terms in Σ^{\dagger} , including $(T_3^{[2]})^{\dagger}$, that are already present in the low-order LMMCC or CR-CCSD[T] and CR-CCSD(T) models and that engage the triply excited moments $\mathcal{M}_{a_1a_2a_3}^{i_1i_2i_3}(2)$, and the quadratic $\frac{1}{2}(T_2^{\dagger})^2$ terms that are present in the CR-CCSD(TQ),b energy and that engage the quadruply excited moments $\mathcal{M}_{a_1 a_2 a_3 a_4}^{i_1 i_2 i_3 i_4}(2)$, are contained in the QMMCC(2,6) energy expression, Eq. (99), too. As a result, the QMMCC(2,6) energy formula involves the complete set of the generalized moments of the CCSD equations, including the desired pentuply and hextuply excited moments, $\mathcal{M}_{a_1a_2a_3a_4a_5}^{i_1i_2i_3i_4i_5}(2)$ and $\mathcal{M}_{a_1 a_2 a_3 a_4 a_5 a_6}^{i_1 i_2 i_3 i_4 i_5 i_6}(2)$, respectively, and, at the same time, it contains all lower-order terms of the CR-CCSD(T) and CR-CCSD(TQ) methods. The QMMCC(2,6) method

should give us an accurate description of triple bond breaking due to the presence of the $\mathcal{M}_{a_1a_2a_3a_4a_5}^{i_1i_2i_3i_4i_5}(2)$ and $\mathcal{M}_{a_1a_2a_3a_4a_5a_6}^{i_1i_2i_3i_4i_5i_6}(2)$ moments and the $T_2^{\dagger}(T_3^{[2]})^{\dagger}$ and $\frac{1}{2}[(T_3^{[2]})^{\dagger}]^2$ terms in Eq. (100).

We have also tested the approximate QMMCC schemes in which we ignore the higher-order terms involving the most expensive hextuply or pentuply and hextuply excited CCSD moments. For example, the summation over n in Eq. (101) reduces to $\sum_{n=3}^{5}$ when we neglect the $\frac{1}{2}[(T_3^{[2]})^{\dagger}]^2$ terms. The resulting QMMCC approximation, termed the QMMCC(2,5) method, does not require the calculation of the most expensive hextuply excited moments $\mathcal{M}_{a_1 a_2 a_3 a_4 a_5 a_6}^{i_1 i_2 i_3 i_4 i_5 i_6}$ (2). The QMMCC(2,5) energy expression can be given the following form:

$$E_0^{\text{QMMCC}(2,5)} = E_0^{(\text{CCSD})} + \delta_0^{(\text{CCSD})}(\text{QMMCC}(2,5)),$$
 (103)

where

$$\delta_0^{(CCSD)}(QMMCC(2,5)) = N^{QMMCC(2,5)}/D^{QMMCC(2,5)},$$
 (104)

with

$$N^{\text{QMMCC}(2,5)} = \sum_{n=3}^{5} \sum_{k=3}^{n} \langle \Psi_{0}^{\text{QMMCC}} | Q_{n} C_{n-k}(2) M_{k}(2) | \Phi \rangle$$

$$= \langle \Phi | [T_{1}^{\dagger} T_{2}^{\dagger} + (T_{3}^{[2]})^{\dagger}] M_{3}(2)$$

$$+ [\frac{1}{2} (T_{2}^{\dagger})^{2} + T_{1}^{\dagger} (T_{3}^{[2]})^{\dagger}] [M_{4}(2) + T_{1} M_{3}(2)]$$

$$+ T_{2}^{\dagger} (T_{3}^{[2]})^{\dagger} [M_{5}(2) + T_{1} M_{4}(2) + (T_{2} + \frac{1}{2} T_{1}^{2}) M_{3}(2)] | \Phi \rangle, \quad (105)$$

and

$$D^{\text{QMMCC}(2,5)} = 1 + \langle \Phi | T_1^{\dagger} T_1 | \Phi \rangle + \langle \Phi | [T_2^{\dagger} + \frac{1}{2} (T_1^{\dagger})^2] (T_2 + \frac{1}{2} T_1^2) | \Phi \rangle$$

$$+ \langle \Phi | [T_1^{\dagger} T_2^{\dagger} + (T_3^{[2]})^{\dagger}] (T_1 T_2 + \frac{1}{6} T_1^3) | \Phi \rangle$$

$$+ \langle \Phi | [\frac{1}{2} (T_2^{\dagger})^2 + T_1^{\dagger} (T_3^{[2]})^{\dagger}] (\frac{1}{2} T_2^2 + \frac{1}{2} T_1^2 T_2 + \frac{1}{24} T_1^4) | \Phi \rangle$$

$$+ \langle \Phi | T_2^{\dagger} (T_3^{[2]})^{\dagger} (\frac{1}{2} T_1 T_2^2 + \frac{1}{6} T_1^3 T_2 + \frac{1}{120} T_1^5) | \Phi \rangle. \tag{106}$$

As we will see in Sect. 5.2.2, the absence of the $\mathcal{M}_{a_1a_2a_3a_4a_5a_6}^{i_1i_2i_3i_4i_5i_6}(2)$ moments and the $\frac{1}{2}[(T_3^{[2]})^{\dagger}]^2$ components in the QMMCC(2,5) energy expression has no detrimental effect on the results of the QMMCC calculations for multiple bond breaking. If we further ignore the $T_2^{\dagger}(T_3^{[2]})^{\dagger}$ terms in the QMMCC(2,6) energy formula, Eq. (99), and the $\frac{1}{2}[(T_3^{[2]})^{\dagger}]^2$ terms that have already been neglected in the QMMCC(2,5) approach, we obtain the QMMCC(2,4) method. The QMMCC(2,4) energy is calculated as follows:

$$E_0^{\text{QMMCC}(2,4)} = E_0^{(\text{CCSD})} + \delta_0^{(\text{CCSD})}(\text{QMMCC}(2,4)),$$
 (107)

where

$$\delta_0^{(CCSD)}(QMMCC(2,4)) = N^{QMMCC(2,4)}/D^{QMMCC(2,4)},$$
 (108)

with

$$N^{\text{QMMCC}(2,4)} = \sum_{n=3}^{4} \sum_{k=3}^{n} \langle \Psi_0^{\text{QMMCC}} | Q_n C_{n-k}(2) M_k(2) | \Phi \rangle$$

$$= \langle \Phi | [T_1^{\dagger} T_2^{\dagger} + (T_3^{[2]})^{\dagger}] M_3(2)$$

$$+ [\frac{1}{2} (T_2^{\dagger})^2 + T_1^{\dagger} (T_3^{[2]})^{\dagger}] [M_4(2) + T_1 M_3(2)] | \Phi \rangle, \qquad (109)$$

and

$$D^{\text{QMMCC}(2,4)} = 1 + \langle \Phi | T_1^{\dagger} T_1 | \Phi \rangle + \langle \Phi | [T_2^{\dagger} + \frac{1}{2} (T_1^{\dagger})^2] (T_2 + \frac{1}{2} T_1^2) | \Phi \rangle$$

$$+ \langle \Phi | [T_1^{\dagger} T_2^{\dagger} + (T_3^{[2]})^{\dagger}] (T_1 T_2 + \frac{1}{6} T_1^3) | \Phi \rangle$$

$$+ \langle \Phi | [\frac{1}{2} (T_2^{\dagger})^2 + T_1^{\dagger} (T_3^{[2]})^{\dagger}] (\frac{1}{2} T_2^2 + \frac{1}{2} T_1^2 T_2 + \frac{1}{24} T_1^4) | \Phi \rangle. \quad (110)$$

As we can see, the QMMCC(2,4) method requires that we only consider the triply and quadruply excited moments of the CCSD equations, $\mathcal{M}_{a_1a_2a_3}^{i_1i_2i_3}(2)$ and $\mathcal{M}_{a_1a_2a_3a_4}^{i_1i_2i_3i_4}(2)$, respectively. In consequence, the QMMCC(2,4) energy formulas, Eqs. (107)–(110), resemble the expressions defining the CR-CCSD(TQ),b approach described in Sect. 4.2 (cf. Eqs. (70), (72), and (74)). The lowest level of the QMMCC approximations, i.e. the QMMCC(2,3) approach, is obtained by neglecting the $\left[\frac{1}{2}(T_2^{\dagger})^2 + T_1^{\dagger}(T_3^{[2]})^{\dagger}\right]$ terms in Eqs. (109) and (110), so that the only moments of the CCSD equations that are included in the QMMCC(2,3) calculations are the triply excited $\mathcal{M}_{a_1a_2a_3}^{i_1i_2i_3}(2)$ moments. We calculate the QMMCC(2,3) energy by using the formula

$$E_0^{\text{QMMCC(2,3)}} = E_0^{(\text{CCSD})} + \delta_0^{(\text{CCSD})}(\text{QMMCC(2,3)}),$$
 (111)

where

$$\delta_0^{(CCSD)}(QMMCC(2,3)) = N^{QMMCC(2,3)}/D^{QMMCC(2,3)},$$
 (112)

with

$$N^{\mathrm{QMMCC}(2,3)} = \langle \Psi_0^{\mathrm{QMMCC}} | Q_3 \, C_0(2) \, M_3(2) | \Phi \rangle$$

$$= \langle \Phi | [T_1^{\dagger} T_2^{\dagger} + (T_3^{[2]})^{\dagger}] M_3(2) | \Phi \rangle, \tag{113}$$

and

$$D^{\text{QMMCC}(2,3)} = 1 + \langle \Phi | T_1^{\dagger} T_1 | \Phi \rangle + \langle \Phi | [T_2^{\dagger} + \frac{1}{2} (T_1^{\dagger})^2] (T_2 + \frac{1}{2} T_1^2) | \Phi \rangle$$
$$+ \langle \Phi | [T_1^{\dagger} T_2^{\dagger} + (T_3^{[2]})^{\dagger}] (T_1 T_2 + \frac{1}{6} T_1^3) | \Phi \rangle. \tag{114}$$

The QMMCC(2,3) energy formulas, Eqs. (111)–(114), are practically identical to the CR-CCSD[T] or CR-CCSD(T) expressions, Eqs. (51) and (52). Thus, we can expect that the QMMCC(2,3) results are virtually identical to the CR-CCSD[T] or CR-CCSD(T) results.

The formal similarity of the QMMCC(2,4) and CR-CCSD(TQ),b approximations immediately implies that the computer costs of the QMMCC(2,4) calculations resemble those of the CR-CCSD(TQ),b calculations. Thus, in analogy to the CR-CCSD(TQ),b method and its standard CCSD(TQ_f) counterpart, the cost of calculating the QMMCC(2,4) energy correction, Eq. (108), is $n_o^2 n_u^5$, where n_o and n_u are the numbers of occupied and unoccupied orbitals, respectively. The QMMCC(2,5) and QMMCC(2,6) methods are somewhat more expensive, although, as shown in Section 5.2.2, we can ignore the most expensive pentuply and hextuply excited moments, $\mathcal{M}_{a_1 a_2 a_3 a_4 a_5}^{i_1 i_2 i_3 i_4 i_5}$ (2) and $\mathcal{M}_{a_1 a_2 a_3 a_4 a_5}^{i_1 i_2 i_3 i_4 i_5}$ (2), respectively, in the QMMCC(2,5) and QMMCC(2,6) energy formulas, Eqs. (103) and (99), respectively, without affecting the excellent QMMCC(2,5) and QMMCC(2,6) results.

The most expensive steps of the full QMMCC(2,6) approximation, on which all

other QMMCC methods are based, scale as $n_o^3 n_u^5$. The relatively low, n^8 -like, cost of computing the noniterative QMMCC(2,6) energy correction may be somewhat surprising, since the hextuply excited moments $\mathcal{M}_{a_1 a_2 a_3 a_4 a_5 a_6}^{i_1 i_2 i_3 i_4 i_5 i_6}(2)$ are twelve-index quantities, but one has to keep in mind the highly factorized character of the QMMCC energy corrections. For example, the most expensive $\frac{1}{2} \langle \Phi | [(T_3^{[2]})^{\dagger}]^2 M_6(2) | \Phi \rangle$ term of the QMMCC(2,6) method has the following form:

$$\frac{1}{2}\langle\Phi|[(T_3^{[2]})^{\dagger}]^2 M_6(2)|\Phi\rangle = \frac{1}{48}\langle\Phi|[(T_3^{[2]})^{\dagger}]^2 (V_N T_2^4)_C|\Phi\rangle, \tag{115}$$

since

$$\mathcal{M}_{a_1 a_2 a_3 a_4 a_5 a_6}^{i_1 i_2 i_3 i_4 i_5 i_6}(2) = \frac{1}{24} \langle \Phi_{i_1 i_2 i_3 i_4 i_5 i_6}^{a_1 a_2 a_3 a_4 a_5 a_6} | (V_N T_2^4)_C | \Phi \rangle, \tag{116}$$

where, as usual, V_N represents the two-body part of the Hamiltonian in the normal-ordered form. The highly factorized character of Eq. (115) allows us to form the intermediates from the $(T_3^{[2]})^{\dagger}$ deexcitation and T_2 excitation cluster amplitudes by connecting the $(T_3^{[2]})^{\dagger}$ and T_2 diagrams with at least two fermion lines. In consequence, we do not have to construct and store the twelve-index hextuply excited moments $\mathcal{M}_{a_1 a_2 a_3 a_4 a_5 a_6}^{i_1 i_2 i_3 i_4 i_5 i_6}(2)$ to calculate terms, such as Eq. (115). This leads to a reduction of the operation count to the $n_o^3 n_u^5$ or less expensive noniterative steps. Similar remarks apply to the QMMCC(2,5) theory, which formally uses the moments $\mathcal{M}_{a_1 a_2 a_3 a_4 a_5}^{i_1 i_2 i_3 i_4 i_5}(2)$. Again, all terms entering the QMMCC(2,5) energy formula are highly factorized and we can completely eliminate the need for calculating and storing ten-index quantities, such as $\mathcal{M}_{a_1 a_2 a_3 a_4 a_5}^{i_1 i_2 i_3 i_4 i_5}(2)$, by connecting the T_2^{\dagger} and $T_3^{(2)}$ vertices entering the pentuply

excited part of Eq. (105) with the T_1 and T_2 vertices entering

$$\mathcal{M}_{a_1 a_2 a_3 a_4 a_5}^{i_1 i_2 i_3 i_4 i_5}(2) = \langle \Phi_{i_1 i_2 i_3 i_4 i_5}^{a_1 a_2 a_3 a_4 a_5} | [V_N(\frac{1}{6}T_2^3 + \frac{1}{4}T_1^2 T_2^2)]_C | \Phi \rangle$$
 (117)

to form the relevant intermediates.

Let us summarize our discussion of the QVMMCC, LMMCC, and QMMCC methods. The QMMCC(2,4) theory is similar in content and computer cost to the existing CR-CCSD(TQ),b method, described in Sect. 4.2. The CR-CCSD(TQ),b method can be viewed as a slightly modified version of the QMMCC(2,4) theory, in which the only bilinear term of the $\frac{1}{2}(\Sigma^{\dagger})^2$ type, multiplying $[M_4(2) + T_1M_3(2)]$, is the lowest-order $\frac{1}{2}(T_2^{\dagger})^2$ term. As demonstrated in Sect. 5.2.2, the QMMCC(2,4) and CR-CCSD(TQ), b results are virtually identical. The LMMCC approach is equivalent to the CR-CCSD[T] method, which is, in turn, only slightly less accurate than the CR-CCSD(T) and QMMCC(2,3) approaches, and considerably less accurate than the CR-CCSD(TQ), b method in applications involving multiple bond breaking (see Sect. 5.2.2). Finally, the QMMCC(2,4) approach represents an approximation to the more complete QMMCC(2,5) and QMMCC(2,6) models. This means that the CR-CCSD(TQ), b or QMMCC(2,4) approaches can be regarded as intermediate steps between the less accurate LMMCC = CR-CCSD[T], CR-CCSD(T), and QMMCC(2,3)methods, which work very well for the ground-state PESs involving single bond breaking (see Sects. 4.2 and 5.2.2), and the more accurate QMMCC(2,5) and QMMCC(2,6) approaches, which, as shown in Sect. 5.2.2, are capable of providing an accurate description of the PESs involving multiple bond breaking. We expect, therefore, to observe the following accuracy patterns in the actual calculations for bond breaking:

$$\begin{split} LMMCC &\equiv CR\text{-}CCSD[T] \lesssim CR\text{-}CCSD(T) \approx QMMCC(2,3) \\ &< CR\text{-}CCSD(TQ), b \approx QMMCC(2,4) \\ &< QMMCC(2,5) \lesssim QMMCC(2,6) \equiv QMMCC \lesssim Full CI. \quad (118) \end{split}$$

5.2.2. Examples of Applications

In order to test the performance of the QMMCC methods, we implemented the entire family of the QMMCC approximations described in the previous section. As in the case of the CI-corrected MMCC(2,5) and MMCC(2,6) methods, we used the spin-adapted CCSD code of Piecuch and Paldus to generate the required T_1 and T_2 cluster amplitudes. The RHF calculations needed to generate molecular orbitals and the integral transformation from the atomic to molecular orbital basis were performed with GAMESS. In programming the QMMCC methods, we relied on the expressions for the generalized moments of the CCSD equations given in Appendices B and C (obtained using the diagrammatic method of MBPT; see Appendix B for the details). We tested the performance of the QMMCC methods by performing the calculations for single bond breaking in HF, double bond breaking in H₂O, triple bond breaking in N₂, and the very challenging type of bond breaking in C₂. In all cases, we used the relatively small DZ basis set, which allowed us to compare the QMMCC results with those obtained with the exact full CI approach.

We already know that all types of single bond breaking (such as bond breaking in HF) are accurately described by the lowest-order MMCC(2,3) approximations, including the CISDt-corrected MMCC(2,3) approach discussed in Sect. 4.1 and the completely renormalized CCSD[T] and CCSD(T) approaches discussed in Sect. 4.2. According to Eq. (118), we expect the results from the QMMCC(2,3) and CR-CCSD[T] or CR-CCSD(T) calculations for single bond breaking in HF to be almost identical. Our test calculations for HF using the QMMCC(2,3) method confirmed this expectation: The QMMCC(2,3) results turned out to be virtually identical (to within less than a millihartree) to the CR-CCSD[T] and CR-CCSD(T) results. Thus, in the following, we focus on the higher-level QMMCC(2,4), QMMCC(2,5), and QMMCC(2,6) approximations. In the case of HF, the small ~1 millihartree unsigned errors in the QMMCC(2,4) results in the entire $R_e \leq R \leq 5R_e$ region are practically identical to the CR-CCSD(TQ) results (see Tables 1 and 6). This is a clear reflection of the accuracy patterns described by Eq. (118). The higher level QMMCC(2,5) and QMMCC(2,6) calculations provide results that are very similar to their lower level QMMCC(2,4) counterparts (see Table 6). This indicates that the inclusion of the more expensive pentuply and hextuply excited moments of the CCSD equations, $\mathcal{M}_{a_1 a_2 a_3 a_4 a_5}^{i_1 i_2 i_3 i_4 i_5}(2)$ and $\mathcal{M}_{a_1 a_2 a_3 a_4 a_5 a_6}^{i_1 i_2 i_3 i_4 i_5 i_6}(2)$, is not providing us with any additional improvements in the QMMCC(2,4) or CR-CCSD(TQ) results for processes involving a dissociation of a single chemical bond. In these cases, the very simple MMCC(2,3)approximations, such as CR-CCSD(T), are sufficient for an accurate description of single bond breaking and the QMMCC(2,4) or CR-CCSD(TQ) approaches provide additional small improvements.

The QMMCC approximations have been developed primarily to improve the poor description of multiple bond dissociation by the standard CC methods, such as CCSD, CCSD[T], CCSD(T), or CCSD(TQ_f). In the context of the simultaneous breaking of both O-H bonds in the H₂O molecule, we would like to reduce, if not completely eliminate, the large negative errors resulting from the CCSD[T], CCSD(T), and $CCSD(TQ_f)$ calculations in the $R = 2R_e$ region (cf. Table 2). We have already discussed the considerable improvements in the results of the standard CC calculations for the double dissociation of water by the completely renormalized CC approaches, such as CR-CCSD(T) or CR-CCSD(TQ) (see Sect. 4.2). In particular, the CR-CCSD(T) and CR-CCSD(TQ) methods reduce the large negative ((-6)-(-11)) millihartree) errors, relative to full CI, obtained in the CCSD[T], CCSD(T), and CCSD(TQ_f) calculations at $R = 2R_e$ to small (< 2-3 millihartree) positive errors (cf. Table 2). We have also mentioned that we can obtain similar improvements in the results of the standard CC calculations by switching to the CI-corrected MMCC(2,3) and MMCC(2,4) methods (see Sect. 4.1; particularly Table 2). The CISDt-corrected MMCC(2,3) method or the CISDtq-corrected MMCC(2,4) approach reduces the larger negative errors in the CCSD[T], CCSD(T), and CCSD(TQ_f) results for $R = 2R_e$ to relatively small ~ 2 millihartree positive errors. As shown in Sect. 5.1, the CISDtqp-corrected MMCC(2,5) scheme and the CISDtqph-corrected MMCC(2,6)approach reduce these errors further, to 0.730 and 0.538 millihartree, respectively (see Table 4). It is interesting to examine whether the QMMCC methods, which can be viewed as the natural extensions of the "black-box" CR-CCSD[T], CR-CCSD(T), and CR-CCSD(TQ) approaches, are capable of providing similar accuracies.

The QMMCC(2,4), QMMCC(2,5), and QMMCC(2,6) results for the H₂O molecule are listed in Table 4. As expected (cf. Eq. (118)), the QMMCC(2,4) approximation, defined by Eqs. (107)-(110), provides results that are virtually identical to the CR-CCSD(TQ) results shown in Table 2. In analogy to the CR-CCSD(TQ) case, the small ~ 0.3 millihartree error in the QMMCC(2,4) energy at $R=R_e$ monotonically increases with R to reach \sim 2 millihartree in the $R=2R_e$ region (cf. Table 4). The QMMCC(2,4) results are also similar to the results of the CISDtq-corrected MMCC(2,4) calculations (cf. Tables 2 and 4). This is quite promising, since, unlike the CISDtq-corrected MMCC(2,4) theory, the QMMCC(2,4) method does not require selecting active orbitals. The QMMCC(2,5) and QMMCC(2,6) methods provide further improvements in the description of the double dissociation of water, particularly in the $R = 2R_e$ region. The 1.163-2.853 millihartree errors in the CR-CCSD[T], CR-CCSD(T), CR-CCSD(TQ), and QMMCC(2,4) results at $R = 2R_e$ reduce to < 0.6 millihartree when the QMMCC(2,5) and QMMCC(2,6) methods are employed. The description of the double dissociation of the H_2O molecule by the QMMCC(2,6) method is as good as the excellent description of this process by the CISDtqphcorrected MMCC(2,6) approach, which requires that we first perform multireferencelike CISDtqph calculations (see Table 4). It is remarkable to observe that the 1.790, 5.590, and 9.333 millihartree errors in the CCSD results at $R = R_e$, 1.5 R_e , and $2R_e$, respectively, can be reduced to < 0.7 millihartree in the entire $R = R_e - 2R_e$ region by adding to the CCSD energies, the a posteriori noniterative QMMCC energy corrections, employing only T_1 and T_2 components obtained in the CCSD calculations.

The results of the QMMCC(2,5) calculations are somewhat surprising (in a pos-

itive sense). The QMMCC(2,5) energies are essentially identical to the excellent QMMCC(2,6) energies at all values of R. This implies that we can almost certainly ignore the most expensive hextuply excited $\mathcal{M}_{a_1a_2a_3a_4a_5a_6}^{i_1i_2i_3i_4i_5i_6}(2)$ moments and the corresponding $\frac{1}{2}[(T_3^{[2]})^\dagger]^2|\Psi_0\rangle$ wave function components that are present in the QMMCC(2,6) energy expression without sacrificing the high quality of the QMMCC results. In fact, we can neglect the $\mathcal{M}_{a_1 a_2 a_3 a_4 a_5}^{i_1 i_2 i_3 i_4 i_5}(2)$ and $\mathcal{M}_{a_1 a_2 a_3 a_4 a_5 a_6}^{i_1 i_2 i_3 i_4 i_5 i_6}(2)$ moments in the complete QMMCC or QMMCC(2,6) energy formula, Eq. (99), without compromising the excellent QMMCC(2,6) results. The 0.2-0.7 millihartree errors in the QMMCC results for H₂O, obtained by zeroing the $\mathcal{M}^{i_1i_2i_3i_4i_5}_{a_1a_2a_3a_4a_5}(2)$ and $\mathcal{M}^{i_1i_2i_3i_4i_5i_6}_{a_1a_2a_3a_4a_5a_6}(2)$ moments in the QMMCC(2,6) energy formulas, are as small as the errors in the results of the complete QMMCC(2,6) calculations, in which all generalized moments of the CCSD equations are included (see Table 4). By ignoring the $\mathcal{M}_{a_1a_2a_3a_4a_5}^{i_1i_2i_3i_4i_5}(2)$ and $\mathcal{M}_{a_1a_2a_3a_4a_5a_6}^{i_1i_2i_3i_4i_5i_6}(2)$ moments of the CCSD equations in the QMMCC(2,6) energy expression, we are essentially preserving the simplicity and the relatively low cost of the CR-CCSD(TQ) calculations. This means that we may be able to obtain < 1 millihartree errors for cases involving a simultaneous breaking of two single bonds with an effort comparable to the CR-CCSD(TQ) calculations. Based on the results of the QMMCC calculations for H₂O, shown in Table 4, the QMMCC method, in which the $\mathcal{M}_{a_1a_2a_3a_4a_5}^{i_1i_2i_3i_4i_5}(2)$ and $\mathcal{M}_{a_1a_2a_3a_4a_5a_6}^{i_1i_2i_3i_4i_5i_6}(2)$ moments are ignored, is definitely worth further exploration. We can also use the QMMCC(2,5) method, defined by Eq. (103), and obtain results for the double dissociation of water that can only be matched by the excellent results of the QMMCC(2,6) or CISDtqph-corrected MMCC(2,6) calculations (see Table 4). Our benchmark calculations for the water molecule clearly reflect the accuracy pattern described by Eq. (118).

The most critical test of the QMMCC theory is provided by triple bond breaking in N₂. As mentioned in Sect. 4.2, the ground-state PESs obtained in the CR-CCSD(T) and CR-CCSD(TQ) calculations for dissociations of single and double bonds are usually very good but, when triple bond breaking is involved, the CR-CCSD(T) and CR-CCSD(TQ) results become less accurate. For example, the 25.069 millihartree error in the CR-CCSD(TQ), b results for N_2 at $R=2R_e$, although much smaller than the 246.405 and 92.981 millihartree errors obtained with the standard CCSD(T) and $CCSD(TQ_f)$ approaches, is far too big for the highly accurate description of the potential energy curve for N₂. The CR-CCSD(T) results for N₂ at larger values of R are even worse than the CR-CCSD(TQ) results (see Table 3). Thus, the CR-CCSD(T) and CR-CCSD(TQ) methods are not sufficient to obtain highly accurate PESs involving multiple bond breaking, although, undoubtedly, the CR-CCSD(TQ), b results for N₂ are much better than the results of the standard CC calculations (including the relatively expensive full CCSDT and CCSDT(Q_f) calculations; cf. Table 3 and Fig. 2). The unphysical humps and other unphysical features of PESs obtained in the standard CCSD, CCSD(T), CCSD(TQ_f), CCSDT, and $CCSDT(Q_f)$ calculations are almost entirely eliminated by the CR-CCSD(TQ), b approach (see Table 3 and Fig. 2), but the 10-25 millihartree differences between the CR-CCSD(TQ), b and full CI energies at intermediate and larger values of the N-N separation R are too large for the majority of applications including the dynamics describing the N_2 molecule. We already know that the CISDtqph-corrected MMCC(2,6) approach provides the desired improvements in the description of triple

bond breaking in N₂, reducing the 10-25 millihartree differences between the CR-CCSD(TQ), b and full CI energies at intermediate and larger internuclear separations R to 4.0-4.5 millihartree (see Sect. 5.1, particularly Table 5 and Fig. 3). We must keep in mind, however, that the CISDtqph-corrected MMCC(2,6) approach requires that we select active orbitals for the CISDtqph calculations that are needed to construct wave function $|\Psi_0\rangle$ entering the MMCC(2,6) energy expression (82). In other words, although the CISDtqph-corrected MMCC(2,6) can be viewed as a noniterative CC approximation that provides an excellent description of triple bond breaking, this method is not a pure "black-box" of the CCSD(T) or CCSD(TQ_f) type, since we must make some arbitrary decisions about active orbitals in order to carry out the related CISDtoph calculations (and these calculations also increase the computer effort). Clearly, it is interesting to examine if we can reduce the 10-25 millihartree errors resulting from the CR-CCSD(TQ), b calculations at larger values of R to a few millihartree by using the QMMCC(2,6) method, which is a "black-box" equivalent of the highly successful CISDtqph-corrected MMCC(2,6) approximation.

The QMMCC results for the N_2 molecule obtained by adding the QMMCC(2,4), QMMCC(2,5), and QMMCC(2,6) corrections to the CCSD energies according to Eqs. (99)–(110), are shown in Table 5 and Fig. 4. As we can see, the QMMCC(2,5) and QMMCC(2,6) methods are capable of providing an excellent description of the entire $R = 0.75R_e - 2.25R_e$ region of the N_2 potential energy curve. The very large negative errors in the CCSD results for N_2 in the $R > 1.75R_e$ region and the 13.517, 25.069, and 14.796 millihartree errors in the CR-CCSD(TQ),b results at $R = 1.75R_e$, $2R_e$, and $2.25R_e$, are reduced by the complete QMMCC(2,6) method to 1.380, 6.230, and -3.440

millihartree, respectively. This is quite remarkable, considering the single-reference and noniterative character of the QMMCC energy corrections and the complete failure of the CCSD approximation, on which the QMMCC(2,6) and other QMMCC methods are based, at larger internuclear separations. As in the case of H₂O, the QMMCC(2,5) results for N₂ are almost identical to the excellent QMMCC(2,6) results.

As shown in Fig. 4, the QMMCC(2,6) potential energy curve for N₂ is located above the full CI curve in the entire $R < 2.25R_e$ region, in spite of the catastrophic failure and the apparently non-variational behavior of the CCSD method at larger N-N separations. The QMMCC(2,6) potential energy curve and the full CI curve almost overlap in the entire $0.75R_e \leq R \leq 2.25R_e$ region. The QMMCC(2,6) potential is a monotonically increasing function in the entire 2.068 bohr $\leq R \leq$ 4.35 bohr region (recall that R = 2.068 bohr is the equilibrium bond length in N_2). It is only when $R \approx 2.25R_e$ that the QMMCC(2,6) energies slightly decrease, but even in this case the errors in the QMMCC(2,6) results, relative to full CI, are less (in absolute value) than 3.5 millihartree (see Table 5). The approximate dissociation energy D_e , calculated by forming the difference between the QMMCC(2,6) energies at R=4.35bohr and $R = R_e$, is 6.59 eV, in excellent agreement with the full CI value of D_e of 6.61 eV. Thus, the QMMCC theory represents an approximately variational formalism, which is capable of providing an excellent description of the large part of the potential energy curve of N_2 .

Our experience with the QMMCC results for the simultaneous dissociation of both O-H bonds in H₂O tells us that it might be worth examining the effect of neglecting the most expensive moments of the CCSD equations, i.e. $\mathcal{M}_{a_1 a_2 a_3 a_4 a_5}^{i_1 i_2 i_3 i_4 i_5}$ (2) and

 $\mathcal{M}_{a_1 a_2 a_3 a_4 a_5 a_6}^{i_1 i_2 i_3 i_4 i_5 i_6}(2)$, in the QMMCC calculations for N_2 . We have already noticed that the QMMCC(2,5) method, in which the $\mathcal{M}_{a_1a_2a_3a_4a_5a_6}^{i_1i_2i_3i_4i_5i_6}(2)$ moments are ignored, provides results of the full QMMCC(2,6) quality (cf. Table 5 and Fig. 4). The large, 30-120 millihartree, unsigned errors in the CCSD results in the $R \geq 1.5R_e$ region are reduced to 3.756 millihartree at $R = 1.5R_e$, 1.415 millihartree at $R = 1.75R_e$, 6.672 millihartree at $R = 2R_e$, and 2.638 millihartree at $R = 2.25R_e$ when the QMMCC(2,5) approach is employed. When the pentuply and hextuply excited moments, $\mathcal{M}_{a_1 a_2 a_3 a_4 a_5}^{i_1 i_2 i_3 i_4 i_5}(2)$ and $\mathcal{M}_{a_1 a_2 a_3 a_4 a_5 a_6}^{i_1 i_2 i_3 i_4 i_5 i_6}(2)$, respectively, are neglected, the errors in the QMMCC(2,6) calculations increase slightly, but the overall performance of the QMMCC(2,6) approximation, in which $\mathcal{M}_{a_1a_2a_3a_4a_5}^{i_1i_2i_3i_4i_5}(2)$ and $\mathcal{M}_{a_1a_2a_3a_4a_5a_6}^{i_1i_2i_3i_4i_5i_6}(2)$ are zeroed, remains very good (see Table 5). The potential energy curve of N₂, obtained by performing the QMMCC(2,6) calculations in which the pentuply and hextuply excited moments are zeroed, is monotonically increasing in the entire $R_e \leq R \leq 2R_e$ region. The approximate dissociation energy D_e , obtained by forming the difference between the QMMCC(2,6)($\mathcal{M}_{a_1a_2a_3a_4a_5}^{i_1i_2i_3i_4i_5}(2) = \mathcal{M}_{a_1a_2a_3a_4a_5a_6}^{i_1i_2i_3i_4i_5i_6}(2) = 0$) energies at $R = 2R_e$ and $R = R_e$, is 6.54 eV, in very good agreement with the full CI D_e value of 6.61 eV. The somewhat more complete QMMCC(2,6) calculations, in which only the hextuply excited $\mathcal{M}_{a_1a_2a_3a_4a_5a_6}^{i_1i_2i_3i_4i_5i_6}(2)$ moments are zeroed, and the QMMCC(2,5) calculations produce D_e values, which are only slightly more accurate than the value of D_e resulting from the QMMCC(2,6)($\mathcal{M}_{a_1a_2a_3a_4a_5}^{i_1i_2i_3i_4i_5}(2) = \mathcal{M}_{a_1a_2a_3a_4a_5a_6}^{i_1i_2i_3i_4i_5i_6}(2) = 0$) calculations (6.59 and 6.61 eV, respectively). Based on the results of the QMMCC calculations for the N₂ molecule, we can conclude that it is not absolutely necessary to include the pentuply and hextuply excited moments of the CCSD equations in order to obtain an excellent description of triple bond breaking as long as we maintain the specific, highly factorized, many-body structure of the noniterative energy corrections defining the QMMCC(2,5) and QMMCC(2,6) approaches (cf. Eqs. (100)-(102) and (104)-(106)).

As in the case of H_2O (and as predicted by Eq. (118)), the QMMCC(2,4) results for N_2 are essentially identical to those obtained with the CR-CCSD(TQ),b approach (cf. Tables 3 and 5 or Figs. 2 and 4). This implies that we cannot ignore the $T_2^{\dagger}(T_3^{[2]})^{\dagger}$ terms in the QMMCC(2,6) or QMMCC(2,5) energy expressions, Eqs. (99)–(106), although, as shown above, we can certainly ignore the corresponding pentuply excited $\mathcal{M}_{a_1a_2a_3a_4a_5}^{i_1i_2i_3i_4i_5}$ (2) moments. Our QMMCC(2,5) calculations imply that we can safely neglect the $\frac{1}{2}[(T_3^{[2]})^{\dagger}]^2$ terms and the corresponding hextuply excited $\mathcal{M}_{a_1a_2a_3a_4a_5a_6}^{i_1i_2i_3i_4i_5i_6}$ (2) moments in the QMMCC(2,6) energy expressions. The accuracy patterns described by Eq. (118) are clearly reflected in our calculations for the N_2 molecule. This means that the noniterative QMMCC corrections provide us with a systematic way of improving the standard and renormalized CC results for multiple bond breaking.

We also applied the QMMCC methods to the very complicated case of bond breaking in the C_2 molecule. The C_2 molecule is characterized by an unusual ordering of the $\sigma(2p)$ and $\pi(2p)$ shells and the proximity of the highest occupied π and lowest unoccupied σ orbitals, which cause a quasi-degeneracy of the ground-state wave function even at the equilibrium geometry. In analogy to N_2 , the C_2 molecule is characterized by large T_n effects, where n > 2, even at the equilibrium geometry. The effect of T_3 clusters in C_2 for the DZ basis set at $R = R_e$, as measured by the difference between the CCSDT and CCSD energies, is 18.593 millihartree. The difference between the

 T_4 clusters are important too. As in the N_2 case, all standard single-reference CC approaches, including the iterative CCSD and CCSDT methods and their perturbative CCSD(T) and CCSD(TQ_f) extensions, fail to provide a correct description of the potential energy curve of C_2 (see Fig. 5).

As shown in Table 7, the error in the CCSD result at $R=R_e$ is 20.684 millihartree. For $R \geq 1.75R_e$, the CCSD results seem to improve, providing unsigned errors of 36.280, 15.772, and 3.422 millihartree at $R = 1.75R_e$, $2R_e$, and $2.5R_e$, respectively. However, at $R \approx 2.5R_e$, the CCSD potential energy curve goes below the full CI curve (see Table 7 and Fig. 5). This is a clear indication of the imminent breakdown of the CCSD theory at larger internuclear C-C separations. The standard noniterative CC methods, such as CCSD(T) and $CCSD(TQ_f)$, in which the effects due to triples and quadruples are obtained from MBPT, provide reasonable results for $R < 1.75R_e$, but in the $R > 1.75R_e$ region, the CCSD(T) and CCSD(TQ_f) approaches completely fail. The unsigned errors in the CCSD(T) and CCSD(TQ_f) calculations, which are 80.231 and 29.196 millihartree, respectively, at $R = 2.5R_e$, increase to 96.055 and 67.237 millihartree at $R = 3R_e$. The CCSD, CCSD(T), and full CCSDT curves have big humps in the region of intermediate R values (see Fig. 5). The CR-CCSD(TQ),b approach is capable of reducing the large errors in the standard CC results in the $R \geq 2R_e$ region to ~20 millihartree, and the shape of the CR-CCSD(TQ),b curve is qualitatively correct, but it is interesting to examine if we can get further improvements in the results for C₂ by switching to the QMMCC theory. As shown in Table 7, the QMMCC(2,4), QMMCC(2,5), and QMMCC(2,6) methods reduce the 20.684 millihartree error in the CCSD result at $R=R_e$ to 2.875-4.991 millihartree. For

stretched geometries, the improvements offered by the QMMCC approximations are even more dramatic. In particular, the huge errors in the CCSD(T) and CCSD(TQ_f) results in the $R = 2.5R_e - 3R_e$ region reduce to relatively small ~11-13 millihartree errors when the QMMCC(2,5) and QMMCC(2,6) calculations are performed. The QMMCC(2,5) and QMMCC(2,6) potential energy curves are located near the full CI curve and all QMMCC energies are invariably above their exact full CI counterparts (see Fig. 5 and Table 7). In analogy to the N₂ molecule, the QMMCC(2,4) results are not as good as the QMMCC(2,5) and QMMCC(2,6) results. As one might expect based on Eq. (118), the QMMCC(2,4) results are almost identical to the CR-CCSD(TQ),b results.

It is again interesting to note that the QMMCC(2,5) and QMMCC(2,6) results are almost identical (see Table 7). Indeed, the energy differences of the QMMCC(2,5) and QMMCC(2,6) results in the entire $R=0.75R_e-3R_e$ region do not exceed 0.012 millihartree. This means that we can ignore the most expensive hextuply excited moments, $\mathcal{M}_{a_1a_2a_3a_4a_3a_6}^{i_1i_2i_3i_4i_5i_6}(2)$, in the calculations for C_2 without affecting the results. In analogy to the N_2 molecule, the simplified QMMCC(2,6) method, obtained by zeroing the $\mathcal{M}_{a_1a_2a_3a_4a_3}^{i_1i_2i_3i_4i_5}(2)$ and $\mathcal{M}_{a_1a_2a_3a_4a_5a_6}^{i_1i_2i_3i_4i_5i_6}(2)$ moments, produces results that are similar to the results of the complete QMMCC(2,6) calculations. The fact that we still have 11-23 millihartree errors in the $R \geq 1.5R_e$ region with the QMMCC(2,5) and QMMCC(2,6) methods needs to be addressed, but we must keep in mind the challenging nature of the bond breaking in C_2 on the one hand and the single-reference character of the noniterative QMMCC corrections on the other hand. We think that one of the reasons why we find these relatively large deviations from the full CI re-

sults with the QMMCC methods is the fact that the CCSD approach, on which the QMMCC approximations are based, provides cluster amplitudes that are much too unphysical to yield a highly accurate description of the C₂ curve by means of noniterative QMMCC corrections. In Sect. 6, we suggest a method that might improve the QMMCC results for C₂ in the region of intermediate and large C-C separations.

5.2.3. Conclusion

In this section, we introduced the new classes of the MMCC "black-box" approximations, referred to as the QVMMCC and QMMCC models. As in all MMCC methods, the main idea of the QVMMCC and QMMCC approximations is that of the noniterative energy corrections which, when added to the energies obtained in the standard CC (e.g., CCSD) calculations, provide highly accurate description of quasi-degenerate states and bond breaking.

We demonstrated that the QMMCC corrections to the standard CCSD energies lead to an excellent description of double dissociation of water and triple bond breaking in N_2 . The QMMCC corrections are capable of restoring the virtually exact description of the large part of the N_2 potential energy curve, in spite of the apparent failure of the CCSD theory at larger internuclear separations and in spite of the fact that we only use the CCSD values of the T_1 and T_2 cluster amplitudes in constructing the QMMCC corrections obtained with the RHF reference.

The QMMCC methods can be regarded as the higher-order analogs of the previ-

ously proposed (also MMCC-based) CR-CCSD[T], CR-CCSD(T), and CR-CCSD(TQ) approximations, which work well for single and double bond breaking, but which fail to provide a highly accurate description of triple bond breaking. The QVMMCC and QMMCC methods provide a systematic way of improving the CR-CCSD[T], CR-CCSD(T), and CR-CCSD(TQ) results, particularly when multiple bond breaking is considered.

The main reason for the success of the QMMCC methods is a specific, highly factorized, many-body structure of the corresponding energy corrections $\delta_0^{(\text{CCSD})}$, which would have never been discovered if we had only relied on the conventional MBPT arguments in the design of these corrections. The presence of the higher-order pentuply and hextuply excited moments of the CCSD equations in the QMMCC energy expressions seems to be of secondary significance. The presence of various bilinear terms, such as $\frac{1}{2}(T_2^{\dagger})^2$ and $T_2^{\dagger}(T_3^{[2]})^{\dagger}$, seems to be much more important in reducing the huge errors in the CCSD results for multiple bond breaking to a few millihartree, rather than the presence of the pentuply and hextuply excited CCSD moments.

6. Summary, Concluding Remarks, and Future Perspectives

In this thesis, we have described several new ideas in the area of highly accurate coupled-cluster (CC) calculations for molecular potential energy surfaces involving bond breaking. The main focus of this work has been the extension of the applicability of the method of moments of coupled-cluster equations (MMCC) and renormalized coupled-cluster approaches of Kowalski and Piecuch to multiple bond breaking. We have accomplished this goal by developing new classes of the CI-corrected MMCC methods and quasi-variational (QV) and quadratic (Q) MMCC approaches.

The main idea of all MMCC methods, including new methods developed in this work, is that of noniterative energy corrections which, when added to the energies obtained in the standard CC calculations, such as CCSD, recover a virtually exact description of many-electron systems. The MMCC formalism provides us with rigorous relationships between the standard CC energies and their exact full CI counterparts. By estimating the differences of the full CI and CC energies in a given basis set using the MMCC expressions, we can obtain results that are significantly better than the results of standard CC calculations. This is particularly true in quasi-degenerate situations, such as bond breaking, where the conventional arguments originating from MBPT, on which the standard noniterative CC approximations, such as CCSD(T), are based, fail due to the divergent behavior of the MBPT expansions at larger internuclear separations.

The MMCC formalism leads to various approximations, including the renormalized (R) and completely renormalized (CR) CCSD(T) and CCSD(TQ) methods. The

CR-CCSD(T) and CR-CCSD(TQ) approaches remove the pervasive failing of the standard CCSD(T) and $CCSD(TQ_f)$ approximations for single bond breaking and some cases of multiple bond dissociation, but in severe cases of multiple bond breaking, they do not work well. We can use the CI-corrected MMCC(2,3) and MMCC(2,4) methods instead of the CR-CCSD(T) and CR-CCSD(TQ) approaches, but their performance in cases of multiple bond breaking is almost identical to the performance of the CR-CCSD(T) and CR-CCSD(TQ) methods.

In order to change this situation, we have proposed two new classes of the MMCC approximations: (i) the CI-corrected MMCC(2,5) and MMCC(2,6) methods and (ii) the QVMMCC and QMMCC approaches. In the former methods, we design the MMCC corrections to the CCSD energies by utilizing all or almost all generalized moments of the CC equations, and by performing the *a priori* limited CI calculations with a small set of pentuple and hextuple excitations defined through active orbitals that provide the wave function $|\Psi_0\rangle$ entering the MMCC energy expressions. Our test calculations for the double dissociation of water and triple bond breaking in N₂ clearly indicate that the CI-corrected MMCC(2,6) approach is capable of providing \sim 1 millihartree or better accuracies in the description of multiple bond breaking. This is an important finding, demonstrating the usefulness of the MMCC theory in designing noniterative CC methods for molecular potential energy surfaces.

Two factors contribute to the success of the CI-corrected MMCC(2,6) method. First of all, the MMCC(2,6) approach is the lowest-order MMCC approximation that utilizes the complete set of moments of the CCSD equations, including the pentuply and hextuply excited moments ignored in the earlier studies. Second, the CISDtqph

wave function $|\Psi_0\rangle$ used in the design of the MMCC(2,6) energy correction provides a reasonable description of multiple bond breaking. By inserting the CISDtqph wave function $|\Psi_0\rangle$ into the MMCC(2,6) energy expression, we obtain a virtually exact description of multiple bond dissociation.

The only practical problem with the CI-corrected MMCC(2,6) approach is that this method requires defining active orbitals. In other words, the CI corrected MMCC(2,6) method is not as easy to use as the standard and renormalized CCSD(T) and CCSD(TQ) approaches. This issue has been addressed in this thesis research by developing the QVMMCC and QMMCC methods. The QMMCC methods can be regarded as the higher-order extensions of the existing "black-box" CR-CCSD(T) and CR-CCSD(TQ) approaches that work for single as well as multiple bond breaking. We confirmed this by performing calculations for the double dissociation of water and triple bond breaking in N_2 , obtaining ~ 1 millihartree accuracies in both cases. For single bond breaking (we used HF as a test case), the QMMCC methods work as well as the CR-CCSD(T) and CR-CCSD(TQ) approximations, which provide excellent results in this case.

The only case where the QMMCC methods did not work as well as expected was the bond breaking in C_2 . The QMMCC methods provide significant improvements over the standard and renormalized CCSD(T) and CCSD(TQ) results in this case, but the potential energy curves obtained in the QMMCC calculations are characterized by 10–20 millihartree errors at larger C–C separations. The main reason for this poorer performance of the QMMCC methods is the extremely low quality of the T_1 and T_2 cluster amplitudes used to construct the QMMCC corrections.

The poorer performance of the QMMCC approximations for C_2 calls for further studies. We believe that the best course of action in this area will be to improve the quality of the T_1 and T_2 cluster operators that are used in the design of the QMMCC and other MMCC energy corrections. We might, for example, try to minimize the expectation value of the Hamiltonian with the CCSD wave function, i.e.,

$$E_0^{\text{VCC}}(T_1, T_2) = \langle \Phi | e^{T_1^{\dagger} + T_2^{\dagger}} H e^{T_1 + T_2} | \Phi \rangle / \langle \Phi | e^{T_1^{\dagger} + T_2^{\dagger}} e^{T_1 + T_2} | \Phi \rangle , \qquad (119)$$

with respect to cluster amplitudes $t_{a_1}^{i_1}$ and $t_{a_1a_2}^{i_1i_2}$ defining T_1 and T_2 instead of calculating T_1 and T_2 by the standard CCSD method. This would enable us to obtain the variationally best T_1 and T_2 operators, which might be better for the MMCC calculations. Unfortunately, it is very difficult to propose an efficient algorithm for calculating the energy expressions of the type of Eq. (119), since the expectation value of the Hamiltonian with a CC wave function represents a nonterminating series in cluster components. 16 There are, however, other ways of improving the quality of T_1 and T_2 clusters. For example, Piecuch et. al. 135,136,144 have recently demonstrated that one can obtain reasonably good T_1 and T_2 cluster amplitudes, in a computationally tractable fashion, without resorting to the nonterminating series in cluster components resulting from Eq. (119), by using the extended CCSD (ECCSD) method or one of its approximate variants based on the ECC theory. 145-155 Just like the standard CCSD theory, the ECCSD approach uses only one and two-body cluster components. The only difference between the standard CCSD method and the ECCSD approach is the use of two independent sets of singly and doubly excited cluster amplitudes in

the ECCSD calculations. As shown by Piecuch $et\ al.,^{135,136,144}$ the T_1 and T_2 clusters resulting from the ECCSD calculations are of much higher quality than the T_1 and T_2 clusters obtained with the standard CCSD method. In particular, the ECCSD method applied to N_2 does not suffer from the non-variational collapse observed in the CCSD calculations at larger N-N separations. Thus, it will be very interesting to examine the effect on the QMMCC and other MMCC results due to using the better T_1 and T_2 clusters resulting from the ECCSD calculations. The preliminary results for the minimum basis set model of N_2 are most encouraging. There is, therefore, some hope that we will have new ways of improving the results for the most challenging types of bond breaking (such as that in C_2) by combining the ECCSD and MMCC ideas.

Appendices

Appendix A. An elementary derivation of Eq. (21)

The MMCC theory and all MMCC approximations, including the renormalized and completely renormalized CCSD[T], CCSD(T), and CCSD(TQ) approaches, the CI-corrected MMCC methods, and the quasi-variational and quadratic MMCC methods, are based on Eq. (21). An elementary derivation of Eq. (21), based on applying the resolution of identity to the asymmetric energy expression, Eq. (24), is presented in this Appendix (see Ref. 46 for the original proof; cf., also, Ref. 45 for the alternative derivation).

First, we insert the resolution of identity,

$$P + \sum_{n=1}^{N} Q_n = 1, (120)$$

where

$$P = |\Phi\rangle\langle\Phi| \tag{121}$$

is the projection operator onto the one-dimensional subspace spanned by the reference configuration $|\Phi\rangle$ and

$$Q_n = \sum_{\substack{i_1 < \dots < i_n \\ a_1 < \dots < a_n}} |\Phi_{i_1 \dots i_n}^{a_1 \dots a_n} \rangle \langle \Phi_{i_1 \dots i_n}^{a_1 \dots a_n}|$$

$$(122)$$

is the projection operator onto the subspace spanned by the *n*-tuply excited configurations relative to $|\Phi\rangle$, into Eq. (24) defining the MMCC functional $\Lambda^{CC}[\Psi]$. We get

$$\Lambda^{\text{CC}}[\Psi] = \langle \Psi | P(H - E_0^{(A)}) e^{T^{(A)}} | \Phi \rangle / \langle \Psi | e^{T^{(A)}} | \Phi \rangle
+ \sum_{n=1}^{N} \langle \Psi | Q_n (H - E_0^{(A)}) e^{T^{(A)}} | \Phi \rangle / \langle \Psi | e^{T^{(A)}} | \Phi \rangle .$$
(123)

The cluster operator $T^{(A)}$ is an excitation operator so that $(T^{(A)})^{\dagger}$ and its positive powers annihilate $|\Phi\rangle$. Thus, the formula for the CC energy can be rewritten as follows (cf. Eq. (16)):

$$E_0^{(A)} = \langle \Phi | e^{-T^{(A)}} H e^{T^{(A)}} | \Phi \rangle = \langle \Phi | H e^{T^{(A)}} | \Phi \rangle. \tag{124}$$

This implies that the first term on the right-hand side of Eq. (123) vanishes. Indeed,

$$\langle \Psi | P(H - E_0^{(A)}) e^{T^{(A)}} | \Phi \rangle / \langle \Psi | e^{T^{(A)}} | \Phi \rangle = \langle \Psi | \Phi \rangle \left(\langle \Phi | H e^{T^{(A)}} | \Phi \rangle - E_0^{(A)} \right) /$$

$$\langle \Psi | e^{T^{(A)}} | \Phi \rangle$$

$$= 0, \qquad (125)$$

so that

$$\Lambda^{\rm CC}[\Psi] = \sum_{n=1}^{N} \langle \Psi | Q_n \left(H - E_0^{(A)} \right) e^{T^{(A)}} | \Phi \rangle / \langle \Psi | e^{T^{(A)}} | \Phi \rangle. \tag{126}$$

Next, we apply the well-known property of the CC exponential ansatz, 15,16,35,38,45

$$He^{T^{(A)}}|\Phi\rangle = e^{T^{(A)}}(He^{T^{(A)}})_C|\Phi\rangle = e^{T^{(A)}}\bar{H}^{(A)}|\Phi\rangle,$$
 (127)

where $\bar{H}^{(A)}$ is the similarity-transformed Hamiltonian of the CC theory, Eq. (9), to obtain the expression

$$Q_n H e^{T^{(A)}} |\Phi\rangle = Q_n e^{T^{(A)}} \bar{H}^{(A)} |\Phi\rangle = \sum_{k=0}^n Q_n (e^{T^{(A)}})_{n-k} \bar{H}_k^{(A)} |\Phi\rangle, \qquad (128)$$

where, in general, O_k represents the k-body component of operator O. We can obtain Eq. (127) by multiplying $He^{T^{(A)}}|\Phi\rangle$ on the left by $e^{T^{(A)}}e^{-T^{(A)}}=1$ and by realizing that the similarity-transformed Hamiltonian $\bar{H}^{(A)}$ can be identified with the connected product of H and $e^{T^{(A)}}$ (see, e.g., Refs. 35, 38, 45 for more information). The k=0 term in Eq. (128) gives the unlinked, energy-dependent, part of $Q_n He^{T^{(A)}}|\Phi\rangle$, namely, $E_0^{(A)}Q_ne^{T^{(A)}}|\Phi\rangle$ (see Eq. (16)). This immediately implies that Eq. (128) can be rewritten in the following form:^{45,46}

$$Q_n (H - E_0^{(A)}) e^{T^{(A)}} |\Phi\rangle = \sum_{k=1}^n Q_n (e^{T^{(A)}})_{n-k} \bar{H}_k^{(A)} |\Phi\rangle = \sum_{k=1}^n Q_n C_{n-k}(m_A) M_k(m_A) |\Phi\rangle,$$
(129)

where $C_{n-k}(m_A)$ is the (n-k)-body component of $e^{T^{(A)}}$, Eq. (22), and $M_k(m_A)|\Phi\rangle$ is defined by Eq. (23). In deriving Eq. (129), we used the identity

$$\bar{H}_k^{(A)}|\Phi\rangle = Q_k \bar{H}^{(A)}|\Phi\rangle \equiv M_k(m_A)|\Phi\rangle.$$
 (130)

Before we proceed further, let us comment on the many-body structure of Eq. (129). Since the zero-body contribution $C_0(m_A) = (e^{T^{(A)}})_0$ equals 1, the k = n term in Eq. (129) corresponds to the connected component of $Q_n He^{T^{(A)}}|\Phi\rangle$, i.e., $Q_n(He^{T^{(A)}})_C|\Phi\rangle$. Thus, all remaining terms in Eq. (129) with 0 < k < n represent the linked but disconnected components of $Q_n He^{T^{(A)}}|\Phi\rangle$ (see Ref. 45 for further details).

In order to complete the derivation of Eq. (21), we substitute Eq. (129) into Eq.

(126) to obtain the following result:

$$\Lambda^{\text{CC}}[\Psi] = \sum_{n=1}^{N} \sum_{k=1}^{n} \langle \Psi | Q_n C_{n-k}(m_A) M_k(m_A) | \Phi \rangle / \langle \Psi | e^{T^{(A)}} | \Phi \rangle.$$
 (131)

From Eq. (24), it immediately follows that we can replace $\Lambda^{\rm CC}[\Psi]$ by the energy difference $E_0 - E_0^{(A)} \equiv \delta_0^{(A)}$, where E_0 is the exact, full CI, energy if $|\Psi\rangle$ is the full CI state $|\Psi_0\rangle$. Thus,

$$\delta_0^{(A)} = \sum_{n=1}^N \sum_{k=1}^n \langle \Psi_0 | Q_n \, C_{n-j}(m_A) \, M_k(m_A) | \Phi \rangle / \langle \Psi_0 | e^{T^{(A)}} | \Phi \rangle \,. \tag{132}$$

Eq. (132) is valid for any values of the cluster amplitudes defining $T^{(A)}$. In practical applications of the MMCC theory, we assume, of course, that $T^{(A)}$ is obtained by solving the standard CC equations, Eq. (8), such that the generalized moments $\mathcal{M}_{a_1...a_k}^{i_1...i_k}(m_A)$ with $k=1,\ldots,m_A$ vanish. This immediately implies that (cf. Eqs. (8), (20), and (23))

$$M_k(m_A)|\Phi\rangle = 0$$
, for $k = 1, \dots, m_A$. (133)

The substitution of Eq. (133) into Eq. (132) reduces the summations over n and k in Eq. (132) to $\sum_{n=m_A+1}^{N} \sum_{k=m_A+1}^{n}$, giving us the desired result, Eq. (21).

Appendix B. The many-body diagrams for the generalized moments of the CCSD equations

The explicit expressions for the generalized moments of the CCSD equations that appear in the MMCC energy formulas can be most conveniently obtained using diagrammatic methods of MBPT. The basic elements of the diagrammatic language used by us in deriving the expressions for the complete set of the CCSD moments, i.e. $\mathcal{M}_{a_1 a_2 a_3}^{i_1 i_2 i_3 i_4}(2)$, $\mathcal{M}_{a_1 a_2 a_3 a_4 a_5}^{i_1 i_2 i_3 i_4 i_5}(2)$, and $\mathcal{M}_{a_1 a_2 a_3 a_4 a_5 a_6}^{i_1 i_2 i_3 i_4 i_5 i_6}(2)$, and the diagrams representing these moments are described in this Appendix. The resulting algebraic expressions in terms of molecular integrals and cluster amplitudes are given in Appendix C.

Basically there are two closely related types of many-body diagrams: the Hugen-holtz diagrams and the Goldstone diagrams. Both are inspired by the Feynman diagrams used in quantum field theory and time-dependent perturbation theory, although in the development of quantum chemical methods, it is sufficient to use the time-independent formulation of diagrammatic techniques introduced to chemistry by Čížek. 15,16

The diagrammatic theory starts from selecting a Fermi vacuum state $|\Phi\rangle$, which is a single-determinantal state that is typically chosen to provide a reasonable approximation to the ground electronic state of a given many-fermion system under consideration. When we promote an electron from a spin-orbital occupied in $|\Phi\rangle$ to a virtual spin-orbital unoccupied in $|\Phi\rangle$, we create a hole in the Fermi vacuum and a particle in the virtual spin-orbital. For example, the Slater determinant $|\Phi^{a_1a_2}_{i_1i_2}\rangle$ is a 2-hole/2-particle state (two electrons occupying hole or occupied spin-orbitals i_1 and

 i_2 are promoted to virtual or unoccupied or particle spin-orbitals a_1 and a_2). As a rule of thumb in drawing diagrams, one says that holes "run backwards in time" and particles "run forward" (although time plays here only a formal role; there is no time in the time-independent description used by us).

There are two conventions for drawing the Goldstone and Hugenholtz diagrams:

(1) the formal time for determining the hole-particle character of single-particle states flows from the right to the left, or (2) the formal time flows from the bottom to the top. We will use the former convention, which is to say that the hole lines (representing occupied single-particle states) run from the left to the right and the particle lines representing the unoccupied single-particle states run from the right to the left. We will use the Hugenholtz diagrams, which are less numerous and easier to draw, when compared to the Goldstone diagrams.

Essentially, every diagrammatic calculation reduces to the following operations:

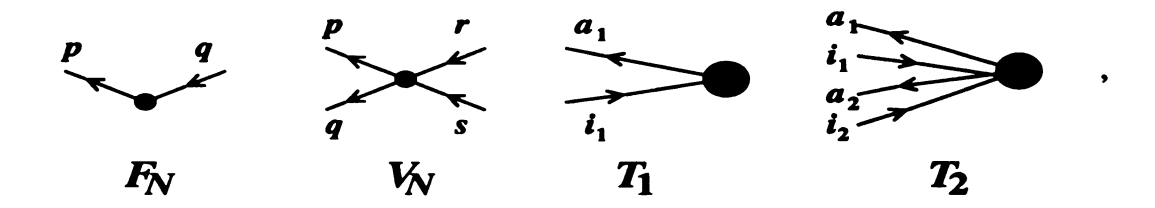
1. First, we represent the second quantized operators A_{μ} , $\mu=1,\ldots,M$, entering a given operator product $\prod_{\mu=1}^{M}A_{\mu}$, by basic diagrams. In the design of these diagrams, we use vertices with incoming lines representing annihilation operators and outgoing lines representing creation operators. Each basic vertex A_{μ} contains information about matrix elements in a spin-orbital basis defining operator A_{μ} . For example, the basic diagrams relevant to our MMCC calculations (in a Hugenholtz representation), representing the one- and two-body parts of the Hamiltonian H_N in a normal-ordered form,

$$F_N = \sum_{p,q} f_p^q N\{c^p c_q\} \equiv f_p^q N\{c^p c_q\}$$
 (134)

and

$$V_N = \frac{1}{4} \sum_{p,q,r,s} v_{pq}^{rs} N\{c^p c^q c_s c_r\} \equiv \frac{1}{4} v_{pq}^{rs} N\{c^p c^q c_s c_r\}, \qquad (135)$$

respectively (f is the Fock operator and $N\{...\}$ is the normal product) and the cluster operators T_1 and T_2 are



respectively.

2. Next, we align the basic diagrams A_{μ} along the invisible horizontal line using the same ordering of these diagrams as in the corresponding operator product $\prod_{\mu=1}^{M} A_{\mu},$



3. In the third step, we connect (contract) the lines of diagrams A_{μ} in all possible ways using the rules

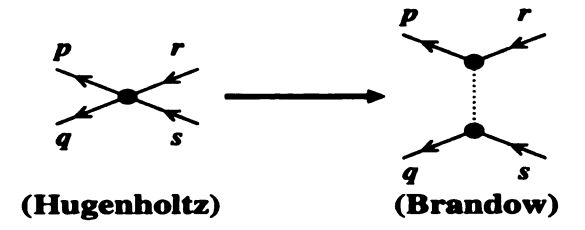
which reflect the fact that the only nonvanishing contractions of creation and annihilation operators are $c^p c_q = \delta_{pq} H(q)$ and $c_p c^q = \delta_{pq} [1 - H(q)]$, where H(q) = 1 for q being a hole and 0 for q representing a particle (δ_{pq} is the usual Kronecker delta). Connecting lines of diagrams is equivalent to using the Wick's theorem. Only nonequivalent resulting diagrams should be considered in the final analysis (some resulting diagrams can be obtained in several ways, but we eliminate these repetitions). Specific expressions (such as those in CC theory) may lead to the elimination of certain types of resulting diagrams.

4. Once the allowed resulting diagrams are drawn, we assign the algebraic expression to each and every one of them using the rules discussed below. The final expression for the operator product of interest, $\prod_{\mu=1}^{M} A_{\mu}$, is a sum of the algebraic expressions corresponding to nonequivalent resulting diagrams allowed by a given many-body theory.

Every resulting diagram consists of one or more basic (e.g., V_N or T_2) vertices that are connected by oriented (i.e. fermion) lines and that may have some external (i.e. uncontracted) lines. In general, we interpret such a diagram by forming a product of (a) the weight factor, (b) the sign factor, (c) the scalar factor, and (for example, in the wave function expressions) (d) the operator part, and by summing the resulting

expressions over all relevant hole and particle indices, if such summations exist in operators A_{μ} . For the Hugenholtz diagrams used here, the weight factor is 2^{-k} , where k is the number of pairs of topologically equivalent (e.g., identically oriented) fermion lines. We must remember that the identically oriented lines carrying fixed (i.e. not summed) spin-orbital indices can never be regarded as equivalent lines. The scalar factor is a product of matrix elements associated with the individual vertices A_{μ} from the product $\prod_{\mu=1}^{M} A_{\mu}$ entering the resulting diagram. The operator part (if it appears in the expression) is a product of the creation and annihilation operators associated with the uncontracted external lines.

The Hugenholtz diagrams do not specify the overall sign of the contribution of the diagram. This is due to the fact that the basic Hugenholtz diagrams, such as V_N or T_2 , use antisymmetrized matrix elements $v_{pq}^{r_s}$, $t_{a_1a_2}^{i_1i_2}$, etc. In order to determine the sign, it is necessary to draw one Goldstone representative, called the Brandow diagram, for each Hugenholtz diagram. This can be done by "expanding" the Hugenholtz vertices. For example, the Hugenholtz V_N vertex in a resulting diagram must be replaced (only for the purpose of sign determination) by



In general, in order to obtain a Brandow representative of a given resulting Hugenholtz diagram, we replace all basic Hugenholtz vertices by Goldstone vertices, as shown above, while keeping the directions of the lines and the connectivity intact. Usually more than one possibility exists, but this is not a problem: we choose any Goldstone representative of a given Hugenholtz diagram as a Brandow diagram. Once the Brandow diagram is drawn, we determine the sign factor for it by counting the number of loops (l) and the number of internal hole lines (h) and by using the sign formula $(-1)^{l+h}$.

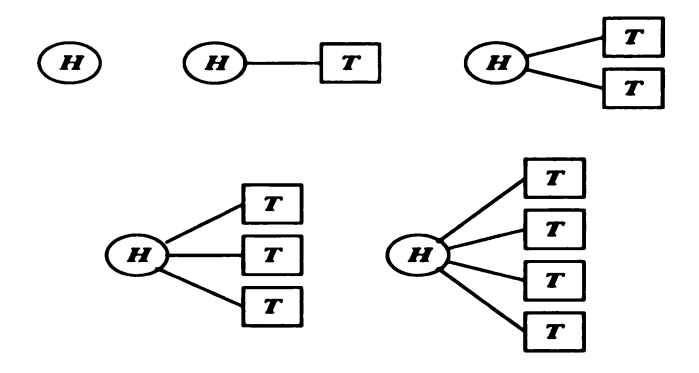
We used the Hugenholtz (and Brandow) diagrams to derive the explicit many-body expressions for all the terms that correspond to the generalized moments $\mathcal{M}_{a_1...a_k}^{i_1...i_k}(m_A)$, k=3-6, Eq. (28). There are several methods of obtaining all resulting Hugenholtz diagrams in a highly efficient manner. We follow the recipe, described in Ref. 156, in which we first draw the nonoriented Hugenholtz skeletons from nonoriented basic vertices representing F_N , V_N , T_1 , and T_2 . The orientations of fermion lines are introduced in a subsequent step, once the nonoriented skeletons are determined. In the case of expressions for the generalized moments of CC equations, where we have to project $(H_N e^{T_1+T_2})_C |\Phi\rangle$ on the excited determinants $|\Phi_{i_1...i_k}^{a_1...a_k}\rangle$, we do not draw the diagram representing the state $\langle \Phi_{i_1...i_k}^{a_1...a_k}|$. Instead, we draw all permissible diagrams for $(H_N e^{T_1+T_2})_C |\Phi\rangle$ with k incoming and k outgoing external lines labeled by fixed indices $i_1, \ldots, i_k, a_1, \ldots, a_k$. This facilitates the process of drawing the resulting diagrams and makes the resulting diagrams less complicated.

We begin our discussion with the $\mathcal{M}_{a_1 a_2 a_3}^{i_1 i_2 i_3}(2)$ moments obtained by projecting the CCSD equations onto triply excited configurations. From Eq. (34), it immediately follows that the following expression must be examined in this case:

$$\mathcal{M}_{a_{1}a_{2}a_{3}}^{i_{1}i_{2}i_{3}}(2) = \langle \Phi_{i_{1}i_{2}i_{3}}^{a_{1}a_{2}a_{3}} | [\frac{1}{2}F_{N}T_{2}^{2} + V_{N}(T_{2} + T_{1}T_{2} + \frac{1}{2}T_{1}^{2}T_{2} + \frac{1}{6}T_{1}^{3}T_{2} + \frac{1}{2}T_{2}^{2} + \frac{1}{2}T_{1}T_{2}^{2})]_{C} | \Phi \rangle,$$

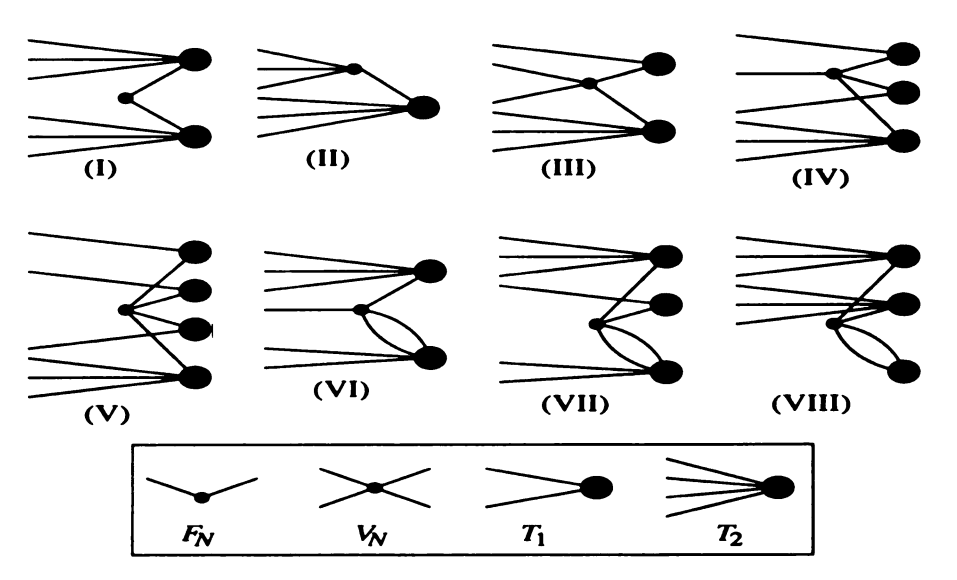
$$(136)$$

where the subscript C designates the connected part of the operator expression. The connected part of an operator expression, such as that in Eq. (136), can be represented graphically by drawing all nonequivalent connected diagrams formed by "connecting" the F_N or V_N vertices with zero, one, two, three, or four T (i.e., T_1 or T_2) vertices, as shown symbolically below.



At most four T cluster components can be attached to the Hamiltonian operator vertex, since $H_N = F_N + V_N$ contains up to two-body interactions.

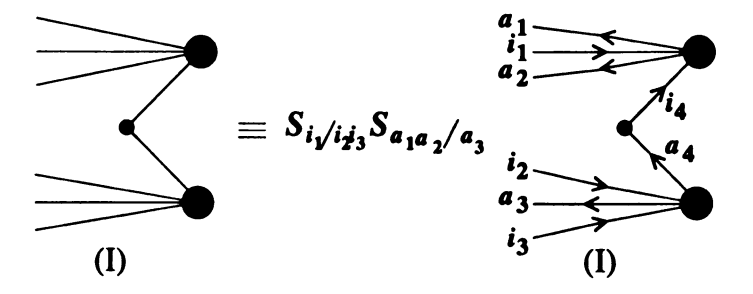
The seven terms in Eq. (136) lead to the following eight nonoriented Hugenholtz diagrams (or skeletons):

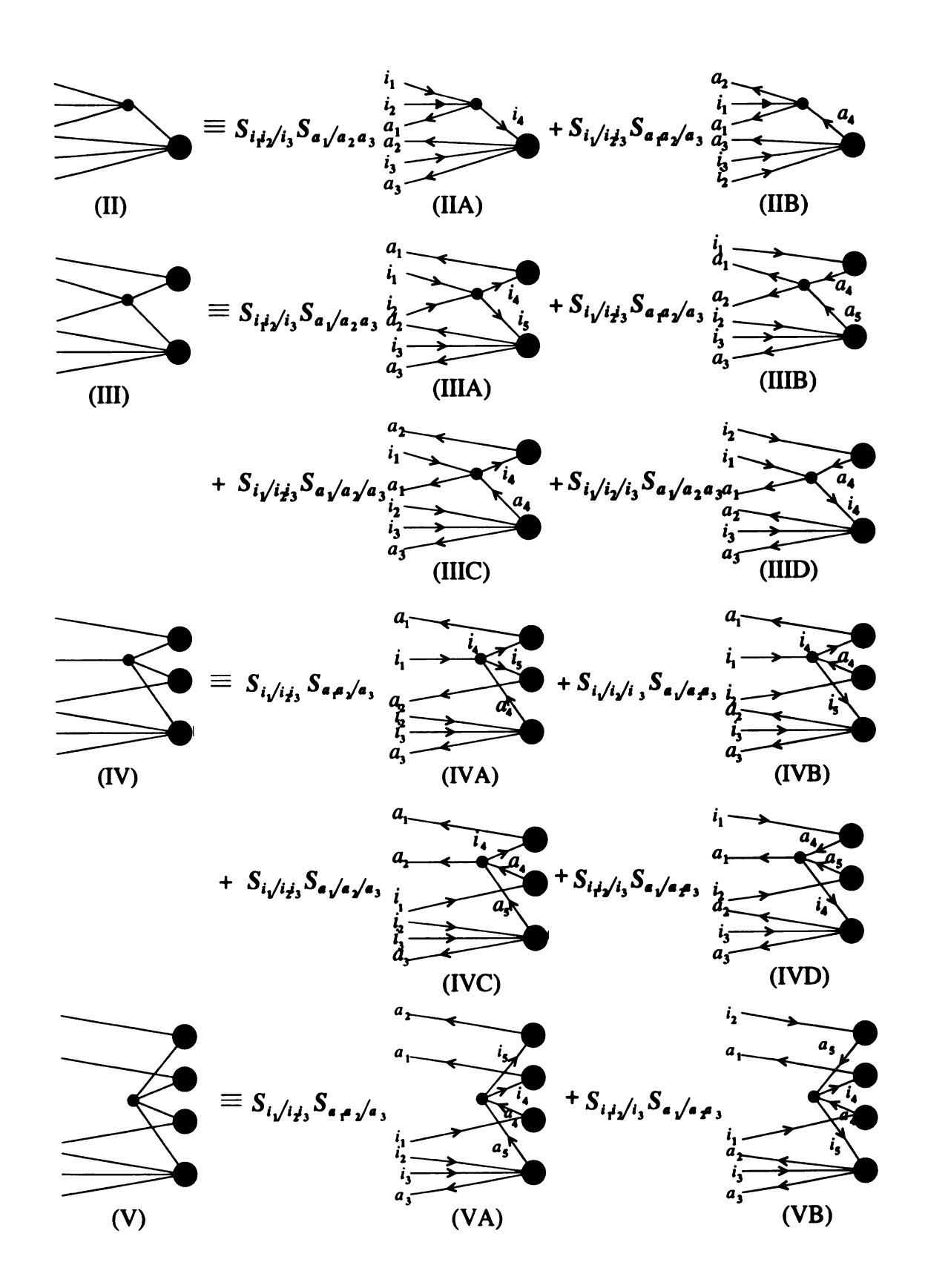


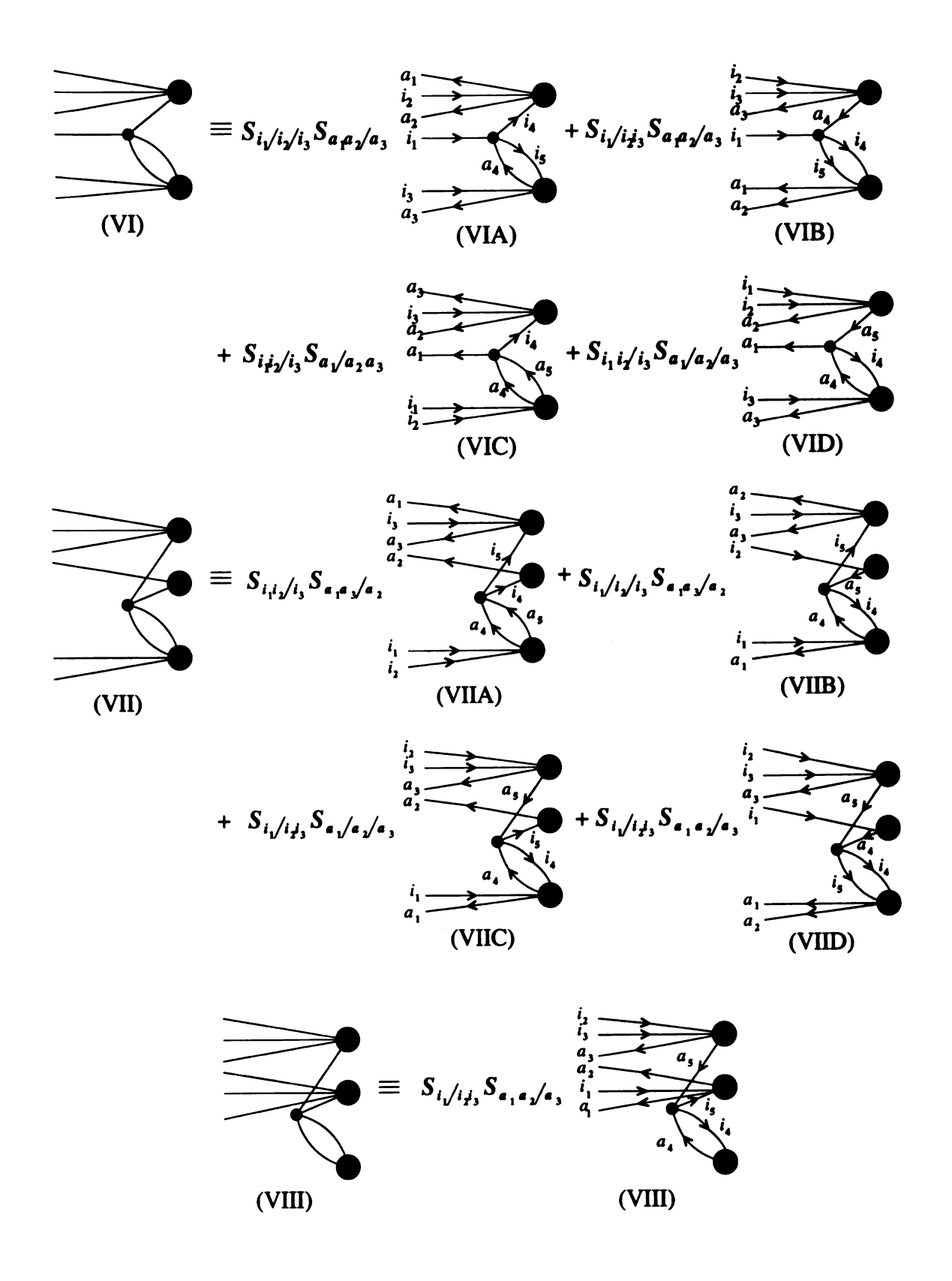
All eight skeletons have six external lines extending to the left that correspond to the

projection of $(H_N e^{T_1+T_2})_C |\Phi\rangle$ in Eq. (34) on triply excited configurations. The final oriented Hugenholtz diagrams corresponding to skeletons (I)–(VIII) are obtained by inserting line orientations in all possible ways. The resulting oriented Hugenholtz diagrams representing moment $\mathcal{M}_{a_1 a_2 a_3}^{i_1 i_2 i_3}(2)$, Eqs. (34) and (136), are given below.

Oriented Hugenholtz diagrams for $\mathcal{M}_{a_1a_2a_3}^{i_1i_2i_3}(2)$ (skeletons I–VIII)







The S operators in front of the Hugenholtz diagrams above (and, also, in the oriented Hugenholtz diagrams corresponding to the remaining moments $\mathcal{M}_{a_1a_2a_3a_4}^{i_1i_2i_3i_4}(2)$, $\mathcal{M}_{a_1a_2a_3a_4a_5}^{i_1i_2i_3i_4i_5i_6}(2)$, and $\mathcal{M}_{a_1a_2a_3a_4a_5a_6}^{i_1i_2i_3i_4i_5i_6}(2)$ considered below) are the diagram symmetrizers that are used to permute the indices labeling external lines for both the occupied and unoccupied spin-orbitals, to obtain the nonequivalent diagrams resulting from the same arrangement of oriented fermion lines in a given skeleton. The actual form of these symmetrizers depends on the topology of a particular diagram and the equivalencies among external lines. For example, the symmetrizers S_{i_1/i_2i_3} and $S_{i_1/i_2/i_3}$ seen in front of several of the diagrams corresponding to the triply excited moments are defined as follows:

$$S_{i_1/i_2i_3} = 1_{i_1i_2i_3} + (i_1i_2) + (i_1i_3), \qquad (137)$$

$$S_{i_1/i_2/i_3} = 1_{i_1i_2i_3} + (i_1i_2) + (i_1i_3) + (i_2i_3) + (i_1i_2i_3) + (i_1i_3i_2), \tag{138}$$

where $1_{i_1i_2i_3}$ is a three-index identity operator, (i_1i_2) , (i_1i_3) , and (i_2i_3) are the two-index permutations (e.g., (i_1i_2) means interchange labels i_1 and i_2), and $(i_1i_2i_3)$ and $(i_1i_3i_2)$ designate the three-index cyclic permutations (e.g., $(i_1i_2i_3)$ indicates that label i_1 is replaced by i_2 , i_2 is replaced by i_3 , and i_3 is replaced by i_1). Notice that in the slashed quantities S_{i_1/i_2i_3} and $S_{i_1/i_2/i_3}$, the only permutations allowed are those which interchange the indices belonging to different groups of symbols separated by the "/" sign. For example, we do not permute i_2 and i_3 in S_{i_1/i_2i_3} . The analogous formulas can be given for the unoccupied labels a_1 , a_2 , etc. and one can easily extend the definitions (137) and (138) to cases involving permutations of more than three indices (needed in the case of higher-than-triply excited moments $\mathcal{M}_{a_1...a_k}^{i_1...i_k}(2)$ with

k > 3).

We can use the above methodology to draw the Hugenholtz diagrams representing the remaining moments $\mathcal{M}_{a_1a_2a_3a_4}^{i_1i_2i_3i_4}(2)$, $\mathcal{M}_{a_1a_2a_3a_4a_5}^{i_1i_2i_3i_4i_5}(2)$, and $\mathcal{M}_{a_1a_2a_3a_4a_5a_6}^{i_1i_2i_3i_4i_5i_6}(2)$. The formulas for the moments $\mathcal{M}_{a_1a_2a_3a_4}^{i_1i_2i_3i_4}(2)$, $\mathcal{M}_{a_1a_2a_3a_4a_5}^{i_1i_2i_3i_4i_5}(2)$, and $\mathcal{M}_{a_1a_2a_3a_4a_5a_6}^{i_1i_2i_3i_4i_5i_6}(2)$ that must be represented diagrammatically are

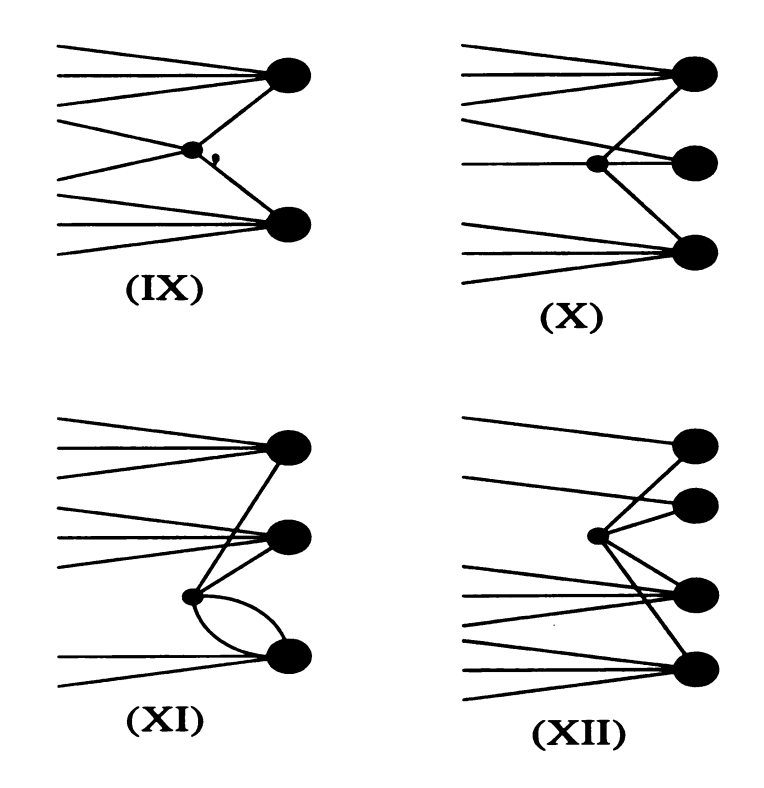
$$\mathcal{M}_{a_1 a_2 a_3 a_4}^{i_1 i_2 i_3 i_4}(2) = \langle \Phi_{i_1 i_2 i_3 i_4}^{a_1 a_2 a_3 a_4} | [V_N(\frac{1}{2}T_2^2 + \frac{1}{2}T_1T_2^2 + \frac{1}{6}T_2^3 + \frac{1}{4}T_1^2T_2^2)]_C | \Phi \rangle, \tag{139}$$

$$\mathcal{M}_{a_1 a_2 a_3 a_4 a_5}^{i_1 i_2 i_3 i_4 i_5}(2) = \langle \Phi_{i_1 i_2 i_3 i_4 i_5}^{a_1 a_2 a_3 a_4 a_5} | [V_N(\frac{1}{6}T_2^3 + \frac{1}{6}T_1 T_2^3)]_C | \Phi \rangle, \tag{140}$$

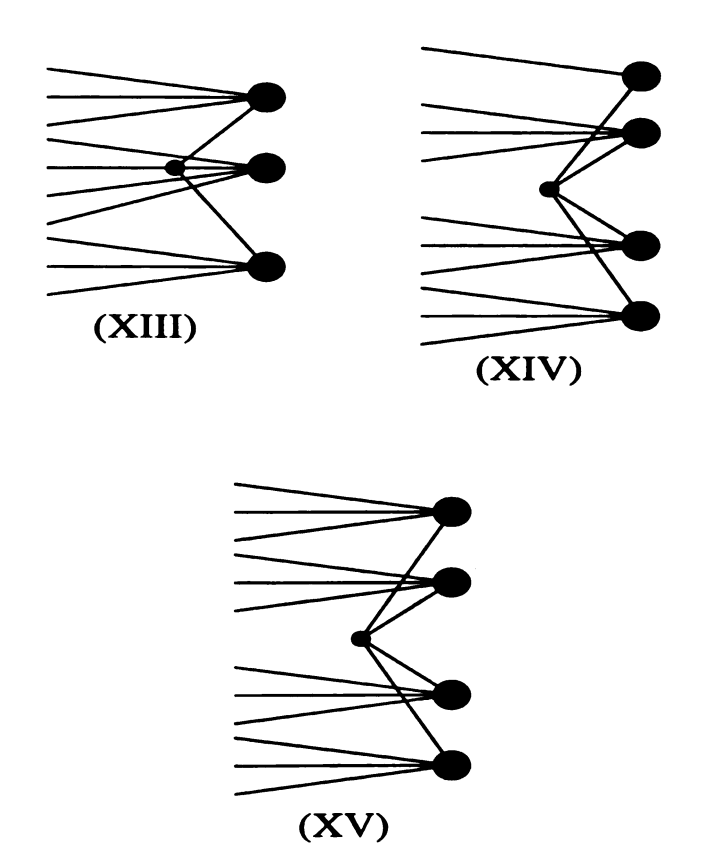
$$\mathcal{M}_{a_{1}a_{2}a_{3}a_{4}a_{5}a_{6}}^{i_{1}i_{2}i_{3}i_{4}i_{5}i_{6}}(2) = \langle \Phi_{i_{1}i_{2}i_{3}i_{4}i_{5}i_{6}}^{a_{1}a_{2}a_{3}a_{4}a_{5}a_{6}} | (\frac{1}{24}V_{N}T_{2}^{4})_{C} | \Phi \rangle.$$
(141)

In the next few pages, the diagrams are written in the following sequence: (i) the nonoriented Hugenholtz skeletons representing $\mathcal{M}_{a_1a_2a_3a_4}^{i_1i_2i_3i_4}(2)$, $\mathcal{M}_{a_1a_2a_3a_4a_5}^{i_1i_2i_3i_4i_5}(2)$, and $\mathcal{M}_{a_1a_2a_3a_4a_5a_6}^{i_1i_2i_3i_4i_5i_6}(2)$, followed by (ii) all oriented Hugenholtz diagrams that result from the nonoriented diagrams for these moments. The Brandow diagrams representing the Hugenholtz diagrams for all CCSD moments $\mathcal{M}_{a_1...a_k}^{i_1...i_k}(2)$, k=3-6, are listed at the end of this Appendix.

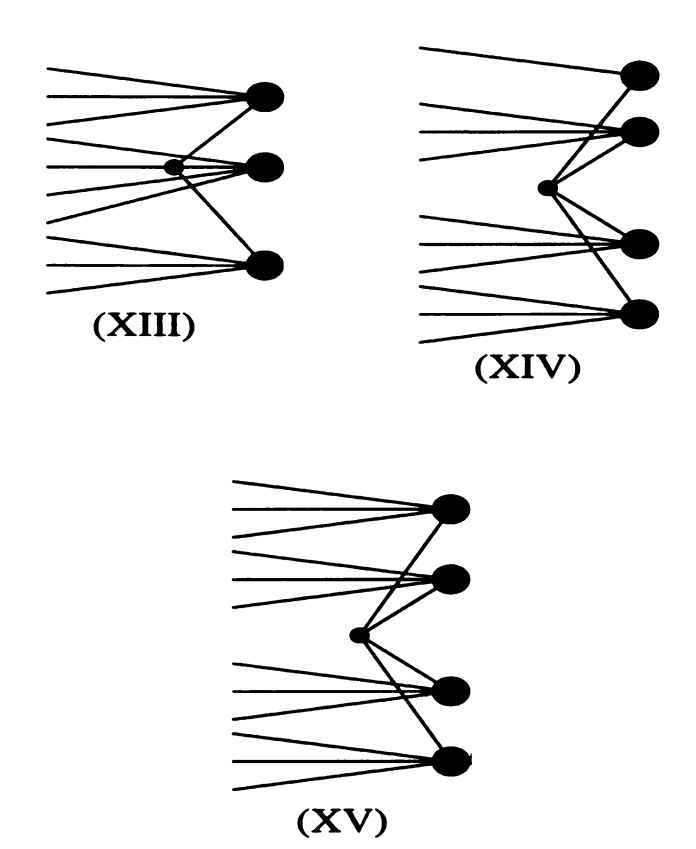
Nonoriented Hugenholtz diagrams for $\mathcal{M}_{a_1 a_2 a_3 a_4}^{i_1 i_2 i_3 i_4}(2)$



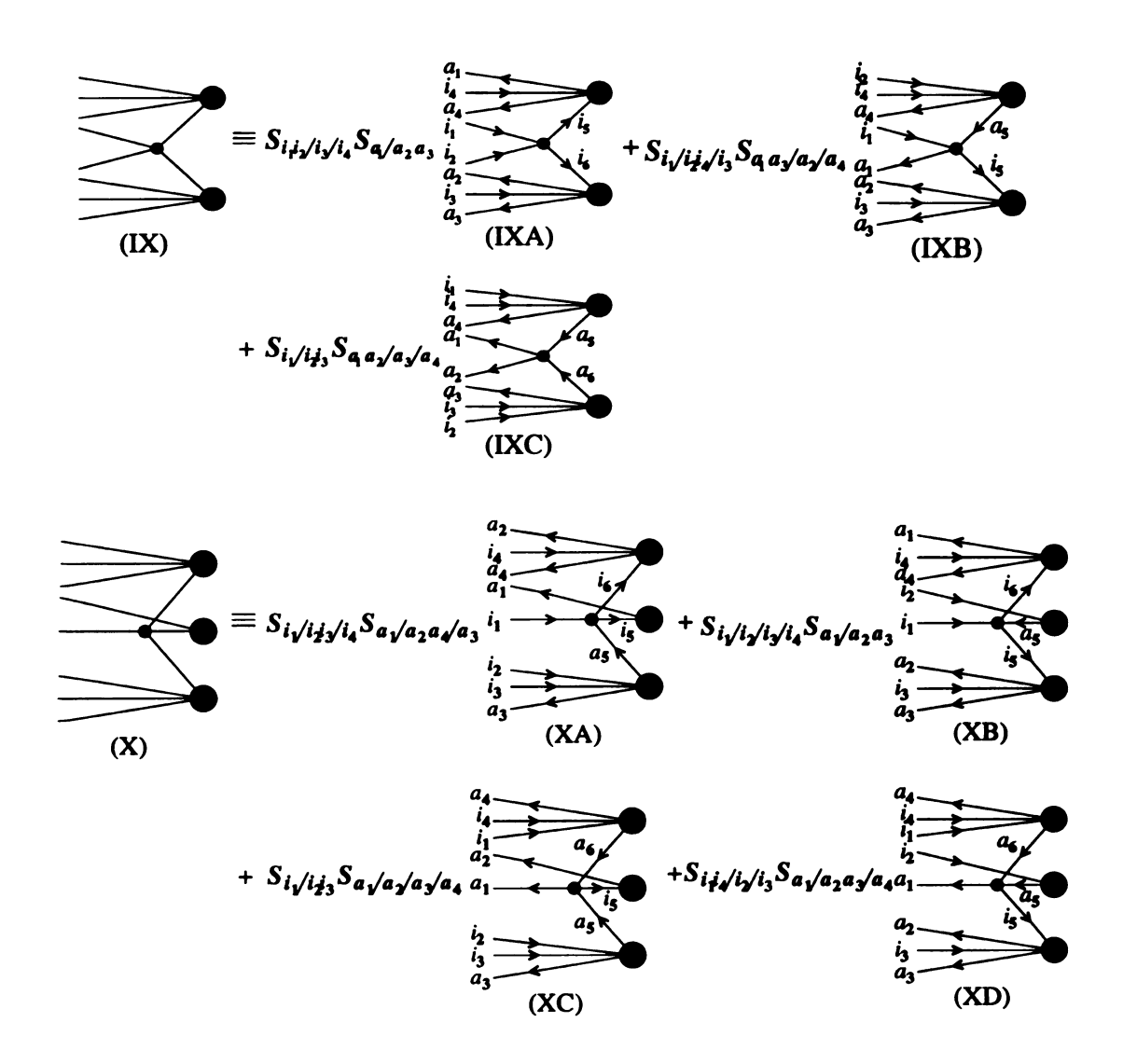
Nonoriented Hugenholtz diagrams for $\mathcal{M}_{a_1a_2a_3a_4a_5}^{i_1i_2i_3i_4i_5}(2)$ ((XIII) and (XIV)) and $\mathcal{M}_{a_1a_2a_3a_4a_5a_6}^{i_1i_2i_3i_4i_5i_6}(2)$ (XV)

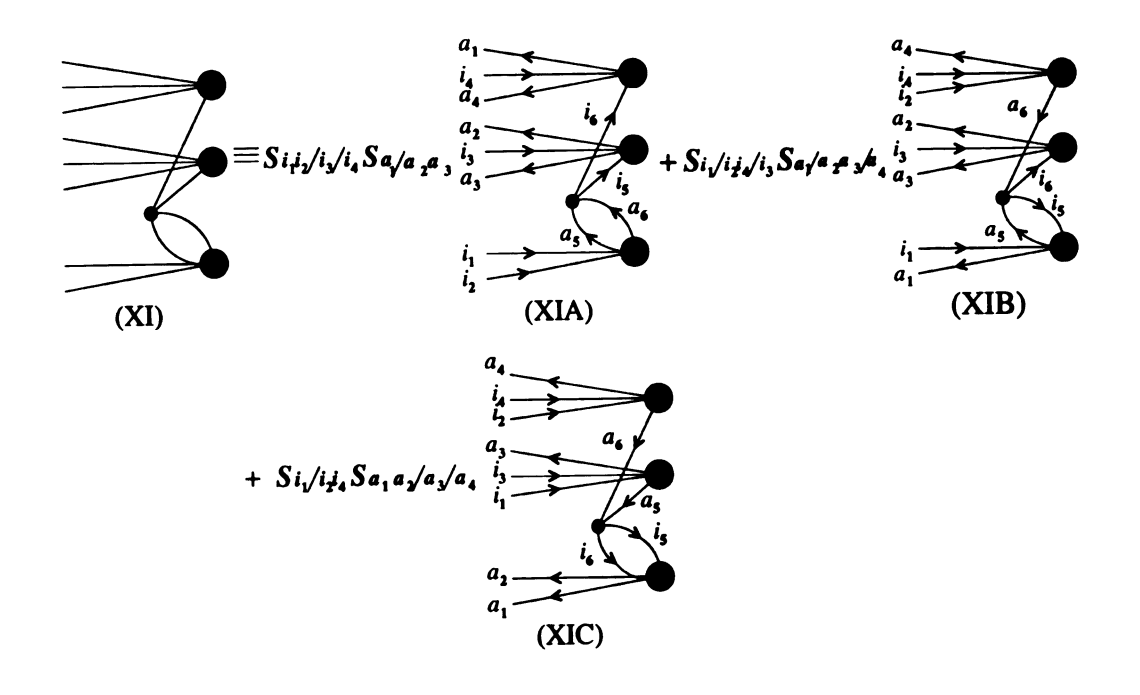


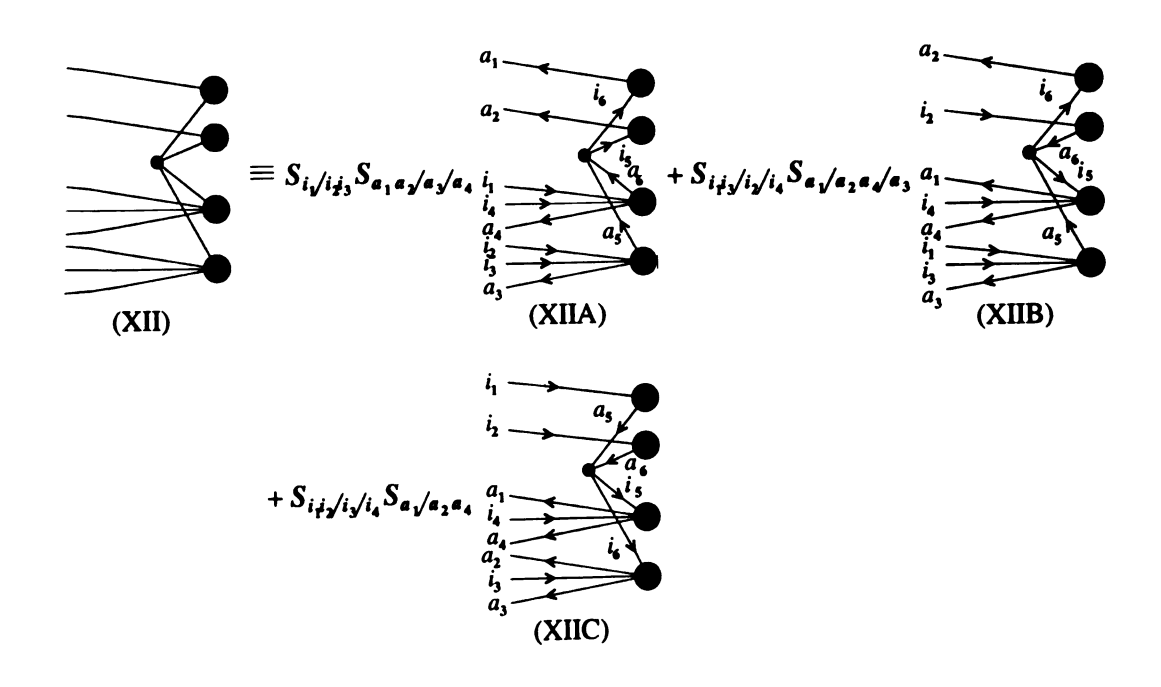
Nonoriented Hugenholtz diagrams for $\mathcal{M}_{a_{1}a_{2}a_{3}a_{4}a_{5}}^{i_{1}i_{2}i_{3}i_{4}i_{5}}(2)$ ((XIII) and (XIV)) and $\mathcal{M}_{a_{1}a_{2}a_{3}a_{4}a_{5}a_{6}}^{i_{1}i_{2}i_{3}i_{4}i_{5}i_{6}}(2)$ (XV)

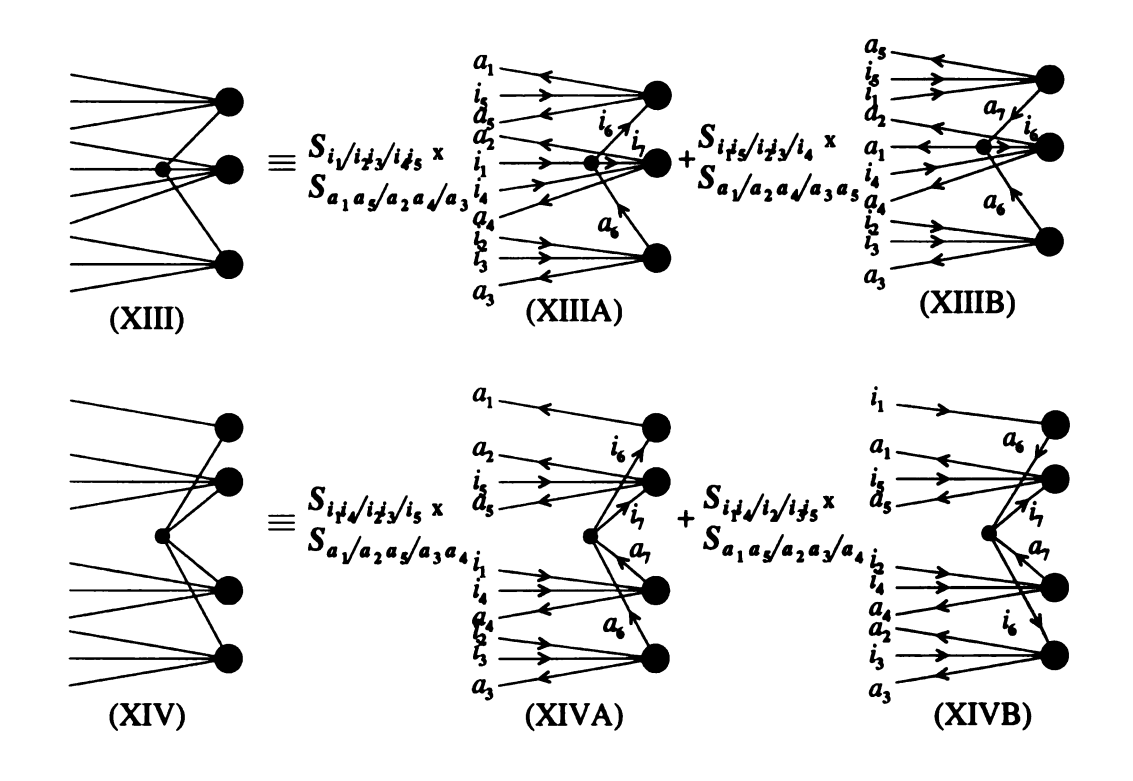


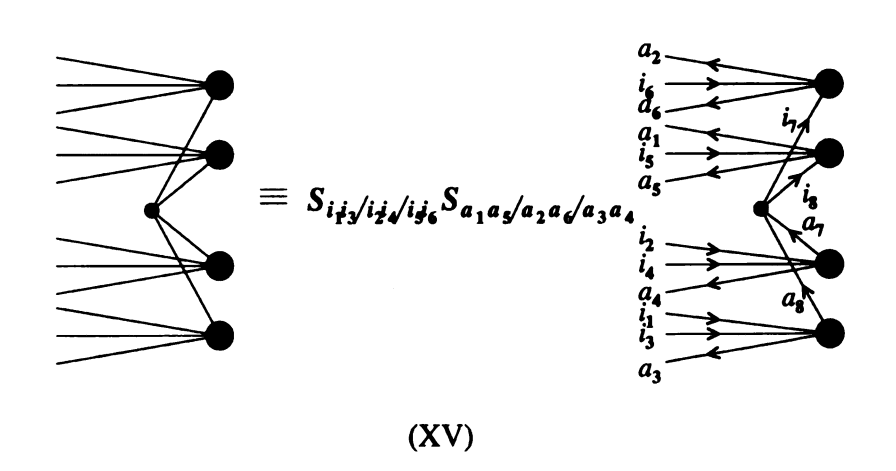
Oriented Hugenholtz diagrams for skeletons (IX)–(XV) representing $\mathcal{M}_{a_1...a_k}^{i_1...i_k}(2)$, with k=4-6



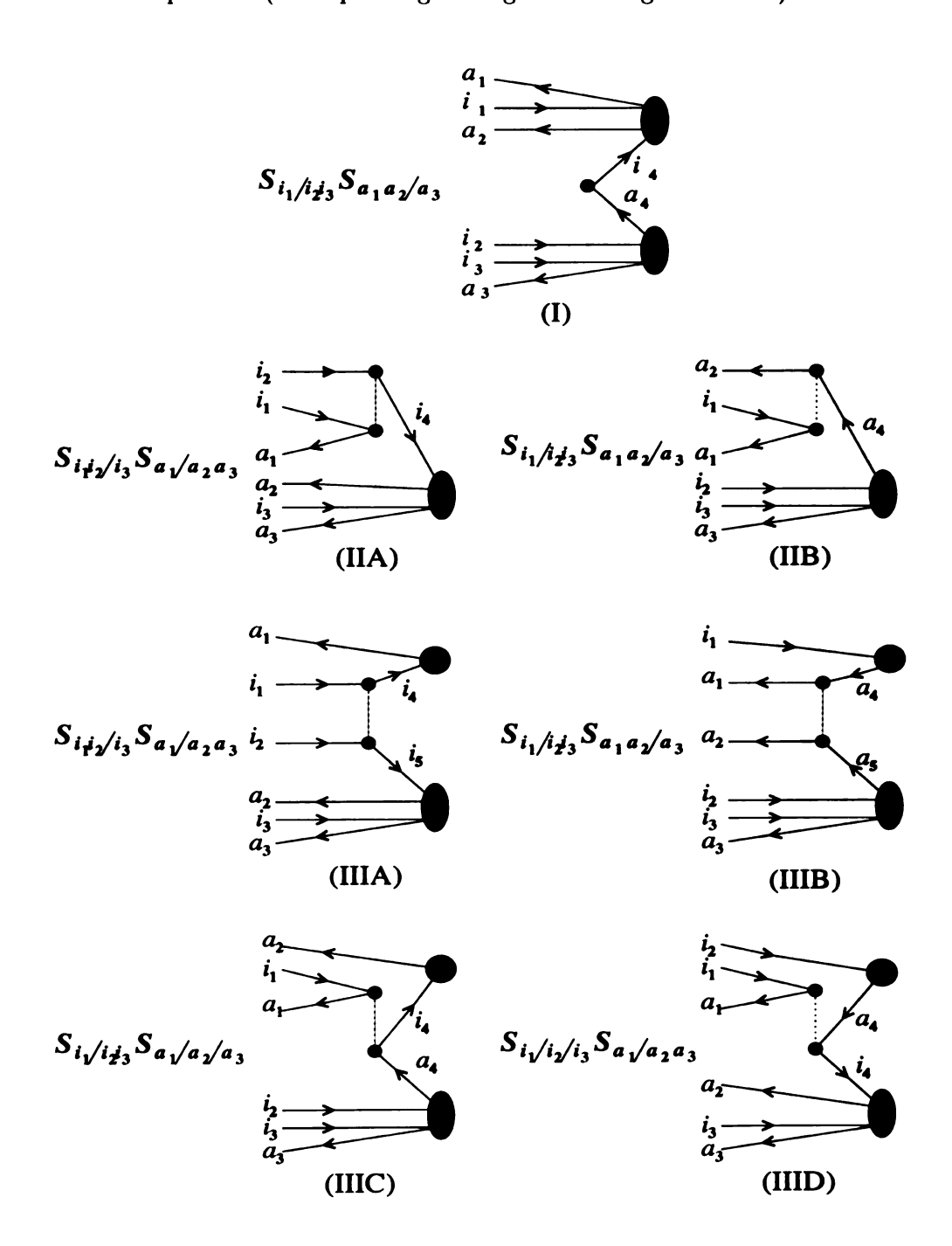


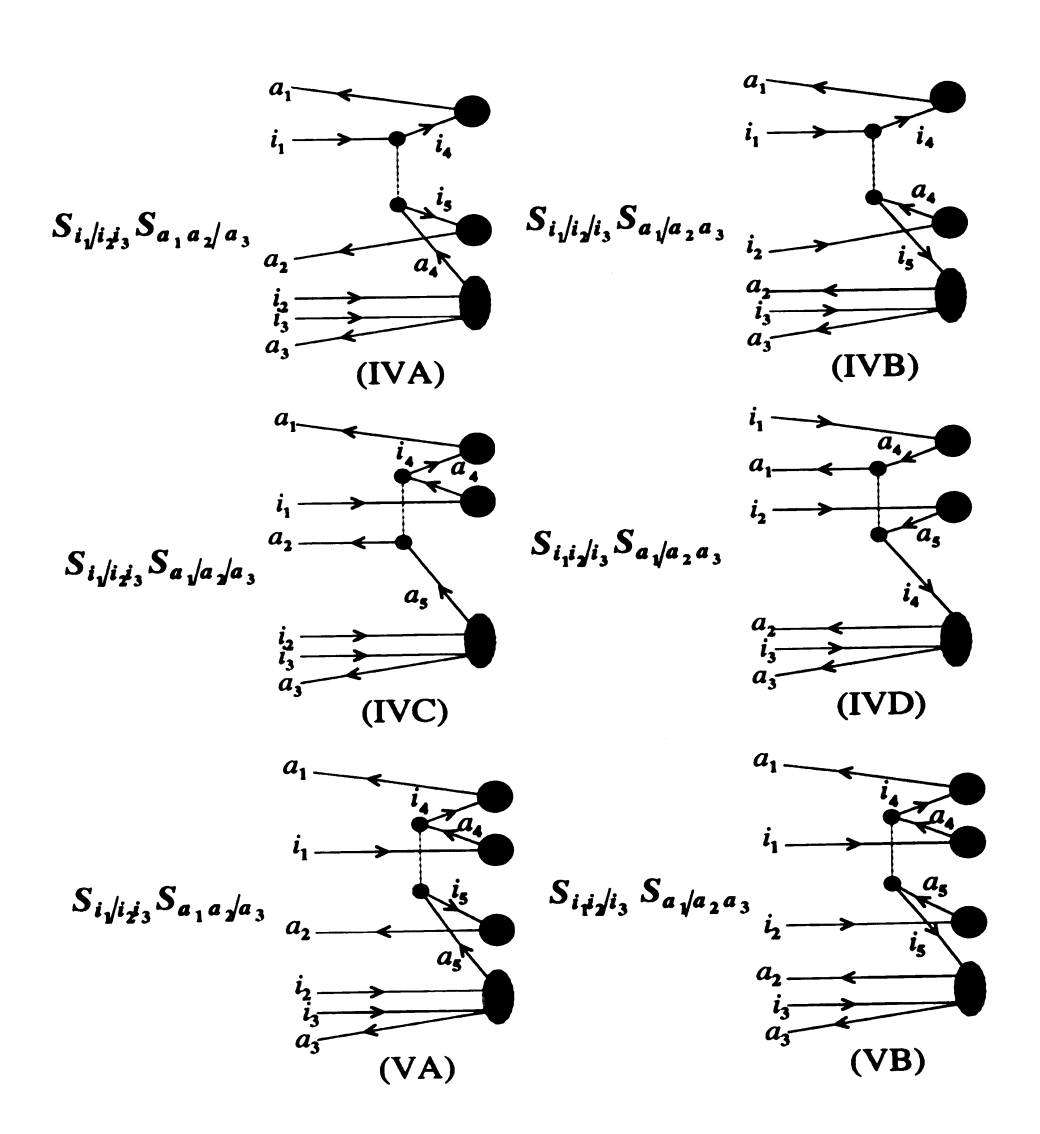


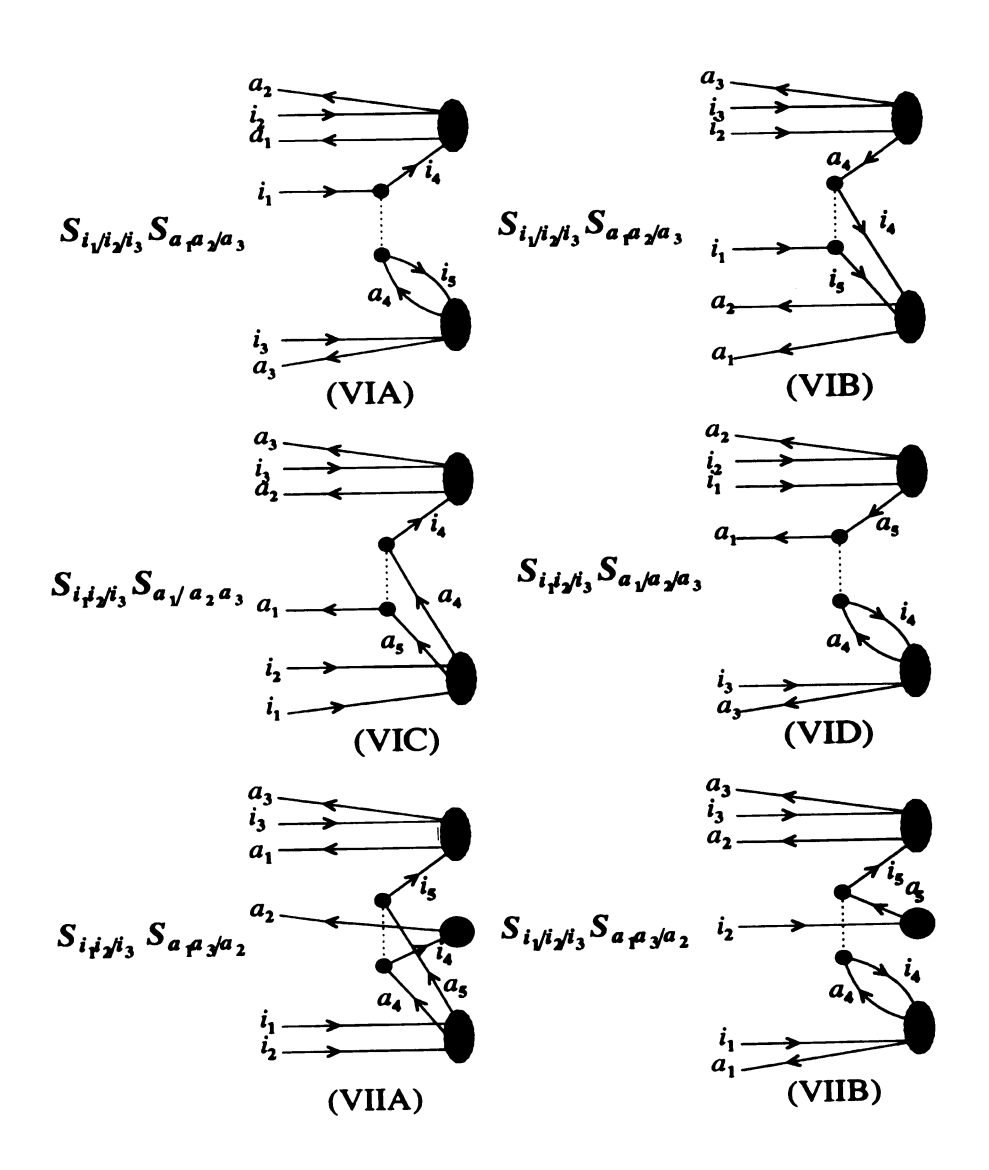


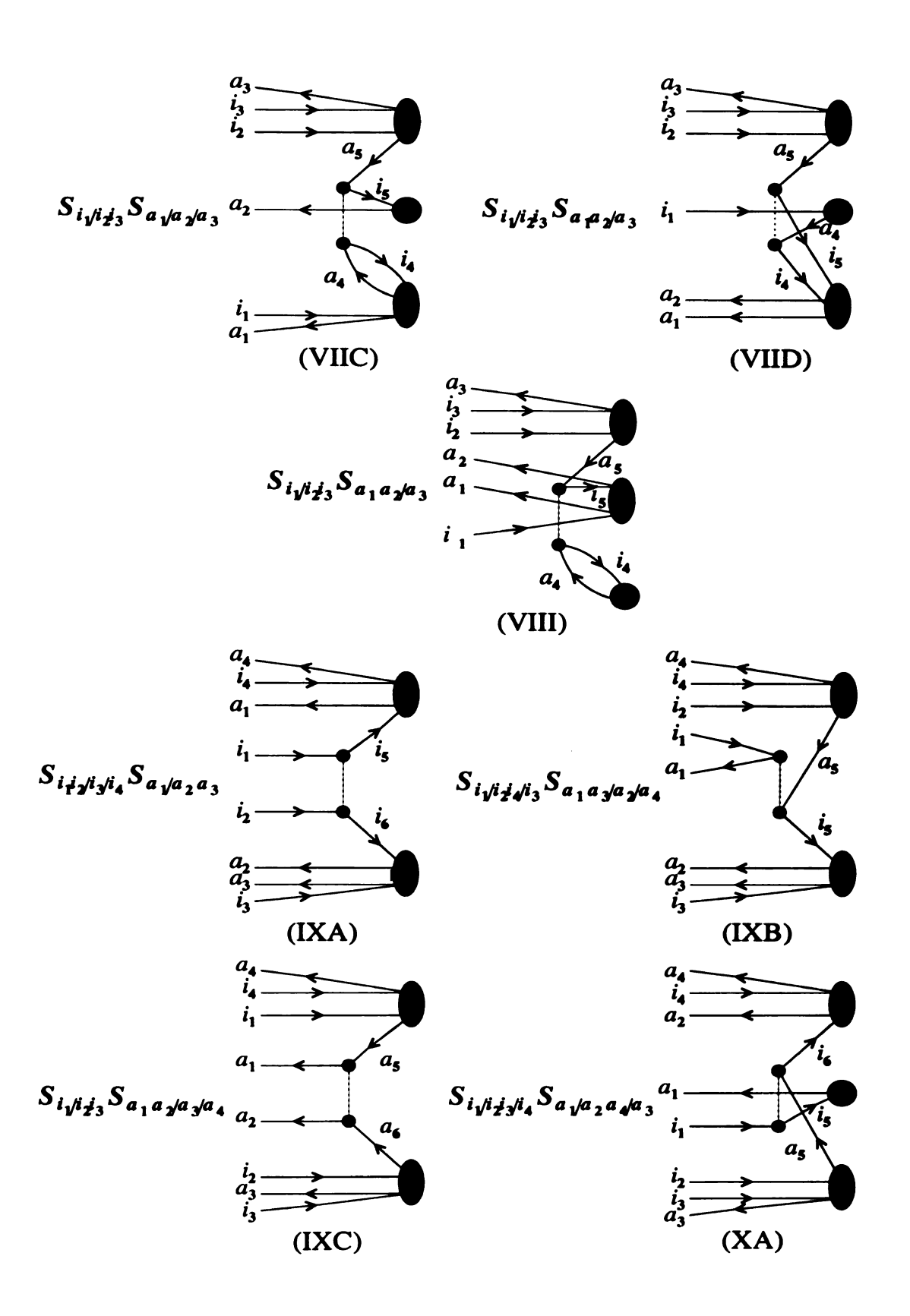


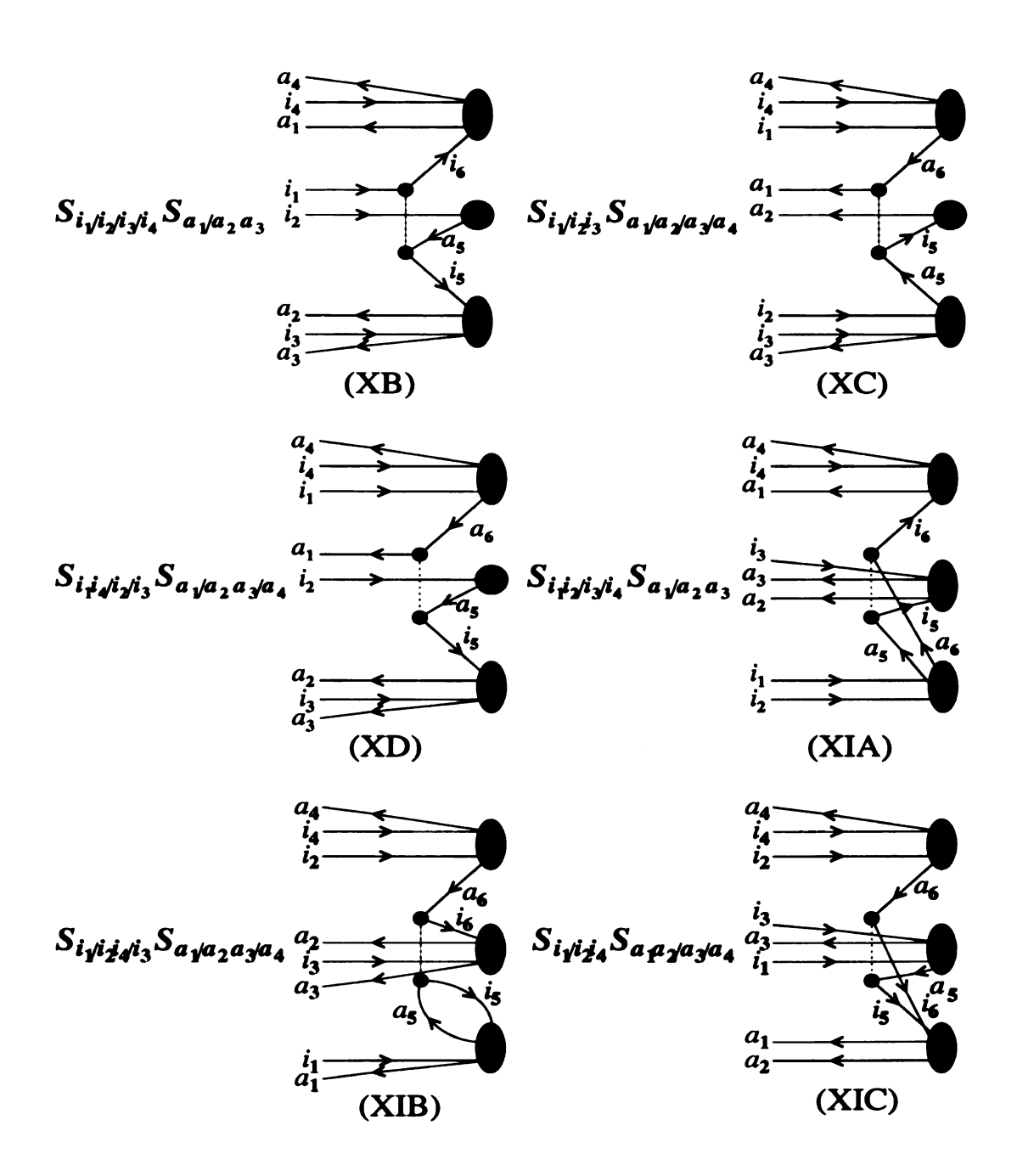
The Brandow diagrams for the complete set of generalized moments of the CCSD equations (corresponding to Hugenholtz diagrams I-XV)

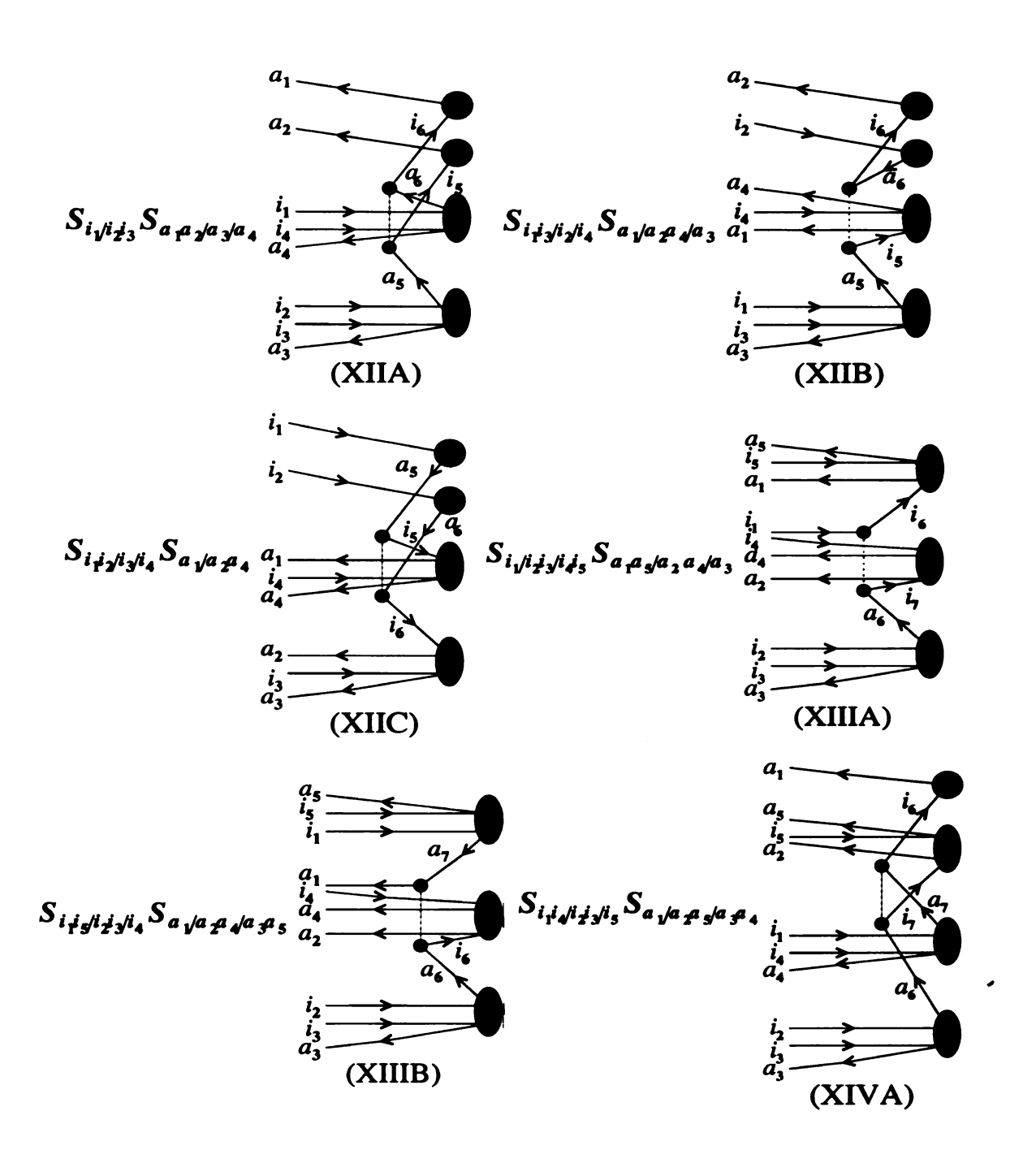


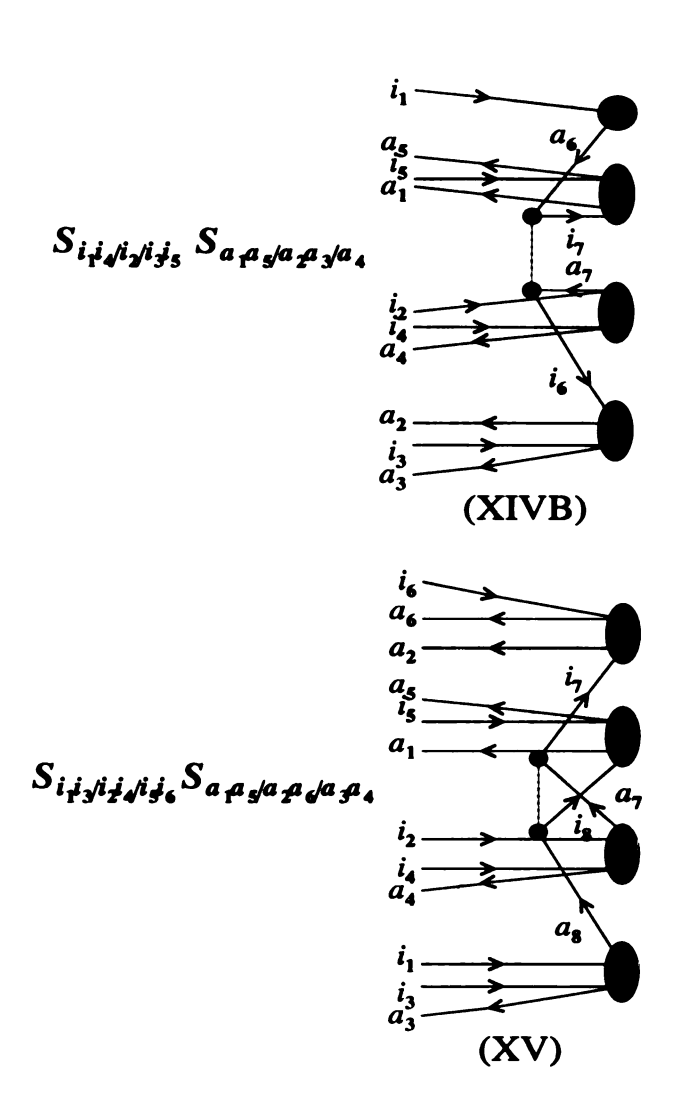












Appendix C. Algebraic expressions for the $\mathcal{M}_{a_1 a_2 a_3}^{i_1 i_2 i_3}(2)$, $\mathcal{M}_{a_1 a_2 a_3 a_4}^{i_1 i_2 i_3 i_4}(2)$, $\mathcal{M}_{a_1 a_2 a_3 a_4 a_5}^{i_1 i_2 i_3 i_4 i_5 i_6}(2)$ moments of the CCSD equations

In this Appendix, we present the final algebraic expressions for the Hugenholtz and Brandow diagrams (I)–(XV) representing the complete set of moments of the CCSD equations used in the MMCC calculations. Let us recall that the weight factor for each diagram is read from the Hugenholtz form of the diagram. The sign factors and the scalar factors, expressed in terms of matrix elements $f_p^q \equiv \langle p|f|q\rangle$, where f is the Fock operator, and $v_{pq}^{rs} \equiv \langle pq|v|rs\rangle_{\mathcal{A}} = \langle pq|v|rs\rangle - \langle pq|v|sr\rangle$, where v is the interaction, and cluster amplitudes $t_{a_1}^{i_1} \equiv \langle a_1|t_1|i_1\rangle$ and $t_{a_1a_2}^{i_1i_2} \equiv \langle a_1a_2|t_2|i_1i_2\rangle_{\mathcal{A}}$ are read from the Brandow diagrams. To properly account for the diagrams resulting from the action of the symmetrizer \mathcal{S} on a specific oriented Hugenholtz diagram, an analogous operator \mathcal{A} , called the antisymmetrizer, must be introduced in the corresponding algebraic expression. For example, the antisymmetrizer \mathcal{A}_{i_1/i_2i_3} corresponding to symmetrizer \mathcal{S}_{i_1/i_2i_3} is defined as

$$\mathcal{A}_{i_1/i_2i_3} = 1_{i_1i_2i_3} - (i_1i_2) - (i_1i_3). \tag{142}$$

Similarly, the four-index antisymmetrizer $A_{i_1i_2/i_3/i_4}$ corresponding to the diagram symmetrizer $S_{i_1i_2/i_3/i_4}$ can be defined as

$$\mathcal{A}_{i_1 i_2 / i_3 / i_4} = 1_{i_1 i_2 i_3 i_4} - (i_1 i_3) - (i_1 i_4) - (i_2 i_3) - (i_2 i_4) - (i_3 i_4) + (i_1 i_3) (i_2 i_4)$$

$$+ (i_1 i_3 i_4) + (i_2 i_3 i_4) + (i_1 i_4 i_3) + (i_2 i_4 i_3) - (i_1 i_3 i_2 i_4), \qquad (143)$$

where $(i_1i_3i_2i_4)$ is a four-index cyclic permutation. In some cases, there are diagrammatic contributions to the quadruply-excited moments $\mathcal{M}_{a_1a_2a_3a_4}^{i_1i_2i_3i_4}(2)$ that do not

require the genuine four-index antisymmetrizers and use the three-index operators instead (see the algebraic expressions below).

The antisymmetrizers, signs, and weights corresponding to the Hugenholtz/Brandow diagrams (I)-(XV) listed in Appendix B are shown in the following table:

Diagram	Antisymmetrizer	Weight	l	h	$Sign \equiv (-1)^{l+h}$
I	$A_{i_1/i_2i_3}A_{a_1a_2/a_3}$	1/4	0	1	-
IIA	${\cal A}_{i_1i_2/i_3}{\cal A}_{a_1/a_2a_3}$	$\frac{1}{4}$	0	1	_
IIB	${\cal A}_{i_1/i_2i_3}{\cal A}_{a_1a_2/a_3}$	$\frac{1}{4}$	0	0	+
IIIA	$\mathcal{A}_{i_1 i_2 / i_3} \mathcal{A}_{a_1 / a_2 a_3}$	$\frac{1}{4}$	0	2	+
IIIB	$\mathcal{A}_{i_1/i_2i_3}\mathcal{A}_{a_1a_2/a_3}$	$\frac{1}{4}$	0	0	+
IIIC	${\cal A}_{i_1/i_2i_3}{\cal A}_{a_1/a_2/a_3}$	$\frac{1}{2}$	0	1	_
IIID	${\cal A}_{i_1/i_2/i_3}{\cal A}_{a_1/a_2a_3}$	$\frac{1}{2}$	0	1	-
IVA	$\mathcal{A}_{i_1/i_2i_3}\mathcal{A}_{a_1a_2/a_3}$	$\frac{1}{4}$	0	2	+
IVB	${\cal A}_{i_1/i_2/i_3}{\cal A}_{a_1/a_2a_3}$	$\frac{1}{2}$	0	2	+
IVC	${\cal A}_{i_1/i_2i_3}{\cal A}_{a_1/a_2/a_3}$	$\frac{1}{2}$	0	1	_
IVD	${\cal A}_{i_1i_2/i_3}{\cal A}_{a_1/a_2a_3}$	$\frac{1}{4}$	0	1	-
VA	${\cal A}_{i_1/i_2i_3}{\cal A}_{a_1a_2/a_3}$	$\frac{1}{4}$	0	2	+
VB	${\cal A}_{i_1i_2/i_3}{\cal A}_{a_1/a_2a_3}$	$\frac{1}{4}$	0	2	+
VIA	${\cal A}_{i_1/i_2/i_3}{\cal A}_{a_1a_2/a_3}$	$\frac{1}{2}$	1	2	_
VIB	${\cal A}_{i_1/i_2i_3}{\cal A}_{a_1a_2/a_3}$	<u>1</u> 8	0	2	+
VIC	${\cal A}_{i_1i_2/i_3}{\cal A}_{a_1/a_2a_3}$	<u>1</u> 8	0	1	_
VID	$\mathcal{A}_{i_1i_2/i_3}\mathcal{A}_{a_1/a_2/a_3}$	$\frac{1}{2}$	1	1	+

Diagram	Antisymmetrizer	Weight	l	h	$Sign \equiv (-1)^{l+h}$
VIIA	$\mathcal{A}_{i_1i_2/i_3}\mathcal{A}_{a_1a_3/a_2}$	18	0	2	+
VIIB	${\cal A}_{i_1/i_2/i_3}{\cal A}_{a_1a_3/a_2}$	$\frac{1}{2}$	1	2	_
VIIC	${\cal A}_{i_1/i_2i_3}{\cal A}_{a_1/a_2/a_3}$	$\frac{1}{2}$	0	2	+
VIID	${\cal A}_{i_1/i_2i_3}{\cal A}_{a_1a_2/a_3}$	$\frac{1}{8}$	0	2	+
VIII	${\cal A}_{i_1/i_2i_3}{\cal A}_{a_1a_2/a_3}$	$\frac{1}{4}$	1	2	_
IXA	${\cal A}_{i_1i_2/i_3/i_4}{\cal A}_{a_1/a_2a_3}$	$\frac{1}{16}$	0	2	+
IXB	${\cal A}_{i_1/i_2i_4/i_3}{\cal A}_{a_1a_3/a_2/a_4}$	$\frac{1}{4}$	0	1	_
IXC	${\cal A}_{i_1/i_2i_3}{\cal A}_{a_1a_2/a_3/a_4}$	$\frac{1}{16}$	0	0	+
XA	${\cal A}_{i_1/i_2i_3/i_4}{\cal A}_{a_1/a_2a_4/a_3}$	$\frac{1}{4}$	0	2	+
XB	$\mathcal{A}_{i_1/i_2/i_3/i_4}\mathcal{A}_{a_1/a_2a_3}$	$\frac{1}{8}$	0	2	+
XC	${\cal A}_{i_1/i_2i_3}{\cal A}_{a_1/a_2/a_3/a_4}$	$\frac{1}{8}$	0	1	_
XD	${\cal A}_{i_1i_4/i_2/i_3}{\cal A}_{a_1/a_2a_3/a_4}$	$\frac{1}{4}$	0	1	_
XIA	${\cal A}_{i_1i_2/i_3/i_4}{\cal A}_{a_1/a_2a_3}$	$\frac{1}{32}$	0	2	+
XIB	${\cal A}_{i_1/i_2i_4/i_3}{\cal A}_{a_1/a_2a_3/a_4}$	$\frac{1}{4}$	1	2	_
XIC	${\cal A}_{i_1/i_2i_4}{\cal A}_{a_1a_2/a_3/a_4}$	$\frac{1}{32}$	0	2	+
XIIA	${\cal A}_{i_1/i_2i_3}{\cal A}_{a_1a_2/a_3/a_4}$	$\frac{1}{16}$	0	2	+
XIIB	${\cal A}_{i_1i_3/i_2/i_4}{\cal A}_{a_1/a_2a_4/a_3}$	$\frac{1}{4}$	0	2	+
XIIC	${\cal A}_{i_1i_2/i_3/i_4}{\cal A}_{a_1/a_2a_4}$	$\frac{1}{16}$	0	2	+
XIIIA	${\cal A}_{i_1/i_2i_3/i_4i_5}{\cal A}_{a_1a_5/a_2a_4/a_3}$	$\frac{1}{16}$	0	2	+
XIIIB	$\mathcal{A}_{i_1i_5/i_2i_3/i_4}\mathcal{A}_{a_1/a_2a_4/a_3a_5}$	$\frac{1}{16}$	0	1	_
XIVA	$\mathcal{A}_{i_1i_4/i_2i_3/i_5}\mathcal{A}_{a_1/a_2a_5/a_3a_4}$	$\frac{1}{16}$	0	2	+
XIVB	$\mathcal{A}_{i_1i_4/i_2/i_3i_5}\mathcal{A}_{a_1a_5/a_2a_3/a_4}$	$\frac{1}{16}$	0	2	+
XV	$\mathcal{A}_{i_1i_3/i_2i_4/i_5i_6}\mathcal{A}_{a_1a_5/a_2a_6/a_3a_4}$	<u>1</u>	0	2	+

The final algebraic expressions for all Hugenholtz/Brandow diagrams (I)–(XV) representing moments $\mathcal{M}_{a_1...a_k}^{i_1...i_k}(2)$, k=3-6, are as follows:

```
I: -\frac{1}{4} \mathcal{A}_{i_1/i_2i_3} \mathcal{A}_{a_1a_2/a_3} \sum \langle i_4|f|a_4\rangle \langle a_1a_2|t_2|i_1i_4\rangle_{\mathcal{A}} \langle a_3a_4|t_2|i_3i_2\rangle_{\mathcal{A}} E_{i_1i_2i_3}^{a_1a_2a_3}
                                                                   a1,a2,a3,a4
IIA: -\frac{1}{4} \mathcal{A}_{i_1 i_2 / i_3} \mathcal{A}_{a_1 / a_2 a_3} \sum \langle i_4 a_1 | v | i_2 i_1 \rangle_{\mathcal{A}} \langle a_2 a_3 | t_2 | i_4 i_3 \rangle_{\mathcal{A}} E_{i_1 i_2 i_3}^{a_1 a_2 a_3}
                                                                         11,12,13,14
                                                                       \sum \langle a_2 a_1 | v | a_4 i_1 \rangle_{\mathcal{A}} \langle a_3 a_4 | t_2 | i_3 i_2 \rangle_{\mathcal{A}} E_{i_1 i_2 i_3}^{a_1 a_2 a_3}
IIB: \frac{1}{4} \mathcal{A}_{i_1/i_2i_3} \mathcal{A}_{a_1a_2/a_3}
                                                                  a1,a2,a3,a4
IIIA: \frac{1}{4} \mathcal{A}_{i_1 i_2 / i_3} \mathcal{A}_{a_1 / a_2 a_3}
                                                                       \sum
                                                                                                \langle i_4 i_5 | v | i_1 i_2 \rangle_A \langle a_1 | t_1 | i_4 \rangle \langle a_2 a_3 | t_2 | i_5 i_3 \rangle_A E_{i_1 i_2 i_3}^{a_1 a_2 a_3}
                                                                      11,12,13,14,15
                      \frac{1}{4}\mathcal{A}_{i_1/i_2i_3}\mathcal{A}_{a_1a_2/a_3}
                                                                           \sum \langle a_1 a_2 | v | a_4 a_5 \rangle_{\mathcal{A}} \langle a_4 | t_1 | i_1 \rangle \langle a_3 a_5 | t_2 | i_3 i_2 \rangle_{\mathcal{A}} E_{i_1 i_2 i_3}^{a_1 a_2 a_3}
IIIB:
                                                                        i1,i2,i3
                                                                  a1,a2,a3,a4,a5
IIIC: -\frac{1}{2}A_{i_1/i_2i_3}A_{a_1/a_2/a_3}
                                                                                                 \langle a_1 i_4 | v | i_1 a_4 \rangle_A \langle a_2 | t_1 | i_4 \rangle \langle a_3 a_4 | t_2 | i_3 i_2 \rangle_A E_{i_1 i_2 i_2}^{a_1 a_2 a_3}
                                                                         a1,a2,a3,a4
IIID: -\frac{1}{2}\mathcal{A}_{i_1/i_2/i_3}\mathcal{A}_{a_1/a_2a_3} \sum \langle a_1i_4|v|i_1a_4\rangle_{\mathcal{A}} \langle a_4|t_1|i_2\rangle \langle a_2a_3|t_2|i_4i_3\rangle_{\mathcal{A}} E_{i_1i_2i_3}^{a_1a_2a_3}
                                                                           11,12,13,14
                                                                         a1,a2,a3,a4
                                                                         \sum
IVA: \frac{1}{4}A_{i_1/i_2i_3}A_{a_1a_2/a_3}
                                                                                            \langle i_4 i_5 | v | i_1 a_4 \rangle_A \langle a_1 | t_1 | i_4 \rangle \langle a_2 | t_1 | i_5 \rangle \langle a_3 a_4 | t_2 | i_3 i_2 \rangle_A
                                                                  11,12,13,14,15
                                                                   a1,a2,a3,a4
                                                                                             \mathbf{x} \; E_{i_1 i_2 i_3}^{a_1 a_2 a_3}
IVB: \frac{1}{2}A_{i_1/i_2/i_3}A_{a_1/a_2a_3}
                                                                           \sum \langle i_4 i_5 | v | i_1 a_4 \rangle_{\mathcal{A}} \langle a_1 | t_1 | i_4 \rangle \langle a_4 | t_1 | i_2 \rangle \langle a_2 a_3 | t_2 | i_5 i_3 \rangle_{\mathcal{A}}
                                                                     11,12,13,14,15
                                                                      a1,a2,a3,a4
                                                                                                 \mathbf{x} \; E_{i_1 i_2 i_3}^{a_1 a_2 a_3}
                                                                                                         \langle i_4 a_2 | v | a_4 a_5 \rangle_{\mathcal{A}} \langle a_1 | t_1 | i_4 \rangle \langle a_4 | t_1 | i_1 \rangle
IVC: -\frac{1}{2}\mathcal{A}_{i_1/i_2i_3}\mathcal{A}_{a_1/a_2/a_3}
                                                                               \sum
                                                                                 11,12,13,14
                                                                            a1,a2,a3,a4,a5
                                                                                                            x \langle a_3 a_5 | t_2 | i_3 i_2 \rangle_A E_{i_1 i_2 i_3}^{a_1 a_2 a_3}
IVD: -\frac{1}{4}\mathcal{A}_{i_1i_2/i_3}\mathcal{A}_{a_1/a_2a_3} \sum \langle a_1i_4|v|a_4a_5\rangle_{\mathcal{A}}\langle a_4|t_1|i_1\rangle\langle a_5|t_1|i_2\rangle
                                                                               11,12,13,14
                                                                          a1,a2,a3,a4,a5
                                                                                                          \mathbf{x} \langle a_2 a_3 | t_2 | i_4 i_3 \rangle_{\mathcal{A}} E_{i_1 i_2 i_3}^{a_1 a_2 a_3}
```

$$\begin{array}{lll} \mathrm{VA}: & \frac{1}{4}\mathcal{A}_{i_{1}/i_{2}i_{3}}\mathcal{A}_{a_{1}a_{2}/a_{3}} \sum_{\substack{i_{1},i_{2},i_{3},i_{4},i_{5} \\ a_{1},a_{2},a_{3},a_{4},a_{5} \\ x}} & \langle i_{4}i_{5}|v|a_{4}a_{5}\rangle_{\mathcal{A}} & \langle a_{1}|t_{1}|i_{4}\rangle & \langle a_{4}|t_{1}|i_{1}\rangle & \langle a_{2}|t_{1}|i_{5}\rangle \\ & \times & \langle a_{3}a_{5}|t_{2}|i_{3}i_{2}\rangle_{\mathcal{A}} E_{i_{1}i_{2}i_{3}}^{a_{1}a_{2}a_{3}} \\ & \times & \langle a_{3}a_{5}|t_{2}|i_{3}i_{2}\rangle_{\mathcal{A}} & \langle a_{1}|t_{1}|i_{4}\rangle & \langle a_{4}|t_{1}|i_{1}\rangle & \langle a_{5}|t_{1}|i_{2}\rangle \\ & \times & \langle a_{2}a_{3}|t_{2}|i_{5}i_{3}\rangle_{\mathcal{A}} & \langle a_{1}|t_{1}|i_{4}\rangle & \langle a_{4}|t_{1}|i_{1}\rangle & \langle a_{5}|t_{1}|i_{2}\rangle \\ & \times & \langle a_{2}a_{3}|t_{2}|i_{5}i_{3}\rangle_{\mathcal{A}} & \langle a_{1}|t_{1}|i_{4}\rangle & \langle a_{4}|t_{1}|i_{1}\rangle & \langle a_{5}|t_{1}|i_{2}\rangle \\ & \times & \langle a_{2}a_{3}|t_{2}|i_{5}i_{3}\rangle_{\mathcal{A}} & \langle a_{1}a_{2}|t_{2}|i_{5}i_{2}\rangle_{\mathcal{A}} & \langle a_{5}a_{4}|t_{2}|i_{5}i_{3}\rangle_{\mathcal{A}} \\ & \times & \langle a_{2}a_{3}|t_{2}|i_{5}i_{3}\rangle_{\mathcal{A}} & \langle a_{1}a_{2}|t_{2}|i_{5}i_{3}\rangle_{\mathcal{A}} & \langle a_{3}a_{4}|t_{2}|i_{3}i_{2}\rangle_{\mathcal{A}} & \langle a_{3}a_{4}|t_{2}|i_{3}i_{5}\rangle_{\mathcal{A}} \\ & \times & \langle a_{1}a_{2}|a_{3}\rangle_{\mathcal{A}} & \times & \langle a_{1}a_{2}|t_{2}|i_{3}i_{2}\rangle_{\mathcal{A}} & \langle a_{1}a_{2}|t_{2}|i_{3}i_{2}\rangle_{\mathcal{A}} & \langle a_{2}a_{3}|t_{2}|t_{2}i_{3}i_{2}\rangle_{\mathcal{A}} & \langle a_{3}a_{4}|t_{2}|i_{3}i_{3}\rangle_{\mathcal{A}} \\ & \times & \langle a_{1}a_{1}|t_{2}|i_{3}\lambda_{\mathcal{A}} & \langle a_{1}a_{2}|t_{2}|t_{2}i_{3}\lambda_{\mathcal{A}} & \langle a_{2}a_{3}|t_{2}|t_{2}i_{3}i_{2}\rangle_{\mathcal{A}} & \langle a_{2}a_{3}|t_{2}|t_{2}i_{3}i_{2}\rangle_{\mathcal{A}} & \langle a_{2}a_{3}|t_{2}|t_{2}i_{3}i_{2}\rangle_{\mathcal{A}} \\ & \times & \langle a_{1}a_{1}|t_{2}|i_{3}\lambda_{\mathcal{A}} & \langle a_{2}a_{3}|t_{2}|t_{2}i_{3}\lambda_{\mathcal{A}} & \langle a_{2}a_{4}|t_{2}|t_{2}i_{3}\lambda_{\mathcal{A}} & \langle a_{2}a_{4}|t_{2}|t_{2}\lambda_{\mathcal{A}} & \langle a_{2}a_{4}|t_{2$$

$$\begin{array}{c} {\rm XD:} & -\frac{1}{4} {\cal A}_{i_1i_4/i_2/i_3} {\cal A}_{a_1/a_2a_3/a_4} \sum\limits_{\substack{i_1,i_2,i_3,i_4,i_5\\ a_1,a_2,a_3,a_4,a_5,a_6}} & \langle a_1i_5|v|a_5a_5\rangle_{\cal A} \langle a_4a_6|t_2|i_4i_1\rangle_{\cal A} \langle a_5|t_1|i_2\rangle \\ & \times \langle a_2a_3|t_2|i_5i_3\rangle_{\cal A} E_{i_1i_2i_3i_4}^{a_1a_2a_3a_4} \\ {\rm XIA:} & \frac{1}{32} {\cal A}_{i_1i_2/i_3/i_4} {\cal A}_{a_1/a_2a_3} \sum\limits_{\substack{i_1,i_2,i_3,i_4,i_5,i_6\\ a_1,a_2,a_3,a_4,a_5,a_6}} & \times \langle a_5a_6|t_2|i_2i_1\rangle_{\cal A} E_{i_1i_2i_3i_4}^{a_1a_2a_3a_4} \\ {\rm XIB:} & -\frac{1}{4} {\cal A}_{i_1/i_2i_4/i_3} {\cal A}_{a_1/a_2a_3/a_4} \sum\limits_{\substack{i_1,i_2,i_3,i_4,i_5,i_6\\ a_1,a_2,a_3,a_4,a_5,a_6}} & \langle i_5i_6|v|a_5a_6\rangle_{\cal A} \langle a_4a_6|t_2|i_4i_2\rangle_{\cal A} \\ & \times E_{i_1i_2i_3i_4}^{a_1a_2a_3a_4} \\ {\rm XIC:} & \frac{1}{32} {\cal A}_{i_1/i_2i_4} {\cal A}_{a_1a_2/a_3/a_4} \sum\limits_{\substack{i_1,i_2,i_3,i_4,i_5,i_6\\ a_1,a_2,a_3,a_4,a_5,a_6}} & \langle i_5i_6|v|a_5a_6\rangle_{\cal A} \langle a_4a_6|t_2|i_4i_2\rangle_{\cal A} \langle a_3a_5|t_2|i_3i_1\rangle_{\cal A} \\ & \times E_{i_1i_2i_3i_4}^{a_1a_2a_3a_4} \\ {\rm XIIA:} & \frac{1}{16} {\cal A}_{i_1/i_2i_3} {\cal A}_{a_1a_2/a_3/a_4} \sum\limits_{\substack{i_1,i_2,i_3,i_4,i_5,i_6\\ a_1,a_2,a_3,a_4,a_5,a_6}} & \langle i_5i_6|v|a_5a_6\rangle_{\cal A} \langle a_1|t_1|i_6\rangle \langle a_2|t_1|i_5\rangle \\ & \times \langle a_1a_2|t_2|i_5i_4\rangle_{\cal A} \langle a_3a_5|t_2|i_3i_2\rangle_{\cal A} \\ & \times E_{i_1i_2i_3i_4}^{a_1a_2a_3a_4} \\ {\rm XIIB:} & \frac{1}{4} {\cal A}_{i_1i_3/i_2/i_4} {\cal A}_{a_1/a_2a_4/a_3} \sum\limits_{\substack{i_1,i_2,i_3,i_4,i_5,i_6\\ a_1,a_2,a_3,a_4,a_5,a_6}} & \langle i_5i_6|v|a_5a_6\rangle_{\cal A} \langle a_2|t_1|i_6\rangle \langle a_6|t_1|i_2\rangle \\ & \times \langle a_1a_4|t_2|i_5i_4\rangle_{\cal A} \langle a_3a_5|t_2|i_3i_1\rangle_{\cal A} E_{i_1i_2i_3i_4}^{a_1a_2a_3a_4} \\ {\rm XIIC:} & \frac{1}{16} {\cal A}_{i_1i_2/i_3/i_4} {\cal A}_{a_1/a_2a_4} \sum\limits_{\substack{i_1,i_2,i_3,i_4,i_5,i_6\\ a_1,a_2,a_3,a_4,a_5,a_6}} \langle i_5i_6|v|a_5a_6\rangle_{\cal A} \langle a_5|t_1|i_1\rangle \langle a_6|t_1|i_2\rangle \\ & \times \langle a_1a_4|t_2|i_5i_4\rangle_{\cal A} \langle a_2a_3|t_2|i_6i_3\rangle_{\cal A} \\ & \times E_{i_1i_2i_3i_4}^{a_1a_2a_3a_4} \\ & \times E_{i_1i_2$$

$$\text{XIIIA}: \quad \frac{1}{16} \mathcal{A}_{i_{1}/i_{2}i_{3}/i_{4}i_{5}} \mathcal{A}_{a_{1}a_{5}/a_{2}a_{4}/a_{3}} \sum_{\substack{i_{1},i_{2},i_{3},i_{4},i_{5},i_{6},i_{7}\\a_{1},a_{2},a_{3},a_{4},a_{5},a_{6}\\x}} \langle i_{6}i_{7}|v|i_{1}a_{6}\rangle_{\mathcal{A}} \langle a_{1}a_{5}|t_{2}|i_{6}i_{5}\rangle_{\mathcal{A}}$$

$$\times \langle a_{2}a_{4}|t_{2}|i_{7}i_{4}\rangle_{\mathcal{A}} \langle a_{3}a_{6}|t_{2}|i_{3}i_{2}\rangle_{\mathcal{A}}$$

$$\times E_{i_{1}i_{2}i_{3}i_{4}i_{5}}^{a_{1}a_{2}a_{3}a_{4}a_{5}} \times \langle a_{1}i_{6}|v|a_{7}a_{6}\rangle_{\mathcal{A}} \langle a_{5}a_{7}|t_{2}|i_{5}i_{1}\rangle_{\mathcal{A}}$$

$$\times E_{i_{1}i_{2}i_{3}i_{4}i_{5}}^{a_{1}a_{2}a_{3}a_{4}a_{5}} \times \langle a_{1}i_{6}|v|a_{7}a_{6}\rangle_{\mathcal{A}} \langle a_{5}a_{7}|t_{2}|i_{5}i_{1}\rangle_{\mathcal{A}}$$

$$\times E_{i_{1}i_{2}i_{3}i_{4}i_{5}}^{a_{1}a_{2}a_{3}a_{4}a_{5}} \times \langle a_{2}a_{4}|t_{2}|i_{6}i_{4}\rangle_{\mathcal{A}} \langle a_{3}a_{6}|t_{2}|i_{3}i_{2}\rangle_{\mathcal{A}}$$

$$\times E_{i_{1}i_{2}i_{3}i_{4}i_{5}}^{a_{1}a_{2}a_{3}a_{4}a_{5}} \times \langle a_{2}a_{4}|t_{2}|i_{6}i_{4}\rangle_{\mathcal{A}} \langle a_{3}a_{6}|t_{2}|i_{3}i_{2}\rangle_{\mathcal{A}}$$

$$\times E_{i_{1}i_{2}i_{3}i_{4}i_{5}}^{a_{1}a_{2}a_{3}a_{4}a_{5}} \times \langle a_{1}a_{5}|t_{2}|i_{6}i_{4}\rangle_{\mathcal{A}} \langle a_{3}a_{6}|t_{2}|i_{3}i_{2}\rangle_{\mathcal{A}}$$

$$\times E_{i_{1}i_{2}i_{3}i_{4}i_{5}}^{a_{1}a_{2}a_{3}a_{4}a_{5}} \times \langle a_{1}a_{5}|t_{2}|i_{6}i_{4}\rangle_{\mathcal{A}} \langle a_{1}a_{5}|t_{2}|i_{6}i_{4}\rangle_{\mathcal{A}} \langle a_{3}a_{6}|t_{2}|i_{3}i_{2}\rangle_{\mathcal{A}}$$

$$\times E_{i_{1}i_{2}i_{3}i_{4}i_{5}}^{a_{1}a_{5}} \times \langle a_{1}a_{5}|t_{2}|i_{6}i_{4}\rangle_{\mathcal{A}} \langle a_{3}a_{6}|t_{2}|i_{3}i_{2}\rangle_{\mathcal{A}} \times \langle a_{1}a_{5}|t_{2}|i_{6}i_{4}\rangle_{\mathcal{A}} \langle a_{1}a_{5}|t_{2}|i_{6}i_{4}\rangle_{\mathcal{A}} \langle a_{1}a_{5}|t_{2}|i_{6}i_{4}\rangle_{\mathcal{A}} \langle a_{1}a_{5}|t_{2}|i_{6}i_{4}\rangle_{\mathcal{A}} \langle a_{1}a_{5}|t_{2}|i_{6}i_{4}\rangle_{\mathcal{A}} \times \langle a_{1}a_{5}|t_{2}|i_{6}i_{5}\rangle_{\mathcal{A}} \times \langle a_{2}a_{5}|t_{2}|i_{6}i_{4}\rangle_{\mathcal{A}} \langle a_{1}a_{5}|t_{2}|i_{6}i_{4}\rangle_{\mathcal{A}} \langle a_{1}a_{5}|t_{2}|i_{6}i_{4}\rangle_{\mathcal{A}} \langle a_{1}a_{5}|t_{2}|i_{6}i_{4}\rangle_{\mathcal{A}} \langle a_{1}a_{5}|t_{2}|i_{6}i_{4}\rangle_{\mathcal{A}} \langle a_{1}a_{5}|t_{2}|t_{6}|t_{6}\rangle_{\mathcal{A}} \times \langle a_{1}a_{5}|t_{2}|t_{6}|t_{6}\rangle_{\mathcal{A}} \langle a_{1}a_{5}|t_{2}|t_{6}|t_{6}\rangle_{\mathcal{A}} \times \langle a_{1}a_{5}|t_{2}|t_{6}|t_{6}\rangle_{\mathcal{A}} \langle a_{1}a_{5}|t_{2}|t_{6}\rangle_{\mathcal{A}} \langle a_{1}a_{5}|t_{6}|t_{6}\rangle_{\mathcal{A}} \langle a_{1}a_{5}|t_{6}|t_{6}\rangle_{\mathcal{A}} \langle a_{1}a_{5}|t_{6}|$$

References

References

- ¹ Hartree, D.R. Proc. Cam. Phil. Soc. 1928, 24, 89; 1928, 24, 111; 1928, 24, 426.
- ² Fock, V. Z. Physik. 1930, 61, 126.
- ³ Löwdin, P.O. Adv. Chem. Phys. 1959, 2, 207.
- ⁴ Pople, J.A.; Head-Gordon, M.; Raghavachari, K. J. Chem. Phys. 1987, 87, 5968.
- ⁵ Boys, S.F. Proc. Roy. Soc. **1950**, A201, 125.
- ⁶ Löwdin, P.O. Phys. Rev., 1955, 97, 1474.
- ⁷ Löwdin, P.O. Phys. Rev., 1955, 97, 1490.
- ⁸ Löwdin, P.O. Phys. Rev., 1955, 97, 1509.
- ⁹ Pople, J.A.; Binkley, J.S.; Seeger, R. Int. J. Quantum Chem. Symp. 1976, 10, 1.
- ¹⁰ Møller, C.; Plesset, M.S. Phys. Rev. 1934, 46, 618.
- ¹¹ Brueckner, K.A. Phys. Rev. 1955, 97, 1353; 100, 36.
- ¹² Goldstone, J. Proc. Roy. Soc. **1957**, A239, 267.
- ¹³ Hubbard, J. Proc. Roy. Soc. 1957, A240, 539; 1958a, A243, 336; 1958b, A244, 199.
- ¹⁴ Hugenholtz, N.M. Physica **1957**, 23, 481.
- ¹⁵ Čížek, J. J. Chem. Phys. **1966**, 45, 4256.

- ¹⁶ Čížek, J. Adv. Chem. Phys. 1969, 14, 35.
- ¹⁷ Čížek, J.; Paldus, J. Int. J. Quantum Chem. 1971, 5, 359.
- ¹⁸ Coester, F. Nucl. Phys. **1958**, 7, 421.
- ¹⁹ Coester, F.; Kümmel, H. Nucl. Phys. **1960**, 17, 477.
- ²⁰ Langhoff, S.R.; Davidson, E.R. Int. J. Quantum Chem. 1974, 8, 61.
- Davidson, E.R. In The World of Quantum Chemistry; Daudel, R.; Pullmsn, B., Eds.; Reidel: Dordrecht, 1974; pp. 17-30.
- ²² Paldus, J.; Čížek, J.; Shavitt, I. Phys. Rev. 1972, A5, 50.
- ²³ Pople, J.A.; Krishnan, R.; Schlegel, H.B.; Binkley, J.S. Int. J. Quantum Chem. 1978, 14, 545.
- ²⁴ Bartlett, R.J.; Purvis III, G.D. Int. J. Quantum Chem. 1978, 14, 561.
- ²⁵ Purvis III, G.D.; Bartlett, R.J. J. Chem. Phys. 1982, 76, 1910.
- ²⁶ Scuseria, G.E.; Scheiner, A.C.; Lee, T.J.; Rice, J.E.; Schaefer III, H.F. J. Chem. Phys. 1987, 86, 2881.
- ²⁷ Scuseria, G.E.; Janssen C.L.; Schaefer III, H.F. J. Chem. Phys. 1988, 89, 7382.
- ²⁸ Lee, T.J.; Rice, J.E. Chem. Phys. Lett. 1988, 150, 406.
- ²⁹ Piecuch, P.; Paldus, J. Int. J. Quantum Chem. 1989, 36, 429.
- ³⁰ Urban, M.; Noga, J.; Cole, S.J.; Bartlett, R.J. J. Chem. Phys. **1985**, 83, 4041.
- 31 Piecuch, P.; Paldus, J. Theor. Chim. Acta 1990, 78, 65.

- ³² Piecuch, P.; Toboła R.; Paldus, J. Int. J. Quantum Chem. 1995, 55, 133.
- ³³ Raghavachari, K.; Trucks, G.W.; Pople, J.A.; Head-Gordon, M. Chem. Phys. Lett. 1989, 157, 479.
- ³⁴ Kucharski, S.A.; Bartlett, R.J. J. Chem. Phys. 1998, 108, 9221.
- Paldus, J. In Methods in Computational Molecular Physics; Wilson, S.; Diercksen, G.H.F., Eds.; NATO Advanced Study Institute, Series B: Physics, Vol. 293; Plenum: New York, 1992; pp. 99-194.
- Lee, T.J.; Scuseria, G.E. In Quantum Mechanical Electronic Structure Calculations with Chemical Accuracy, Langhoff, S.R., Ed.; Kluwer: Dordrecht, 1995; (Dordrecht: Kluwer), pp. 47-108.
- ³⁷ Bartlett, R.J. In *Modern Electronic Structure Theory*; Yarkony, D.R., Ed.; World Scientific: Singapore, 1995; Part I, pp. 1047-1131.
- 38 Paldus, J.; Li, X. Adv. Chem. Phys. 1999, 110, 1.
- ³⁹ Crawford, T.D.; Schaefer III, H.F. Rev. Comp. Chem. 2000, 14, 33.
- ⁴⁰ Laidig, W.D.; Saxe, P.; Bartlett, R.J. J. Chem. Phys. 1987, 86, 887.
- ⁴¹ Ghose, K.B.; Piecuch, P.; Adamowicz, L. J. Chem. Phys. 1995, 103, 9331.
- ⁴² Piecuch, P.; Špirko, V.; Kondo, A.E.; Paldus, J. J. Chem. Phys. **1996**, 104, 4699.
- ⁴³ Piecuch, P.; Kucharski, S.A.; Bartlett, R.J. J. Chem. Phys. **1999**, 110, 6103.
- ⁴⁴ Piecuch, P.; Kucharski, S.A.; Špirko, V. J. Chem. Phys. 1999, 111, 6679.
- ⁴⁵ Piecuch, P.; Kowalski, K. In *Computational Chemistry: Reviews of Current Trends*; Leszczyński, J., Ed.; World Scientific: Singapore, 2000; Vol. 5, pp. 1-104.
- ⁴⁶ Kowalski, K.; Piecuch, P. J. Chem. Phys. 2000, 113, 18.

- ⁴⁷ Kowalski, K.; Piecuch, P. J. Chem. Phys. **2000**, 113, 5644.
- ⁴⁸ Kowalski, K.; Piecuch, P. Chem. Phys. Lett. 2001, 344, 165.
- ⁴⁹ Piecuch, P.; Kucharski, S.A.; Kowalski, K. Chem. Phys. Lett. **2001**, 344, 176.
- ⁵⁰ Piecuch, P.; Kucharski, S.A.; Špirko, V.; Kowalski, K. J. Chem. Phys. **2001**, 115, 5796.
- ⁵¹ Piecuch, P.; Kowalski, K.; Pimienta, I.S.O.; Kucharski, S.A. In *Low-Lying Potential Energy Surfaces*; Hoffmann, M.R.; Dyall, K.G., Eds.; ACS Symposium Series, Vol. 828; American Chemican Society: Washington, D.C., 2002; pp. 31-64.
- ⁵² Piecuch, P.; Kowalski, K.; Pimienta, I.S.O. Int. J. Mol. Sci. 2002, 3, 475.
- ⁵³ McGuire, M.J.; Kowalski, K.; Piecuch, P. J. Chem. Phys. **2002**, 117, 3617.
- ⁵⁴ Lee, Y.S.; Bartlett, R.J. J. Chem. Phys. **1984**, 80, 4371.
- ⁵⁵ Lee, Y.S.; Kucharski, S.A.; Bartlett, R.J. J. Chem. Phys. 1984, 81, 5906; ibid. 1985, 82, 5761.
- ⁵⁶ Noga, J.; Bartlett, R.J.; Urban, M. Chem. Phys. Lett. 1987, 134, 126.
- ⁵⁷ Trucks, G.W.; Noga, J.; Bartlett, R.J. Chem. Phys. Lett. 1988, 145, 548.
- ⁵⁸ Kucharski, S.A.; Bartlett, R.J. Chem. Phys. Lett. 1989, 158, 550.
- ⁵⁹ Kállay, M.; Surján, P.R. J. Chem. Phys. **2001**, 115, 2945.
- ⁶⁰ Noga, J.; Bartlett, R.J. J. Chem. Phys. **1987**, 86, 7041; ibid. **1988**, 89, 3401.
- 61 Scuseria, G.E.; Schaefer III, H.F. Chem. Phys. Lett. 1988, 152, 382.
- 62 Kucharski, S.A.; Bartlett, R.J. Theor. Chim. Acta 1991, 80, 387.

- 63 Kucharski, S.A.; Bartlett, R.J. J. Chem. Phys. 1992, 97, 4282.
- 64 Oliphant, N.; Adamowicz, L. J. Chem. Phys. 1991, 95, 6645.
- 65 Piecuch, P.; Adamowicz, L. J. Chem. Phys. 1994, 100, 5792.
- 66 Musiał, M.; Kucharski, S.A.; Bartlett, R.J. J. Chem. Phys. 2002, 116, 4382.
- 67 Schütz, M. J. Chem. Phys. 2000, 113, 9986.
- 68 Schütz, M.; Werner, H.-J. Chem. Phys. Lett. 2000, 318, 370.
- 69 Schütz, M. J. Chem. Phys. 2002, 116, 8772.
- ⁷⁰ Pulay, P. Chem. Phys. Lett. 1983, 100, 151.
- ⁷¹ Saebø, S.; Pulay, P. Chem. Phys. Lett. **1985**, 113, 13.
- ⁷² Saebø, S.; Pulay, P. Annu. Rev. Phys. Chem. **1993**, 44, 213.
- ⁷³ Jeziorski, B.; Monkhorst, H.J. Phys. Rev. A 1981, 24, 1668.
- ⁷⁴ Jeziorski, B.; Paldus, J. J. Chem. Phys. 1988, 88, 5673.
- ⁷⁵ Meissner, L.; Jankowski, K.; Wasilewski, J. Int. J. Quantum Chem. 1988, 34, 535.
- Paldus, J.; Pylypow, L.; Jeziorski, B. In Many-Body Methods in Quantum Chemistry, Kaldor, U., Ed.; Lecture Notes in Chemistry, Vol. 52; Springer: Berlin, 1989; pp. 151-170.
- ⁷⁷ Kucharski, S.A.; Bartlett, R.J. J. Chem. Phys. **1991**, 95, 8227.
- ⁷⁸ Balková, A.; Kucharski, S.A.; Meissner, L.; Bartlett, R.J. Theor. Chim. Acta 1991, 80, 335.

- ⁷⁹ Balková, A.; Kucharski, S.A.; Bartlett, R.J. Chem. Phys. Lett. 1991, 182, 511.
- 80 Piecuch, P.; Paldus, J. Theor. Chim. Acta 1992, 83, 69.
- Paldus, J.; Piecuch, P.; Jeziorski, B.; Pylypow, L. In Recent Progress in Many-Body Theories; Ainsworthy, T.L.; Campbell, C.E.; Clements, B.E.; Krotschek, E., Eds.; Plenum: New York, 1992; Vol. 3, pp. 287-303.
- 82 Paldus, J.; Piecuch, P.; Pylypow, L.; Jeziorski, B. Phys. Rev. A 1993, 47, 2738.
- 83 Piecuch, P.; Paldus, J. Phys. Rev. A 1994, 49, 3479.
- 84 Piecuch, P.; Paldus, J. J. Chem. Phys. 1994, 101, 5875.
- 85 Kowalski, K.; Piecuch, P. Phys. Rev. A 2000, 61, 052506.
- 86 Piecuch, P.; Landman, J.I. Parallel Comp. 2000, 26, 913.
- 87 Kowalski, K.; Piecuch, P. J. Mol. Struct.: THEOCHEM 2001, 547, 191.
- 88 Piecuch, P.; Kowalski, K. Int. J. Mol. Sci. 2002, 3, 676.
- 89 Lindgren, I.; Mukherjee, D. Phys. Rep. 1987, 151, 93.
- 90 Mukherjee, D.; Pal, S. Adv. Quantum Chem. 1989, 20, 291.
- ⁹¹ Jeziorski, B.; Paldus, J. J. Chem. Phys. 1989, 90, 2714.
- 92 Bernholdt, D.E.; Bartlett, R.J. Adv. Quantum Chem. 1999, 34, 271.
- ⁹³ Jankowski, K.; Paldus, J.; Grabowski, I.; Kowalski, K. J. Chem. Phys. **1992**, 97, 7600; **1994**, 101, 1759.
- ⁹⁴ Jankowski, K.; Paldus, J.; Grabowski, I.; Kowalski, K. J. Chem. Phys. **1994**, 101, 3085.

- 95 Kowalski, K.; Piecuch, P. Int. J. Quantum Chem. 2000, 80, 757.
- ⁹⁶ Mahapatra, U.S.; Datta, B.; Mukherjee, D. Mol. Phys. **1998**, 94, 157.
- 97 Mahapatra, U.S.; Datta, B.; Mukherjee, D. J. Chem. Phys. 1999, 110, 6171.
- 98 Mach, P.; Mášik, J.; Urban, J.; Hubač, I. Mol. Phys. 1998, 94, 173.
- 99 Mášik, J.; Hubač, I. Adv. Quantum Chem. 1999, 31, 75.
- Pittner, J.; Nachtigall, P.; Čársky, P.; Mášik, J.; Hubač, I. J. Chem. Phys. 1999, 110, 10275.
- ¹⁰¹ Hubač, I.; Pittner, J.; Čársky, P. J. Chem. Phys. **2000**, 112, 8779.
- ¹⁰² Sancho-Garcia, J.C.; Pittner, J.; Čársky, P.; Hubač, I. J. Chem. Phys. 2000, 112, 8785.
- ¹⁰³ Pittner, J.; Nachtigall, P.; Čársky, P.; Hubač, I. J. Phys. Chem. A 2001, 105, 1354.
- ¹⁰⁴ Li, X.; Paldus, J. J. Chem. Phys. **1997**, 107, 6257.
- ¹⁰⁵ Li, X.; Paldus, J. J. Chem. Phys. **1998**, 108, 637.
- ¹⁰⁶ Li, X.; Paldus, J. Chem. Phys. Lett. **1998**, 286, 145.
- ¹⁰⁷ Li, X.; Paldus, J. J. Chem. Phys. **1999**, 110, 2844.
- ¹⁰⁸ Li, X.; Paldus, J. Mol. Phys. **2000**, 98, 1185.
- ¹⁰⁹ Li, X.; Paldus, J. J. Chem. Phys. **2000**, 113, 9966.
- ¹¹⁰ Li, X. J. Mol. Struct.: THEOCHEM 2001, 547, 69.

- 111 Kowalski, K.; Piecuch, P. J. Chem. Phys. 2000, 113, 8490.
- 112 Kowalski, K.; Piecuch, P. J. Chem. Phys. 2001, 115, 643.
- 113 Kowalski, K.; Piecuch, P. Chem. Phys. Lett. 2001, 347, 237.
- ¹¹⁴ Oliphant, N.; Adamowicz, L. J. Chem. Phys. 1991, 94, 1229.
- ¹¹⁵ Oliphant, N.; Adamowicz, L. J. Chem. Phys. 1992, 96, 3739.
- 116 Oliphant, N.; Adamowicz, L. Int. Rev. Phys. Chem. 1993, 12, 339.
- ¹¹⁷ Piecuch, P.; Oliphant, N.; Adamowicz, L. J. Chem. Phys. 1993, 99, 1875.
- ¹¹⁸ Piecuch, P.; Adamowicz, L. Chem. Phys. Lett. **1994**, 221, 121.
- ¹¹⁹ Piecuch, P.; Adamowicz, L. J. Chem. Phys. **1995**, 102, 898.
- ¹²⁰ Ghose, K.B.; Adamowicz, L. J. Chem. Phys. 1995, 103, 9324.
- ¹²¹ Ghose, K.B.; Piecuch, P.; Pal, S.; Adamowicz, L. J. Chem. Phys. 1996, 104, 6582.
- ¹²² Adamowicz, L.; Piecuch, P.; Ghose, K.B. Mol. Phys. 1998, 94, 225.
- ¹²³ Olsen, J. J. Chem. Phys. **2000**, 113, 7140.
- ¹²⁴ Krogh, J.W.; Olsen, J. Chem. Phys. Lett. 2001, 344, 578.
- ¹²⁵ Kállay, M.; Szalay, P.G.; Surján, P.R. J. Chem. Phys. **2002**, 117, 980.
- ¹²⁶ Sherrill, C.D.; Krylov, A.I.; Byrd, E.F.C.; Head-Gordon, M. J. Chem. Phys. 1998, 109, 4171.

- ¹²⁷ Krylov, A.I.; Sherrill, C.D.; Byrd, E.F.C.; Head-Gordon, M. J. Chem. Phys. 1998, 109, 10669.
- ¹²⁸ Gwaltney, S.R.; Head-Gordon, M. Chem. Phys. Lett. 2000, 323, 21.
- ¹²⁹ Gwaltney, S.R.; Sherrill, C.D.; Head-Gordon, M.; Krylov, A.I. J. Chem. Phys. **2000**, 113, 3548.
- ¹³⁰ Gwaltney, S.R.; Head-Gordon, M. J. Chem. Phys. **2001**, 115, 2014.
- ¹³¹ Gwaltney, S.R.; Byrd, E.F.C.; Van Voorhis, T.; Head-Gordon, M. Chem. Phys. Lett. 2002, 353, 359.
- ¹³² Kowalski, K.; Piecuch, P. J. Chem. Phys. **2001**, 115, 2966.
- ¹³³ Kowalski, K.; Piecuch, P. J. Chem. Phys. **2002**, 116, 7411.
- ¹³⁴ Piecuch, P.; Kowalski, K.; Pimienta, I.S.O.; McGuire, M.J. Int. Rev. Phys. Chem. 2002, 21, 527.
- Piecuch, P.; Pimienta, I.S.O.; Fan, P.-D.; Kowalski, K. In Recent Progress in Electron Correlation Methodology; Wilson, A.K., Ed.; ACS Symposium Series, Vol. XXX; American Chemical Society: Washington, D.C., 2003; pp. XX-XXX, in press (37 pages).
- Piecuch, P.; Kowalski, K.; Fan, P.-D.; Pimienta, I.S.O. In *Topics in Theoretical Chemical Physics*; Maruani, J; Lefebvre, R.; Brändas, E., Eds.; Progress in Theoretical Chemistry and Physics, Vol. 12; Kluwer, Dordrecht, 2003; pp. 119-206.
- ¹³⁷ Pimienta, I.S.O.; Kowalski, K.; Piecuch, P. J. Chem. Phys. 2003, 119, 2951.
- ¹³⁸ Piecuch, P.; Kucharski, S.A.; Kowalski, K.; Musiał, M. Comp. Phys. Commun. **2002**, 149, 71.

- Schmidt, M.W.; Baldridge, K.K.; Boatz, J.A.; Elbert, S.T.; Gordon, M.S.; Jensen, J.H.; Koseki, S.; Matsunaga, N.; Nguyen, K.A.; Su, S.J.; Windus, T.L.; Dupuis, M.; Montgomery, J.A. J. Comput. Chem. 1993, 14, 1347.
- ¹⁴⁰ Senekerimyan, V.; McGuire, M.J.; Piecuch, P.; Dantus, M. Chem. Phys. Lett., submitted.
- ¹⁴¹ Dunning, T.H. J. Chem. Phys. 1970, 53, 2823.
- Head-Gordon, M.; Van Voorhis, T.; Gwaltney, S.R.; Byrd, E.F.C. In Low-Lying Potential Energy Surfaces; Hoffmann, M.R.; Dyall, K.G., Eds.; ACS Symposium Series, Vol. 828; American Chemican Society: Washington, D.C., 2002; pp. 93-108.
- ¹⁴³ Van Voorhis, T.; Head-Gordon, M. J. Chem. Phys. **2000**, 113, 8873.
- Piecuch, P.; Kowalski, K.; Pimienta, I.S.O.; Fan, P.-D.; Lodriguito, M.; McGuire, M.J.; Kucharski, S.A.; Kuś, T.; Musiał, M. Theor. Chem. Acct., submitted (44 pages).
- ¹⁴⁵ Piecuch, P.; Bartlett, R.J. Adv. Quantum Chem. 1999, 34, 295.
- ¹⁴⁶ Arponen, J.S. . Ann. Phys. **1983**, 151, 311.
- ¹⁴⁷ Arponen, J.S.; Bishop, R.F.; Pajanne, E. Phys. Rev. A 1987, 36, 2519.
- ¹⁴⁸ Arponen, J.S.; Bishop, R.F.; Pajanne, E. Condensed Matter Theor. 1987, 2, 357.
- Arponen, J.S.; Bishop, R.F.; Pajanne, E. In Aspects of Many-Body Effects in Molecules and Extended Systems; Mukherjee, D., Ed.; Lecture Notes in Chemistry, Vol. 50; Springer, Berlin, 1989; p. 79.
- 150 Bishop, R.F.; Arponen, J.S. Int. J. Quantum Chem. Symp. 1990, 24, 197.
- ¹⁵¹ Arponen, J.S.; Bishop, R.F. Ann. Phys. 1991, 207, 171.

- Bishop, R.F.; Robinson, N.I.; Arponen, J.S. Condensed Matter Theor. 1990, 5, 37.
- 153 Bishop, R.F. Theor. Chim. Acta 1991, 80, 95.
- ¹⁵⁴ Arponen, J.S. Phys. Rev. A 1997, 55, 2686.
- ¹⁵⁵ Arponen, J.S.; Bishop, R.F.; Pajanne, E. Phys. Rev. A 1987, 36, 2539.
- ¹⁵⁶ Paldus, J. In *Diagrammatical Methods for Many-Fermion Systems*, Lecture Notes, the University of Nijmegen, **1981**, unpublished.
- ¹⁵⁷ Brandow, B.H. Rev. Mod. Phys. 1967, 39, 771.
- ¹⁵⁸ Saxe, P.; Schaefer III, H.F.; Handy, N.C. Chem. Phys. Lett. 1981, 79, 202.
- ¹⁵⁹ Harrison, R.J.; Handy, N.C. Chem. Phys. Lett. 1983, 95, 386.
- ¹⁶⁰ Pimienta, I.S.O.; Kowalski, K.; Piecuch, P., unpublished results.

Table 1. A comparison of the standard CC, completely renormalized CCSD[T], CCSD(T), and CCSD(TQ), and CI-corrected MMCC(2,3) and MMCC(2,4) energies with the corresponding full CI, CISDt, and CISDtq results obtained for a few internuclear separations R of the HF molecule, as described by the DZ¹⁴¹ basis set.^a

Method	$R=R_e^{\ b}$	$R=2R_e$	$R=3R_e$	$R = 5R_e$
Full CI ^c	-0.160300	-0.021733	0.014719	0.016707
CCSD	1.634	6.047	11.596	12.291
$CCSDT^c$	0.173	0.855	0.957	0.431
$\mathrm{CCSD}[\mathrm{T}]^d$	-0.070	-2.725	-38.302	-75.101
$\mathrm{CCSD}(\mathrm{T})^d$	0.325	0.038	-24.480	-53.183
$\mathrm{CCSD}(\mathrm{TQ_f})^e$	0.218	-0.081	-18.351	-35.078
$\operatorname{CR-CCSD}[\mathrm{T}]^d$	0.163	0.700	2.508	3.820
$CR-CCSD(T)^d$	0.500	2.031	2.100	1.650
$CR-CCSD(TQ),a^f$	0.053	0.396	0.425	0.454
$CR-CCSD(TQ),b^f$	0.060	0.299	0.316	0.689
$\mathrm{CISDt}^{e,g}$	5.783	16.000	29.238	33.627
$\mathrm{CISDtq}^{e,g}$	5.466	6.730	7.456	7.468
$\mathrm{MMCC}(2,3)/\mathrm{CI}^{e,g}$	1.195	2.708	3.669	3.255
$\mathrm{MMCC}(2,4)/\mathrm{CI}^{e,g}$	1.207	$\boldsymbol{2.225}$	3.015	3.066

^a The full CI total energies are reported as (E+100) hartree. The standard CC, CI, CR-CC, and CI-corrected MMCC energies are in millihartree relative to the corresponding full CI energy values.

^b The equilibrium H-F bond length, R_e , equals 1.7328 bohr.

^c From Ref. 41.

^d From Refs. 45 and 46.

^e From Ref. 52.

f From Ref. 134.

^g The active space consisted of the 3σ , 1π , 2π , and 4σ orbitals.

Table 2. A comparison of the standard CC, completely renormalized CCSD[T], CCSD(T), and CCSD(TQ), and CI-corrected MMCC(2,3) and MMCC(2,4) energies with the corresponding full CI, CISDt, and CISDtq results obtained for the equilibrium and two displaced geometries of the H_2O molecule with the DZ^{141} basis set.^a

Method	$R = R_e^{\ b}$	$R=1.5R_e{}^c$	$R = 2R_e^{\ c}$
Full CI	-0.157866 ^b	-0.014521c	0.094753^{c}
CCSD	1.790	5.590	9.333
CCSDT^d	0.434	1.473	-2.211
$CCSDTQ^e$	0.015	0.141	0.108
$\mathrm{CCSD}[\mathrm{T}]^f$	0.362	0.751	-11.220
$CCSD(T)^f$	0.574	1.465	-7.699
$\mathrm{CCSD}(\mathrm{TQ_f})^f$	0.166	0.094	-5.914
$CR-CCSD[T]^f$	0.560	2.053	1.163
$CR-CCSD(T)^f$	0.738	2.534	1.830
$CR-CCSD(TQ),a^f$	0.195	0.905	1.461
$CR-CCSD(TQ),b^f$	0.195	0.836	2.853
$\mathrm{CISDt}^{g,h}$	6.922	18.884	49.948
$\mathrm{CISDtq}^{g,h}$	2.702	2.919	5.638
$\mathrm{MMCC}(2,3)/\mathrm{CI}^{g,h}$	0.811	2.407	1.631
$\mathrm{MMCC}(2,4)/\mathrm{CI}^{g,h}$	0.501	0.942	2.416

^a The full CI total energies are reported as (E + 76) hartree. The standard CC, CI, CR-CC, and CI-corrected MMCC energies are in millihartree relative to the corresponding full CI energy values.

^b The equilibrium geometry and full CI result from Ref. 158.

^c The geometry and full CI result from Ref. 159.

^d From Ref. 60.

^e From Ref. 63.

f From Ref. 46.

^g From Ref. 52.

^h The active space consisted of the $1b_1$, $3a_1$, $1b_2$, $4a_1$, $2b_1$, and $2b_2$ orbitals.

Table 3. A comparison of the standard CC, completely renormalized CCSD[T], CCSD(T), and CCSD(TQ), and CI-corrected MMCC(2,3) and MMCC(2,4) energies with the corresponding full CI, CISDt, and CISDtq results for a few internuclear separations of the N_2 molecule, as described by the DZ^{141} basis set.^a

Method	$0.75R_e$	$R_e^{\ b}$	$1.25R_e$	$1.5R_e$	$1.75R_e$	$2R_e$	$2.25R_e$
Full CI ^c	0.549027	1.105115	1.054626	0.950728	0.889906	0.868239	0.862125
CCSDT°	3.132	8.289	19.061	33.545	17.714	-69.917	-120.836
	0.580	2.107	6.064	10.158	-22.468	-109.767	-155.656
$ ext{CCSD}(ext{T})^c \ ext{CCSD}(ext{TQ}_f)^c \ ext{CCSDT}(ext{Q}_f)^d$	0.742	2.156	4.971	4.880	-51.869	-246.405	-387.448
	0.226	0.323	0.221	-2.279	-14.243	92.981	334.985
	0.047	-0.010	-0.715	-4.584	3.612	177.641	426.175
CR-CCSD(T) ^c	$,a^{c} 0.448$	3.452	9.230	17.509	-2.347	-86.184	-133.313
CR-CCSD(TQ		1.106	2.474	5.341	1.498	-40.784	-69.259
CR-CCSD(TQ		1.302	3.617	8.011	13.517	25.069	14.796
$ ext{CISDt}^{e,f} \\ ext{CISDtq}^{e,f} $	8.380	19.303	40.247	75.379	126.472	182.996	216.760
	5.101	7.233	10.651	18.003	30.226	41.978	51.126
MMCC(2,3)/C		4.076	10.117	18.926	-0.564	-85.380	-133.437
MMCC(2,4)/C		2.354	5.363	11.639	10.831	-16.086	-30.720

^a The full CI total energies are reported as -(E+108) hartree. The standard CC, CI, CR-CC, and CI-corrected MMCC energies are in millihartree relative to the corresponding full CI energy values. The lowest two occupied and the highest two unoccupied orbitals were frozen in correlated calculations.

^b The equilibrium N-N bond length, R_e , equals 2.068 bohr.

^c From Ref. 47.

^d From Ref. 49.

^e From Ref. 134.

^f The active space consisted of the $3\sigma_g$, $1\pi_u$, $2\pi_u$, $1\pi_g$, $2\pi_g$, and $3\sigma_u$ orbitals.

Table 4. A comparison of the CI-corrected MMCC(2,5) and MMCC(2,6) energies and QMMCC(2,4), QMMCC(2,5), and QMMCC(2,6) energies with the results of the full CI, standard CC, and CISDtqp and CISDtqph calculations for the equilibrium and two displaced geometries of the $\rm H_2O$ molecule with the DZ¹⁴¹ basis set.^a

Method	$R=R_e{}^b$	$R=1.5R_e{}^c$	$R=2R_e^{\ c}$
Full CI	-0.157866 ^b	-0.014521°	0.094753^{c}
CCSD	1.790	5.590	9.333
\mathbb{CCSDT}^d	0.434	1.473	-2.211
CCSDTQ ^e	0.015	0.141	0.108
$CCSD[T]^f$	0.362	0.751	-11.220
$CCSD(T)^f$	0.574	1.465	-7.699
$\mathrm{CCSD}(\mathrm{TQ_f})^f$	0.166	0.094	-5.914
$\mathrm{CISDtqp}^{g,h}$	2.628	2.578	3.732
$\operatorname{CISDtqph}^{g,h}$	2.600	2.187	1.922
$\mathrm{MMCC}(2,5)/\mathrm{CI}^{g,h}$	0.421	0.584	0.730
$\mathrm{MMCC}(2,6)/\mathrm{CI}^{g,h}$	0.417	0.477	0.538
$QMMCC(2,4)^i$	0.271	0.959	2.005
$QMMCC(2,5)^i$	0.202	0.688	0.549
$QMMCC(2,6)^i$	0.202	0.688	0.546
QMMCC(2,6)	0.202	0.688	0.546
$(M_{i_1i_2i_3i_4i_5i_6}^{a_1a_2a_3a_4a_5a_6}(2)=0)^{i}$			
QMMCC(2,6)	0.206	0.708	0.657
$(M_{i_1i_2i_3i_4i_5}^{a_1a_2a_3a_4a_5}(2)=0,$			
$M_{i_1i_2i_3i_4i_5i_6}^{a_1a_2a_3a_4a_5a_6}(2)=0)^{i}$			

^a The full CI total energies are reported as (E+76) hartree. The standard CC, CI, QMMCC, and CI-corrected MMCC energies are in millihartree relative to the corresponding full CI energy values.

^b The equilibrium geometry and full CI result from Ref. 158.

 $^{^{}c}$ The geometry and full CI result from Ref. 159.

^d From Ref. 60.

^e From Ref. 63.

f From Ref. 46.

⁹ From Ref. 134.

^h The active space consisted of the $1b_1$, $3a_1$, $1b_2$, $4a_1$, $2b_1$, and $2b_2$ orbitals.

ⁱ From Ref. 137

Table 5. A comparison of the CI-corrected MMCC(2,5) and MMCC(2,6) energies and QMMCC(2,4), QMMCC(2,5), and QMMCC(2,6) energies with the results of the full CI, standard CC, and CISDtqp and CISDtqph calculations for a few internuclear separations of the N_2 molecule with the DZ^{141} basis set.^a

Method	$0.75R_e$	$R_e^{\ b}$	$1.25R_e$	$1.5R_e$	$1.75R_e$	$2R_e$	$2.25R_e$
Full CI ^c	0.549027 1	.105115 1	1.054626 ().950728 (0.889906	0.868239	0.862125
CCSD	3.132	8.289	19.061	33.545	17.714	-69.917	-120.836
CCSDT ^c	0.580	2.107	6.064	10.158	-22.468	-109.767	-155.656
$ ext{CCSD}(ext{T})^c \ ext{CCSD}(ext{TQ}_{ ext{f}})^c \ ext{CCSDT}(ext{Q}_{ ext{f}})^d$	0.742	2.156	4.971	4.880	-51.869	-246.405	-387.448
	0.226	0.323	0.221	-2.279	-14.243	92.981	334.985
	0.047	-0.010	-0.715	-4.584	3.612	177.641	426.175
$ ext{CISDtqp}^{e,f} \ ext{CISDtqph}^{e,f}$	5.401	6.969	8.880	12.086	20.037	28.161	34.276
	5.390	6.799	7.558	6.707	7.189	7.777	8.372
$MMCC(2,5)/CI^{e_0}$		2.089	3.527	5.493	1.631	-24.410	-39.124
$MMCC(2,6)/CI^{e_0}$		2.022	2.909	3.186	4.048	4.443	4.552
$QMMCC(2,4)^g$ $QMMCC(2,5)^g$ $QMMCC(2,6)^g$	0.458	1.384	3.916	8.362	13.074	22.091	10.749
	0.384	1.012	2.365	3.756	1.415	6.672	-2.638
	0.384	1.012	2.373	3.784	1.380	6.230	-3.440
$\begin{array}{c} \text{QMMCC}(2,6) \\ (M_{i_1 i_2 i_3 i_4 i_5 i_6}^{a_1 a_2 a_3 a_4 a_5 a_6}(2) \end{array}$	0.384	1.013	2.397	3.782	1.378	6.240	-3.418
QMMCC(2,6) $(M_{i_1i_2i_3i_4i_5}^{a_1a_2a_3a_4a_5}(2) = M_{i_1i_2i_3i_4i_5i_6}^{a_1a_2a_3a_4a_5a_6}(2) = 0$	0.387 : 0,	1.040	2.533	4.317	2.062	4.674	-6.499

^a The full CI total energies are reported as -(E+108) hartree. The standard CC, CI, QMMCC, and CI-corrected MMCC energies are in millihartree relative to the corresponding full CI energy values. The lowest two occupied and the highest two unoccupied orbitals were frozen in correlated calculations.

^b The equilibrium N-N bond length, R_e , equals 2.068 bohr.

^c From Ref. 47.

^d From Ref. 49.

e From Ref. 134.

^f The active space consisted of the $3\sigma_g$, $1\pi_u$, $2\pi_u$, $1\pi_g$, $2\pi_g$, and $3\sigma_u$ orbitals.

^g From Ref. 137.

Table 6. A comparison of the QMMCC(2,4), QMMCC(2,5), and QMMCC(2,6) energies with the results of the full CI and standard CC calculations for a few internuclear separations R of the HF molecule, as described by the DZ¹⁴¹ basis set.^a

Method	$R=R_e^{\ b}$	$R=2R_e$	$R = 5R_e$
Full CI ^c	-0.160300	-0.021733	0.016707
CCSD	1.634	6.047	12.291
$CCSDT^c$	0.173	0.855	0.431
$\mathrm{CCSD}[\mathrm{T}]^d$	-0.070	-2.725	-75.101
$CCSD(T)^d$	0.325	0.038	-53.183
$\mathrm{CCSD}(\mathrm{TQ_f})^e$	0.218	-0.081	-35.078
$QMMCC(2,4)^f$	0.198	0.074	0.277
$QMMCC(2,5)^f$	0.091	-0.312	-0.797
$QMMCC(2,6)^f$	0.092	-0.308	-0.798

^a The full CI total energies are reported as (E+100) hartree. The standard CC and QMMCC energies are in millihartree relative to the corresponding full CI energy values.

^b The equilibrium H-F bond length, R_e , equals 1.7328 bohr.

^c From Ref. 41.

^d From Refs. 45 and 46.

e From Ref. 52.

^f From Ref. 160.

Table 7. A comparison of the QMMCC(2,4), QMMCC(2,5), and QMMCC(2,6) energies with the results of the full CI, standard CC, and completely renormalized CCSD(TQ) calculations for a few internuclear separations of the C₂ molecule with the DZ¹⁴¹ basis set.^a

Method	$0.75R_e$	$R_e{}^b$	$1.5R_e$	$1.75R_e$	$2R_e$	$2.5R_e$	$3R_e$
Full CI ^c	0.293301	0.641867	0.519881	0.484166	0.462769	0.449248	0.446985
${f CCSD} \ {f CCSDT^c}$	16.795 0.698	20.684 2.091	37.640 14.393	36.280 17.704	15.772 -4.508	-3.422 -22.502	-7.438 -26.161
CCSDT	-2.791	0.389	11.926	1.877	-35.176	-80.231	-96.055
$\mathrm{CCSD}(\mathrm{TQ_f})^c$	-3.594	-0.735	11.347	12.308	5.800	29.196	67.237
CR-CCSD(TQ),	$b^c 4.096$	4.993	17.830	26.812	24.344	21.096	20.282
$\mathrm{QMMCC}(2,4)^d$ $\mathrm{QMMCC}(2,5)^d$	3.379	4.991	19.325 15.451	27.897 23.468	24.370 18.696	20.237 13.180	19.192 11.646
$\begin{array}{c} \text{QMMCC}(2,6)^d \\ \text{QMMCC}(2,6)^d \end{array}$	2.554 2.555	$2.875 \\ 2.875$	15.451	23.470	18.689	13.169	11.634
QMMCC(2,6) $(M_{i_1 i_2 i_3 i_4 i_5 i_6}^{a_1 a_2 a_3 a_4 a_5 a_6}(2)$	2.555 $= 0)^d$	2.875	15.458	23.469	18.689	13.169	11.634
QMMCC(2,6) $(M_{i_1 i_2 i_3 i_4 i_5}^{a_1 a_2 a_3 a_4 a_5}(2) = M_{i_1 i_2 i_3 i_4 i_5}^{a_1 a_2 a_3 a_4 a_5 a_6}(2) = M_{i_1 i_2 i_3 i_4 i_5 i_6}^{a_1 a_2 a_3 a_4 a_5 a_6}(2) = M_{i_1 i_2 i_3 i_4 i_5 i_6}^{a_1 a_2 a_3 a_4 a_5 a_6}(2) = M_{i_1 i_2 i_3 i_4 i_5 i_6}^{a_1 a_2 a_3 a_4 a_5 a_6}(2) = M_{i_1 i_2 i_3 i_4 i_5 i_6}^{a_1 a_2 a_3 a_4 a_5 a_6}(2) = M_{i_1 i_2 i_3 i_4 i_5 i_6}^{a_1 a_2 a_3 a_4 a_5 a_6}(2) = M_{i_1 i_2 i_3 i_4 i_5 i_6}^{a_1 a_2 a_3 a_4 a_5 a_6}(2) = M_{i_1 i_2 i_3 i_4 i_5 i_6}^{a_1 a_2 a_3 a_4 a_5 a_6}(2) = M_{i_1 i_2 i_3 i_4 i_5 i_6}^{a_1 a_2 a_3 a_4 a_5 a_6}(2) = M_{i_1 i_2 i_3 i_4 i_5 i_6}^{a_1 a_2 a_3 a_4 a_5 a_6}(2) = M_{i_1 i_2 i_3 i_4 i_5 i_6}^{a_1 a_2 a_3 a_4 a_5 a_6}(2) = M_{i_1 i_2 i_3 i_4 i_5 i_6}^{a_1 a_2 a_3 a_4 a_5 a_6}(2) = M_{i_1 i_2 i_3 i_4 i_5 i_6}^{a_1 a_2 a_3 a_4 a_5 a_6}(2) = M_{i_1 i_2 i_3 i_4 i_5 i_6}^{a_1 a_2 a_3 a_4 a_5 a_6}(2) = M_{i_1 i_2 i_3 i_4 i_5 i_6}^{a_1 a_2 a_3 a_4 a_5 a_6}(2) = M_{i_1 i_2 i_3 i_4 i_5 i_6}^{a_1 a_2 a_3 a_4 a_5 a_6}(2) = M_{i_1 i_2 i_3 i_4 i_5 i_6}^{a_1 a_2 a_3 a_4 a_5 a_6}(2) = M_{i_1 i_2 i_3 i_4 i_5 i_6}^{a_1 a_2 a_3 a_4 a_5 a_6}(2) = M_{i_1 i_2 i_3 i_4 i_5 i_6}^{a_1 a_2 a_3 a_4 a_5 a_6}(2) = M_{i_1 i_2 i_3 i_4 i_5 i_5 i_6}^{a_1 a_2 a_3 a_4 a_5 a_6}(2) = M_{i_1 i_2 i_3 i_4 i_5 i_5 i_6}^{a_1 a_2 a_3 a_4 a_5 a_6}(2)$	2.609 = 0,	3.064	15.879	23.777	18.892	13.243	11.665

^a The full CI total energies E [reported as -(E+75)] are given in hartree. The standard CC, CR-CC, and QMMCC energies are reported in millihartree relative to the corresponding full CI energy values. The lowest two occupied and the highest two unoccupied orbitals were frozen in correlated calculations.

^b The equilibrium C-C bond length, R_e , equals 2.348 bohr.

^c From Ref. 51.

^d From Ref. 160.

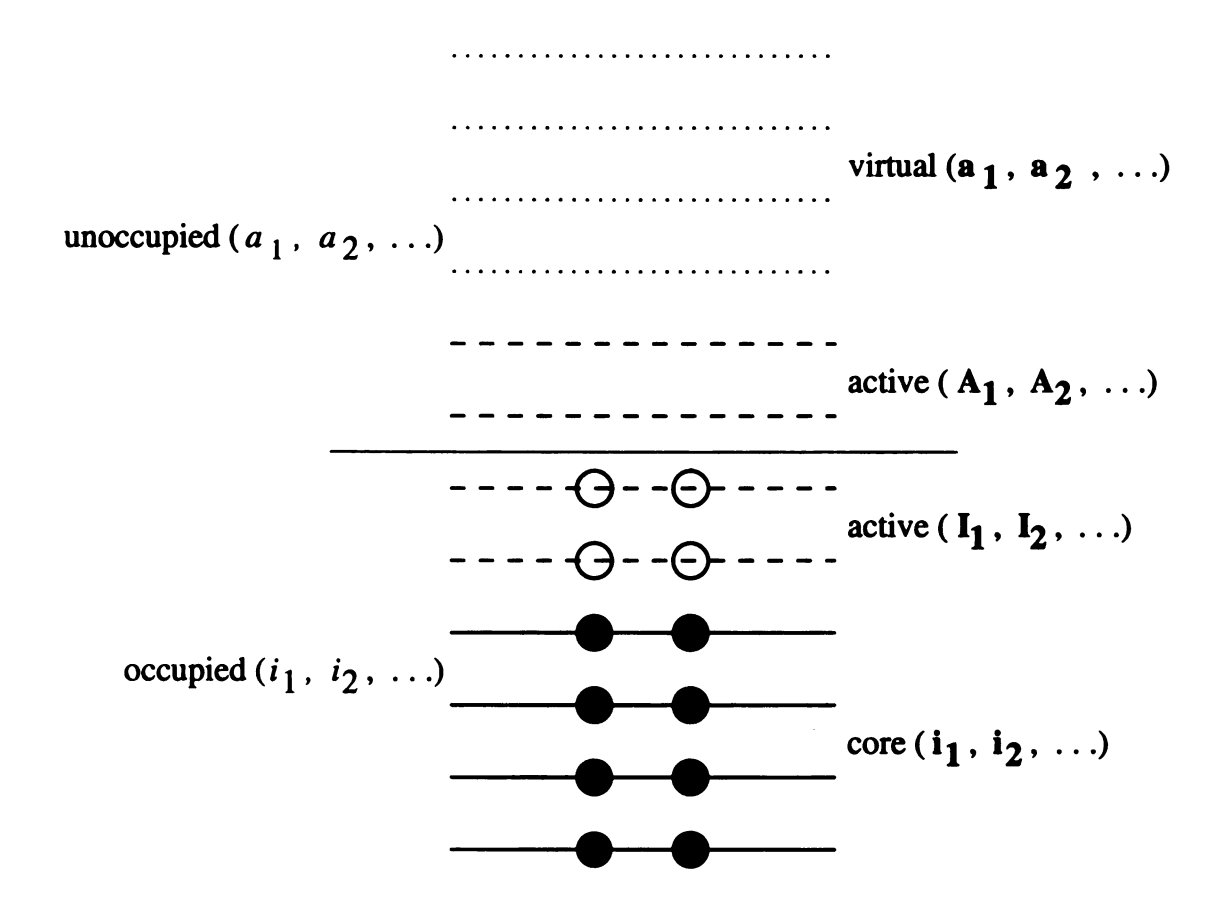


Fig. 1. The orbital classification used in the active-space CI and the CI-corrected MMCC(2,3), MMCC(2,4), MMCC(2,5), and MMCC(2,6) approaches. Core, active, and virtual orbitals are represented by solid, dashed, and dotted lines, respectively. Full and open circles represent core and active electrons of the reference configuration $|\Phi\rangle$.

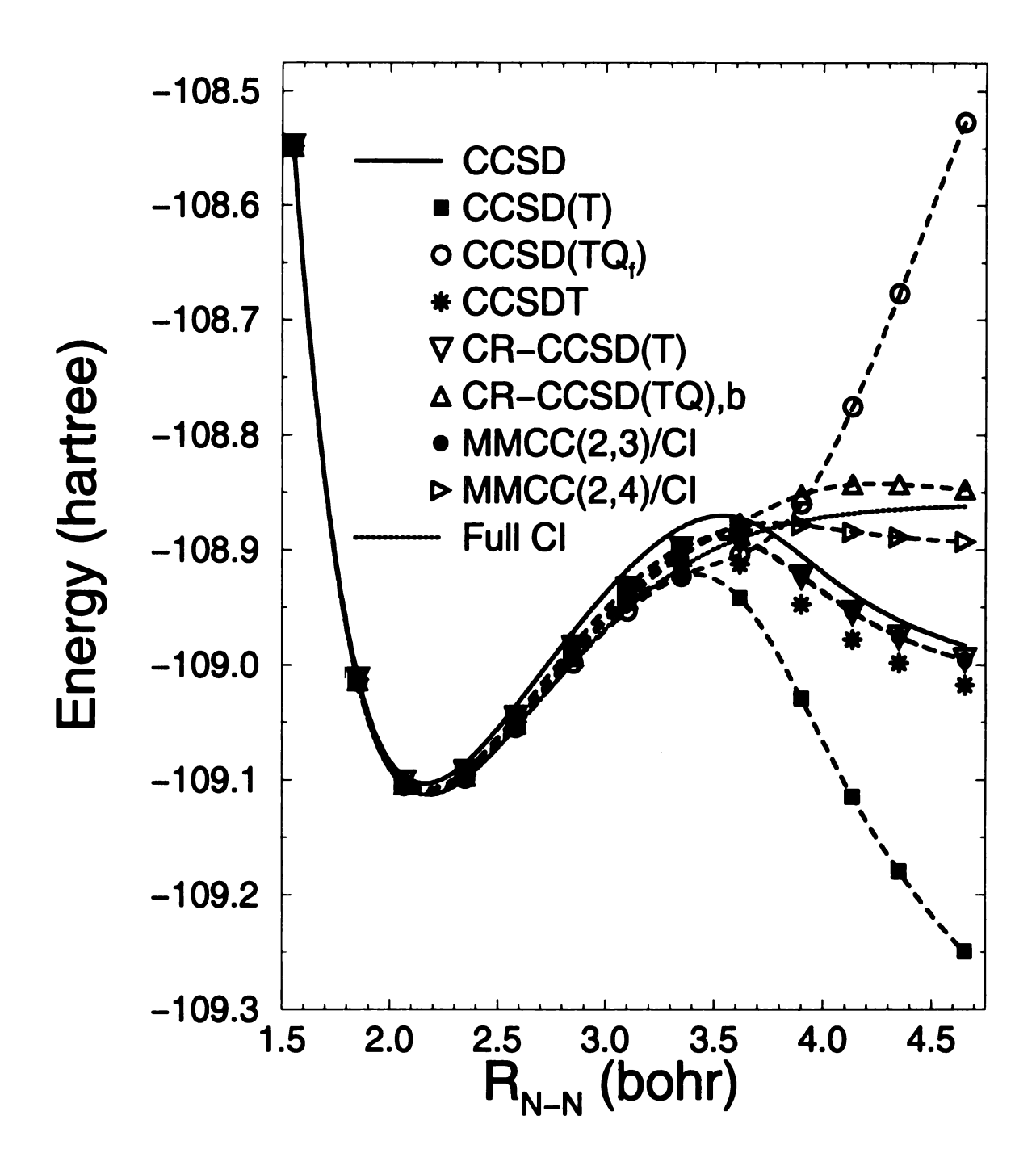


Fig. 2. Potential energy curves for the N_2 molecule, as described by the DZ basis set. A comparison of the results obtained with the CR-CC and CI-corrected MMCC(2,3) and MMCC(2,4) methods with the results of the standard CC and full CI calculations.

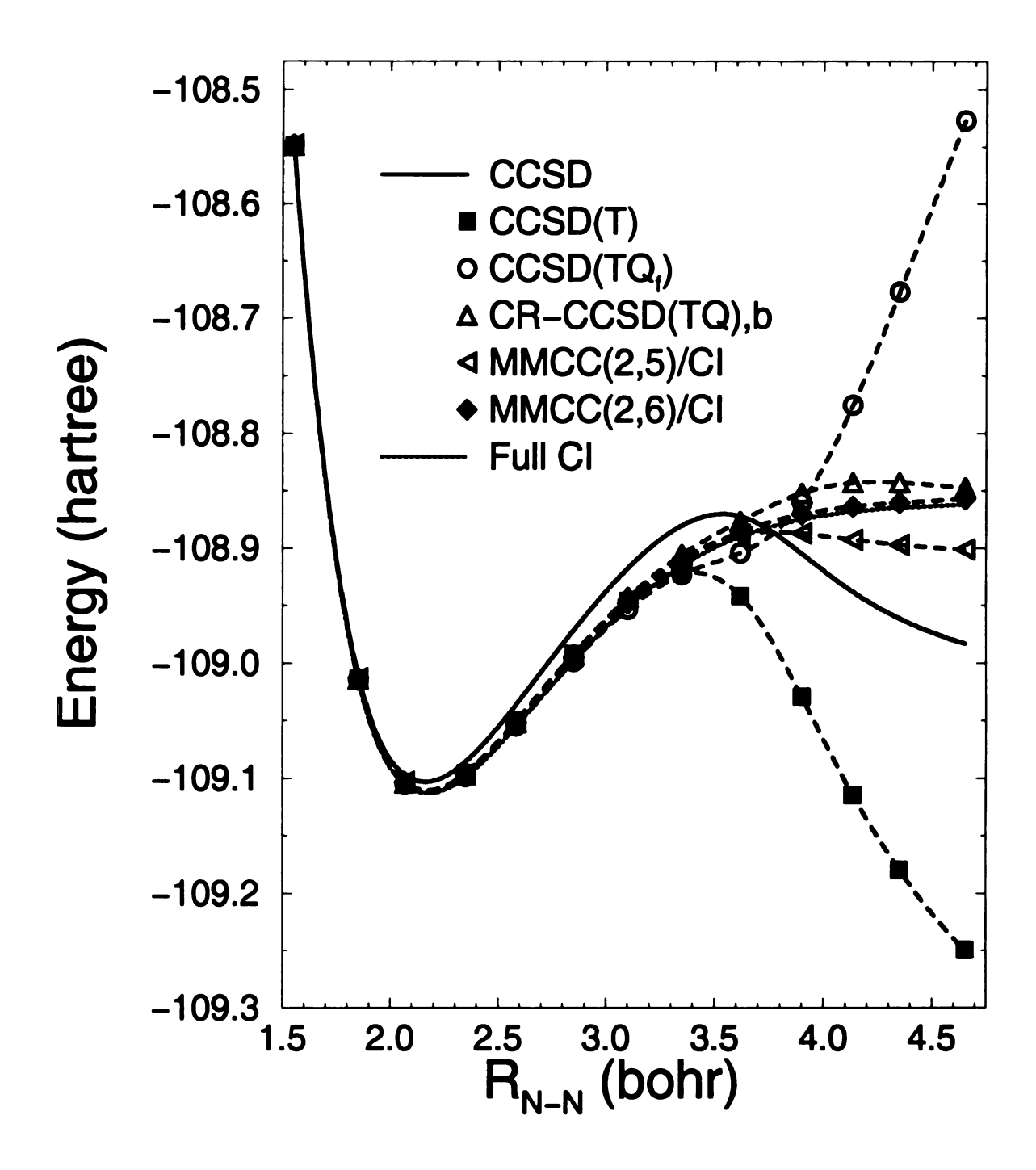


Fig. 3. Potential energy curves for the N_2 molecule, as described by the DZ basis set. A comparison of the results obtained with the CI-corrected MMCC(2,5) and MMCC(2,6) methods with the results of the standard CC, CR-CCSD(TQ), and full CI calculations.

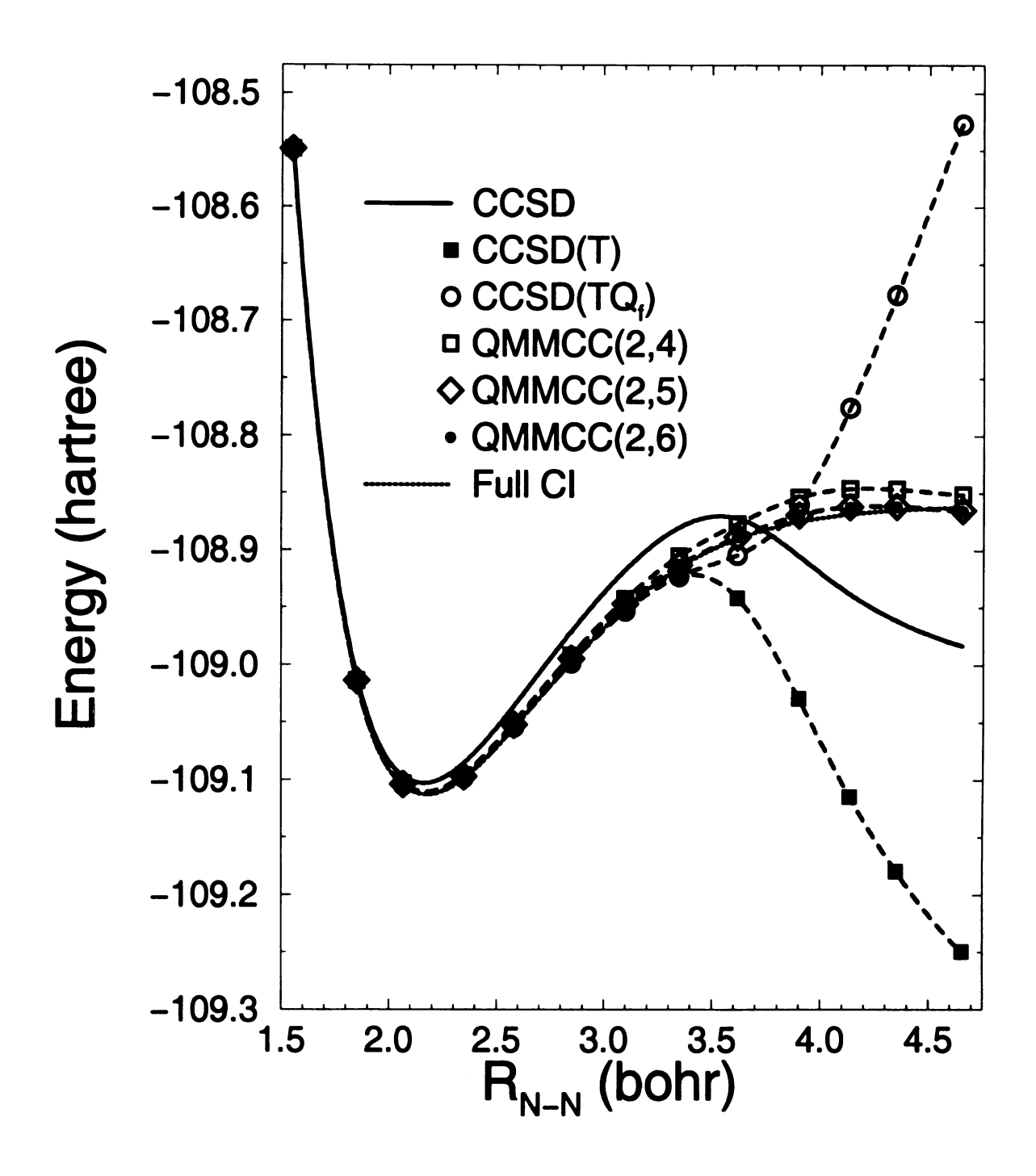


Fig. 4. Potential energy curves for the N₂ molecule, as described by the DZ basis set. A comparison of the results obtained with the QMMCC methods with the results of the standard CC and full CI calculations.

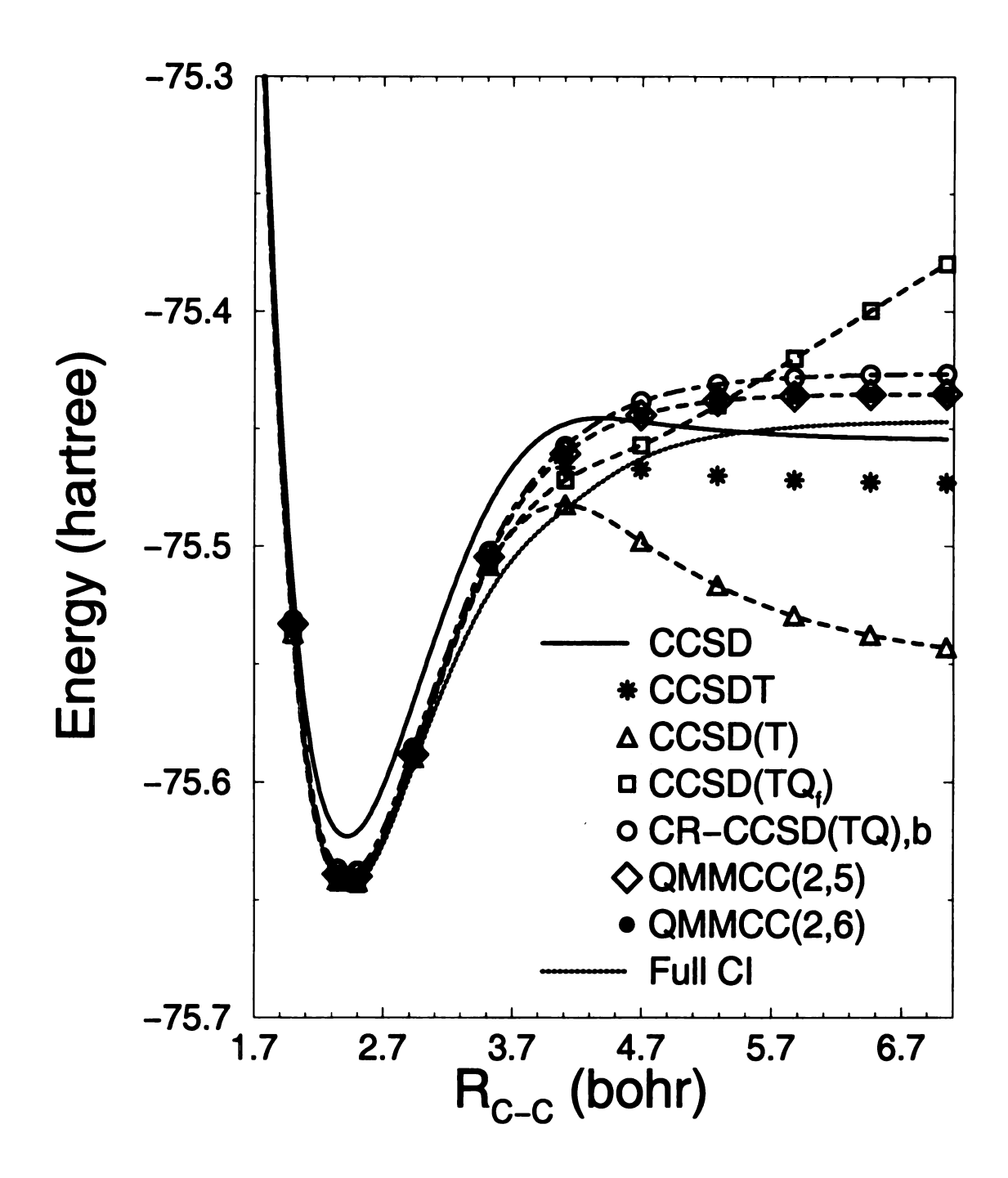


Fig. 5. Potential energy curves for the C₂ molecule, as described by the DZ basis set. A comparison of the results obtained with the QMMCC methods with the results of the standard CC, CR-CCSD(TQ), and full CI calculations.

